

Postglacial colluvium in western Norway: depositional processes, facies and palaeoclimatic record

LARS H. BLIKRA* and W. NEMEC†

**Geological Survey of Norway, PO Box 3006 Lade, N-7002 Trondheim, Norway*

(*E-mail: lars.blikra@ngu.no*)

†*Geological Institute, University of Bergen, N-5007 Bergen, Norway (E-mail: wojtek.nemec@geol.uib.no)*

ABSTRACT

The postglacial Quaternary colluvial systems in western Norway are arrays of steep fans, often coalescing into aprons, developed along the slopes of valley sides and fjord margins. The coarse debris, derived from weathered gneissic bedrock and its glacial-till mantle, varies from highly immature to mature. The depositional processes are mainly avalanches, ranging from rockfalls and debrisflows to snowflows, but include also waterflow and debris creep. The mechanics and sedimentary products of these processes are discussed, with special emphasis on snow avalanches, whose role as an agent of debris transport is little-known to sedimentologists. The subsequent analysis of sedimentary successions is focused on colluvial-fan deltas, which are very specific, yet little-studied, coastal depositional systems. The stratigraphic variation and depositional architecture of the colluvial facies assemblages, constrained by abundant radiometric dates, are used to decipher the signal of regional climatic changes from the sedimentary record. The stratigraphic data from two dozen local colluvial successions are compiled and further compared with other types of regional palaeoclimatic proxy record. The analysis suggests that the colluvial systems, although dependent upon local geomorphic conditions, have acted as highly sensitive recorders of regional climatic changes. The study as a whole demonstrates that colluvial depositional systems are an interesting and important frontier of clastic sedimentology.

INTRODUCTION

This paper discusses the sedimentology of the postglacial Quaternary colluvium in western Norway, based on case studies from two dozen localities in the Møre-Romsdal region (Fig. 1). The colluvium comprises arrays of steep, gravelly fans developed along the valley sides and fjord margins. The depositional processes include a whole range of avalanches, and the paper puts special emphasis on snowflows, whose mechanics and products are little-known to sedimentologists. The paper further focuses on the facies anatomy, chronostratigraphy and depositional history of the colluvium, with emphasis on coastal colluvial systems, which represent a

specific type of fan delta. In the final part, the palaeoclimatic record of the colluvial successions is discussed and compared with other types of regional palaeoclimatic data.

TERMINOLOGY

Colluvium is a general term for clastic slope-waste material, typically coarse grained and immature, deposited in the lower part and foot zone of a mountain slope or other topographic escarpment, and brought there chiefly by sediment-gravity processes (Holmes, 1965; Bates & Jackson, 1987; Blikra & Nemec, 1993a). In geomorphological literature, colluvium is also referred to as 'talus',

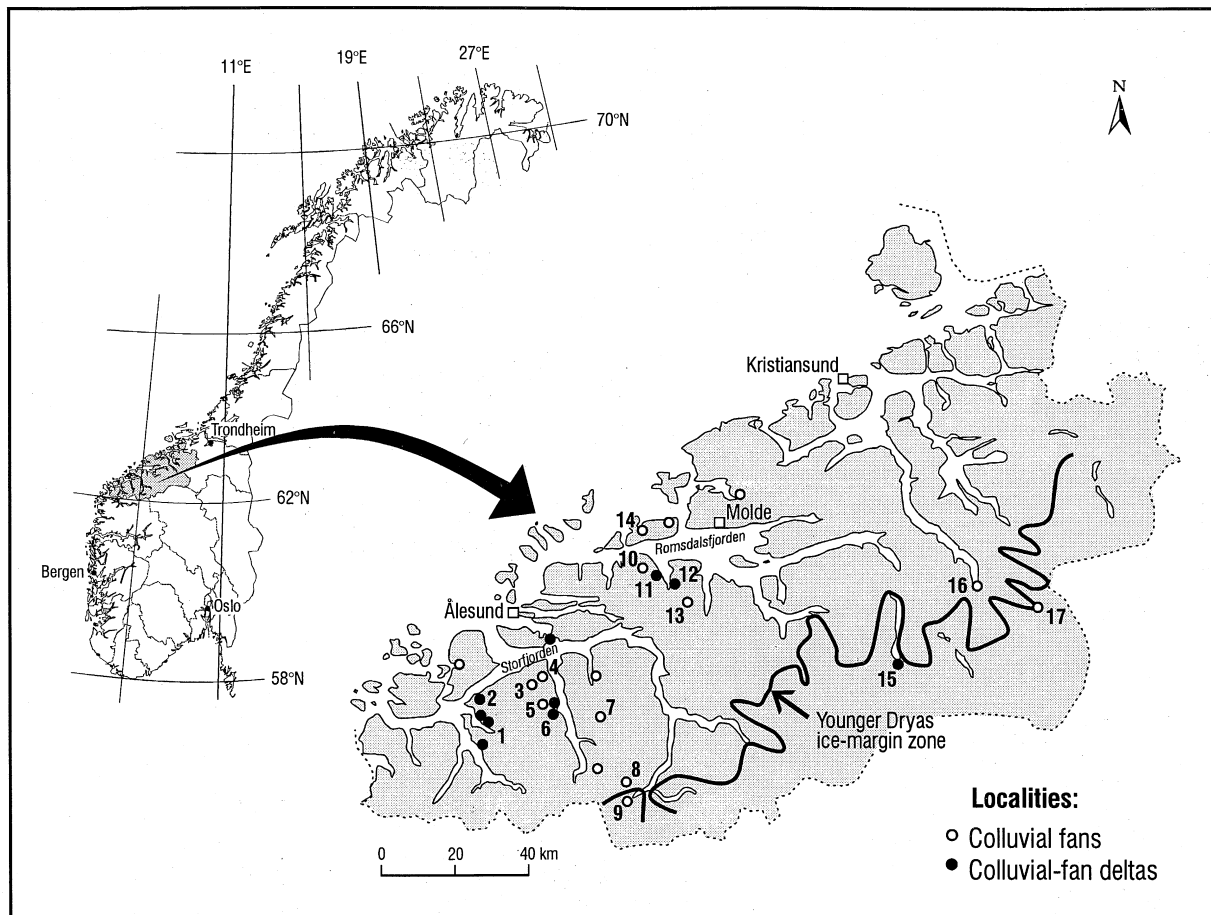


Fig. 1. Locality map of the Møre-Romsdal region, western Norway, showing the main sites of detailed case studies and the position of the Scandinavian ice-sheet margin in the Younger Dryas time. The localities are: (1) Gardvik, Ørstafjorden; (2) Flåskjær; (3) Nordre Vartdal; (4) Tverrelva, Barstadalen; (5) Litlekoppen, Ytre Standal; (6) Tryttesvora and Seljesvora, Hjørundfjorden; (7) Vellesæterdalen; (8) Sunnylvsmoldskreddalen; (9) Korsbrekke, Hellesylt; (10) Fiksdal; (11) Fiksdalstrand; (12) Tomrefjorden; (13) Skorgedalen; (14) Midsund and Stormyr, Oterøya; (15) Eikesdalsvatnet; (16) Sunndalsøra; and (17) Gravem, Sunndalen.

'scree', 'debris slope', 'slope-waste deposits' and 'hillslope (or hillside) deposits'; bedded colluvium is often called 'stratified debris slope'. Colluvial depositional systems have typically the form of relatively steep and short fans, or 'cones', often coalescing into aprons. Modern colluvial fans are readily distinguishable from alluvial fans (Fig. 2), also due to the characteristic products of avalanche processes.

Avalanches are rapid gravitational movements of a wet or dry rock debris, snow, or their mixture, occurring on steep slopes. These mass movements are also called 'catastrophic', because rapid often means faster than an escaping human can run and the speed of large avalanches can be as high as $50\text{--}80\text{ m s}^{-1}$ (Voight, 1978). Colluvial avalanches include rockfalls, debrisfalls, debrisflows, snowflows, and possibly also some slides of rock or debris. The individual processes are

defined and discussed further in the text. (This paper suggests that the terms 'debrisfall' and 'debrisflow' be written as single words, for convenience and in semantic analogy to such terms as rockfall, mudflow and snowflow.) A debrisflow or a snowflow rapidly descending a steep slope is said to be *avalanching*, because the massflow behaviour in such conditions tends to be different than on a gentle slope.

The term 'grainflow' refers to a cohesionless debrisflow, possibly dry, whose movement is characterized by pervasive shear and ubiquitous grain collisions (Bagnold, 1954; Lowe, 1976). Not every cohesionless debrisflow must necessarily be a grainflow (cf. Lowe, 1982), for the phenomenon of grain collisions – the defining feature of a grainflow – may be of minor volumetric importance in many such frictional massflows (Nemec, 1990b). This notion is particularly true



TYPICAL CHARACTERISTICS	colluvial fan	alluvial fan
Geomorphic setting:	mountain slope and its base (slope fan)	mountain footplain or broad valley floor (footplain fan)
Catchment:	mountain-slope ravine	intramontane valley or canyon
Apex location:	high on the mountain slope (at the base of ravine)	at the base of mountain slope (valley/canyon mouth)
Depositional slope:	35-45° near the apex, to 15-20° near the toe	seldom more than 10-15° near the apex, often less than 1-5° near the toe
Plan-view radius:	less than 0.5 km, rarely up to 1-1.5 km	commonly up to 10 km, occasionally more than 100 km
Sediment:	mainly gravel, typically very immature	gravel and/or sand, immature to mature
Grain-size trend:	coarsest debris in the lower/toe zone	coarsest debris in the upper/apical zone
Depositional processes:	avalanches, including rockfall, debrisflow and snowflow; minor waterflow, with streamflow chiefly in gullies	debrisflow and/or waterflow (braided streams)
EXAMPLES	 <p>The Brotfonna colluvial fan, Trollvegen near Romsdal, Norway; one of the world's largest colluvial fans, with a height of 830 m and a plan-view radius of 1.5 km.</p>	 <p>The Badwater alluvial fan, eastern side of Death Valley, California; a modest fan, with a radius of c. 6 km.</p>

Fig. 2. A comparison of the distinctive features of colluvial fans and alluvial fans.

for relatively thick, arenitic sandflows, which often carry 'floating' cobbles or boulders. As pointed out by Middleton & Southard (1978, chapt. 8), 'the idea that grainflow alone is responsible for the emplacement of thick, massive beds of sand ... can only have been based on a misunderstanding of Bagnold's theory'.

Some authors have considered 'avalanche' to be a specific type of mass movement, different from rockfall, debrisflow or slide (e.g. Selby, 1982, 1994; Cas & Wright, 1987). However, the definitions offered are quite odd, suggesting a mechanism analogous to Bagnoldian grainflow and depositional features similar to those of rockfalls and many cohesive debrisflows. Likewise, some authors have oddly restricted the term 'avalanche' to snowflows only. The reader should also be aware that many colluvial avalanches, including rockfalls and debrisflows, have been described under the misleading label 'landslide' – which in geomorphology means little more than a mass movement.

The descriptive terminology for gravel characteristics, including clast fabric notation, used in the present study is after Harms *et al.* (1975) and Collinson & Thompson (1982). The fabric notation uses symbols *a* and *b* to denote the long and intermediate axes of the clast, indices (t) and (p)

refer to the axes orientation transverse or parallel to flow direction, respectively, and index (i) indicates axis imbrication.

DEPOSITIONAL SETTING

The Møre-Romsdal region (Fig. 1) is representative of the postglacial development and geomorphic conditions in western Norway. The region has a rugged topography, with mountain peaks of up to 1800 m, rolling plateaux, glacial cirques, large valleys and deep fjords. The bedrock, chiefly Precambrian gneisses, is strongly fractured and weathered, but has been eroded by glaciers and its primary weathering cover is thus thin and irregular. The NE topographic trend of the main valleys and fjords is related to the Møre-Trøndelag Fault Zone, an early Mesozoic offshore lineament that impinges onto the Scandinavian landmass in the region (Gabrielsen *et al.*, 1984). Other fjords and valleys, trending NW or NNW, are related to an older fault system that has been reactivated in Mesozoic times and parallels the Jan Mayen Fracture Zone (Aanstad *et al.*, 1981).

The region was covered by the Scandinavian ice-sheet during the last-glacial (Late Weichselian) maximum, when the floors and slopes of the

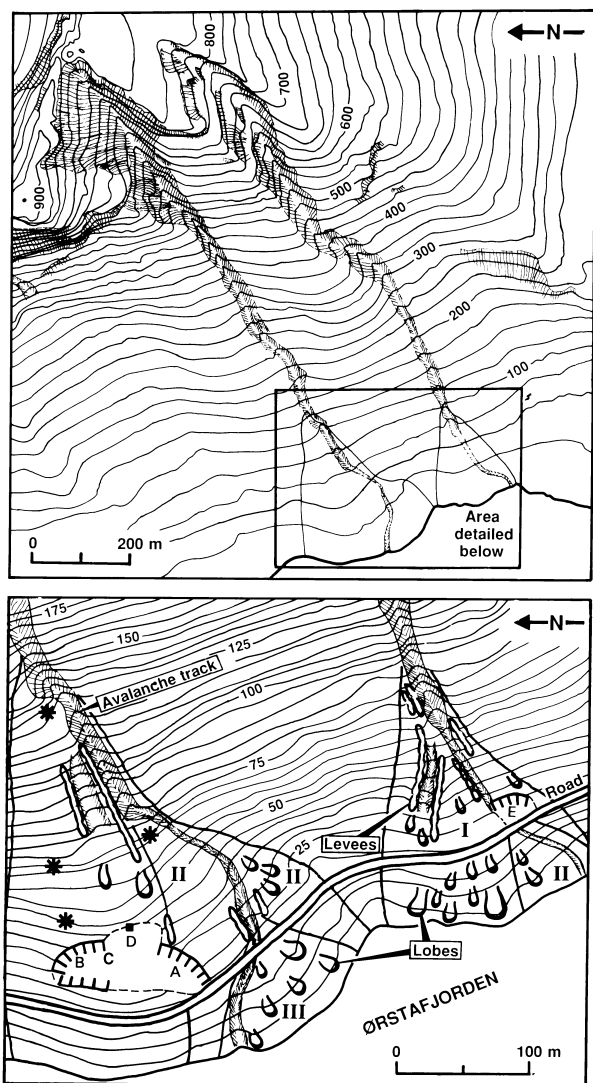


Fig. 3. Map showing the geomorphic setting and morphometry of two colluvial-fan deltas at Gardvik (locality 1 in Fig. 1). Note that the successive lobes (I–III) of the now-emerged fan deltas were built at progressively lower relative sea level. The fan surfaces show numerous debrisflow lobes and levées, and some fresh snowflow deposits (asterisks). Letters A–E denote outcrop sections in the gravel pits.

mountain valleys were mantled with glacial till. It is uncertain whether the highest peaks protruded above the ice-sheet, as nunataks (Sollid & Sørbel, 1979; Nesje *et al.*, 1987; Follestad, 1990; Larsen *et al.*, 1995). The region was deglaciated, from the outer coast progressively to the south-east, between *c.* 13 000 and 10 000 years BP (Mangerud *et al.*, 1979; Mangerud, 1980; Fareth, 1987; Larsen *et al.*, 1991). Since then, the glacial till and local kame terraces, perched on the valley sides, have been subject to erosion and intense resedimenta-

tion by gravitational processes, resulting in arrays of colluvial fans, solitary (Fig. 3) or coalescing into aprons (Figs 4 and 5). Many of these have prograded into deep-water fjords, forming colluvial-fan deltas (Figs 3 and 5D).

Studies of the Holocene glaciers in western Norway have indicated that the postglacial climate fluctuated considerably (Nesje & Kvamme, 1991; Matthews & Karlén, 1992; Nesje & Dahl, 1993; Dahl & Nesje, 1994; Nesje *et al.*, 1995). For example, a major climatic deterioration occurred near the end of the deglaciation phase, in the Younger Dryas time (*c.* 11 000–10 000 years BP), when the shrinking ice-sheet re-advanced (Fig. 1) and local alpine glaciers developed (Reite, 1967; Larsen *et al.*, 1984). The Younger Dryas climate was cold-oceanic (Larsen *et al.*, 1984) and caused a marked increase in avalanche processes (Blikra & Nemec, 1993a; Nesje *et al.*, 1994a; Blikra & Nesje, 1997).

The present-day annual temperatures at sea level range between 12 and 14°C (July) and $\pm 1^\circ\text{C}$ (February), averaging 6–7°C. On higher mountain slopes, the mean annual temperatures are lower, ranging between 2°C and -4°C , respectively. The mean annual precipitation is between 1500 and 2200 mm at sea level and even greater at higher altitudes. The snow accumulation potential is greatest on mountain slopes facing the SE, E and NE, due to the prevalent winds in these directions. Modern avalanches abound, many reaching the shoreline and causing considerable damage to the local vegetation and roads (Lied, 1989), with occasional loss of human life.

The region has a well-established curve of postglacial relative sea-level changes (Svendsen & Mangerud, 1987, 1990), which is used as a palaeogeographic reference framework in the present study. The postglacial isostatic uplift has considerably exceeded the eustatic sea-level rise, resulting in a relative sea-level fall by 50–80 m and gradual emergence of the colluvial-fan deltas (Figs 3 and 5D). Modern human activity, with numerous roadcuts and gravel pits, has created good outcrops of the colluvium.

COLLUVIAL PROCESSES AND FACIES

The colluvium is associated with bedrock mountain slopes of 35° to 50°. The slopes have varied morphometric profiles, with local inclinations from 25–30° to as much as 70–90°. The colluvial fans and aprons that abut these slopes are steep, although their surface inclination depends upon

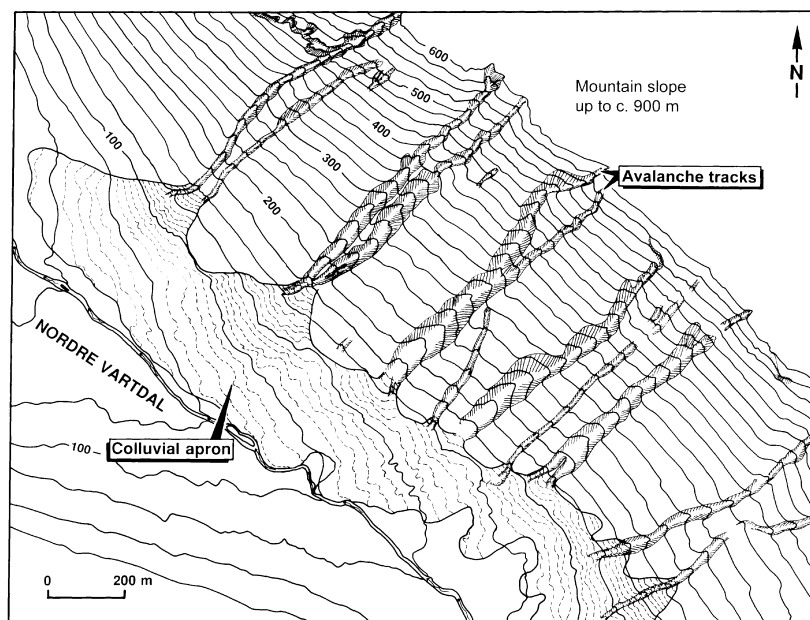


Fig. 4. Map showing the geomorphic setting and morphometry of a subaerial colluvial apron in Nordre Vartdal (locality 3 in Fig. 1). Note that this valley-side apron is an array of coalesced colluvial fans.

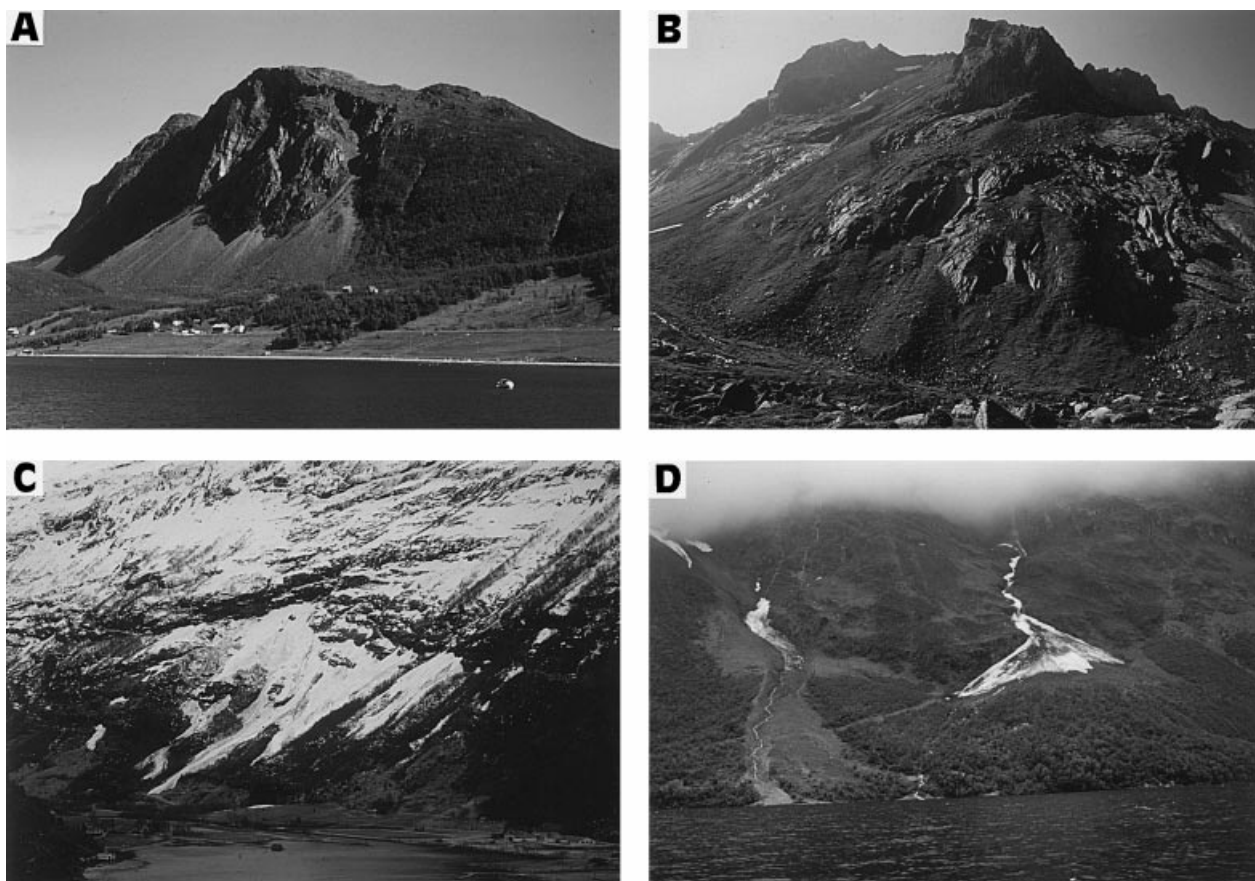


Fig. 5. Examples of colluvial systems in the study area: (A) coalescent colluvial fans dominated by rockfalls, in Oterøya; (B) a valley-side colluvial apron formed by debrisflows, rockfalls and subordinate snowflows, at Litlekopen; (C) coastal colluvial apron dominated by snowflows, in fjord-head area at Korsbrekke; and (D) coalescent colluvial-fan deltas dominated by snowflows, at Eikesdalsvatnet. Photographs from late spring 1992; for localities, see Fig. 1.

SEDIMENTARY FEATURES	DEPOSITIONAL PROCESSES			
	rockfall/debrisfall	debrisflow	snowflow	waterflow
TYPE/GEOMETRY OF DEPOSITS	Fresh rock debris Resedimented gravel Upslope fining Varied runout Scattered clasts Lobate or "patchy" accumulations of debris; scattered large "outrunners"	High-viscosity debrisflow Relatively broad lobes Levées Spill-over lobes Highly elongate, tongue-shaped lobes (upslope fining!)	Low-viscosity/watery debrisflow Toolmark grooves "Debris horn" Longitudinal grooves, debris ridges & clast-thick levées One clast-thick levée Small "digitated" lobe with frontal wash-out sand "Pachy" lobes Scattered clasts Drier snowflows Slushflow	Waterflow Levées of bypassing debrisflows Overbank sand Narrow, gully-type channels; or shallow channels with braid-bars
three-dimensional view				
vertical cross-section	Upward fining Openwork Infilled by "tail"	Tabular beds Large "floating" clasts	Indistinct boundaries Melt-out clasts in precarious positions Stratified waterlain infill of larger interstices Redeposited humic soil Waterlain infill	Remnant debrisflow deposits Tractional infill Isolated channel-fills (up to 1.5 m thick)
TEXTURE AND STRUCTURE	Highly immature debris; mainly angular clasts Boulder to sand size grade. Clast-supported and commonly openwork, with pebbly to sandy infill at the top. Deposits often infilled with waterlain sand and/or redeposited soil material.	Matrix-rich to clast-supported. Sandy/muddy matrix. Common "coarse-tail" inverse grading and outsized cobbles or boulders.	Unsorted, scattered clasts and gravel "patches" infilled with waterlain sand or pebbly sand. The sand in large interstices shows stratification, but is massive, very fine/silty and possibly shell-bearing in submarine deposits.	Clast-supported, pebbly to cobbly gravel interlayered with poorly sorted/stratified sand. Matrix-supported gravel occurs as debrisflow remnants.
CLAST FABRIC	Boulders and large cobbles often show "rolling" fabric, $a(t)$ or $a(t)l(i)$, when emplaced frontally in isolation. Many large clasts upslope show "sliding" fabric $a(p)$, but a disorderly "adjustment" fabric predominates; "shear" fabric $a(p)$ often typifies the avalanche's overriding tail, when evolved into a grainflow.	Large clasts mainly aligned downflow, $a(p)$ or $a(p)l(i)$, but showing $a(t)$ orientation along the lobe front.	Mainly disorderly (chaotic "melt-out" fabric). Boulders and cobbles deposited from turbulent snowflows may have "rolling" fabric $a(t)$, but the scattered debris is vulnerable to rotation by subsequent avalanches. Dense snowflows and slushflows may create "shear" fabric $a(p)$, but this loses order during the melt-out.	Common tractional fabric; poorly developed in gullies due to clast pivoting and adjustment to banks. Many large clasts are rotated <i>in situ</i> to $a(p)$ position by less competent waterflow.
DEBRIS SOURCE	Weathered bedrock. Glacial till and valley-side kame terraces.	Glacial till, kame terraces and upper-slope colluvium.	Glacial till and upper-slope colluvium, including fresh bedrock. Common slope-soil erosion.	Upper slope colluvium and glacial till.

Fig. 6. Summary of the main depositional processes and facies of colluvial fans/aprons, with special reference to the postglacial colluvium in western Norway.

the depositional processes. Fans dominated by rockfalls are generally much steeper and shorter than those formed by debrisflows, whereas fans dominated by snowflows have intermediate gradients. Fan slope depends also upon the prevalent avalanche size and headwall characteristics (Blikra, 1994). The steepest fans have slopes of 43–45° (apex) to 20–30° (toe) and the least steep fans, 30–36° to 5–15°, respectively. Fans dominated by waterflow processes, or long-runout snow avalanches, are no steeper than 13–15° and morphometrically transitional to common alluvial fans.

The main depositional processes responsible for the development of the colluvial systems are summarized in Fig. 6 and discussed in the following sections. The review combines general knowledge with our field observations and gives the genetic facies criteria used in the present study.

Rockfall avalanches

Rockfall is a gravitational movement of a mass of fragmented bedrock liberated abruptly from a cliff

or steep headwall, whose components tumble freely downslope by rolling, bouncing and sliding; or it may be an analogous movement of a solitary rock fragment. The rock debris is characteristically angular, very immature. Large blocks often disintegrate upon impact, spawning smaller clasts. Rockfalls have been studied extensively (Kent, 1965; Bjerrum & Jørstad, 1968; Carson & Kirkby, 1972; Whalley, 1984; Statham & Francis, 1986; Selby, 1994).

In a rockfall, clasts move through a series of impacts on the colluvial slope, which may retard the clast, accelerate it, or stop it instantly. Factors that control the runout of a falling clast include clast size (weight) and shape and the gradient and roughness of the slope surface (Parsons & Abrahams, 1987). Slope roughness is considered in terms of the ratio of the diameter of the falling clast to the diameter of the clasts resting on the slope. Clasts roll down easier on relatively smooth, low-roughness slopes.

The mobility of a rockfall avalanche depends also upon the amount of the debris involved. Colluvial fans formed by larger rockfalls are longer and less steep (Statham & Francis, 1986).

In a voluminous rockfall, the interacting clasts tend to exchange and share their momentum, in a manner similar to that prevailing in a grainflow (Bagnold, 1954; Lowe, 1976; Campbell, 1990; Campbell & Brennen, 1983, 1985). However, the concentration and collision frequency of clasts in a rockfall are lower than in a grainflow, which renders the larger clasts relatively free to move downslope and segregate according to sizes (Campbell & Gong, 1986; Savage & Hutter, 1991). The heavier the clast, the greater its momentum, whereby large clasts tend to move faster and outpace the smaller ones. The tongues of rockfall gravel thus show a marked downslope coarsening and a corresponding increase in surface roughness (Figs 6 and 7). The downslope part of a rockfall deposit is typically openwork, composed of boulders and large cobbles, often with some blocks scattered further downslope as 'out-runners'. The upslope part is thinner, comprised of finer gravel and often infiltrated with granule sand.

In a rockfall avalanche, the faster-moving large clasts usually come to rest first, and the trailing mass of finer debris then overrides this frontal deposit, resulting in an apparent normal grading (Fig. 6). When a series of rockfall avalanches descend the slope along the same track, one after the other, the effective runout of the successive avalanches may be shortened, resulting in an overall upward coarsening (Statham & Francis, 1986; Parsons & Abrahams, 1987; Nemec, 1990b, fig. 11).

The role of clast interactions in a rockfall avalanche increases with the volumetric concentration. The collisional stress component becomes dominant when the concentration of clasts

exceeds *c.* 18 vol.% (Campbell, 1989a), at which point the rockfall regime turns into the shear-flow regime of an avalanching grainflow (Nemec, 1990b, fig. 9). This type of dynamic transformation is common in the finer-grained 'tails' of rockfall avalanches (Bolt *et al.*, 1975; Hsü, 1975; Wasson, 1979; Cruden & Hungr, 1986; Grimstad & Nesdal, 1991; Nemec & Kazancı, 1999).

Rockfall debris is often subject to transient accumulation in a ravine or other slope recess, and subsequently tumbles down as a loose mass once the threshold of frictional yield has been exceeded. Likewise, rockfall gravel that has accumulated in the apical part of a colluvial fan often loses stability and avalanches further downslope as a secondary rockfall, or a debrisflow. The latter may be a grainflow, or a cohesive flow if the fan-head gravel has been illuviated with mud (Nemec & Kazancı, 1999).

Deposits. Colluvial rockfall deposits range from scattered or randomly clustered boulders and cobbles, to distinct, tongue-shaped beds of immature coarse gravel characterized by marked upslope fining, common normal grading and mainly openwork texture (Figs 6 and 7). The openwork texture may be well-preserved (Nemec & Kazancı, 1999), but the gravel in the present case is more often illuviated with sand and mud (Fig. 8). This secondary infill includes soil material rich in plant detritus, derived by contemporaneous slope wash processes. Where emplaced subaqueously, the rockfall gravel is commonly filled with a wave-derived silt or fine sand, possibly bearing fauna shells or their crumbs.

The clast fabric of rockfall deposits is varied. Boulders and cobbles may show a 'rolling' fabric, *a(t)* or *a(t)b(i)*, when emplaced solitarily or as the

Fig. 7. An openwork, bouldery gravel lobe formed by several modern rockfall avalanches, with numerous 'out-runner' blocks, up to 4–5 m long, in the forefront; note the slushflow tongue to the left. Valley-side colluvial apron in Glomsdalen. Photograph by P.A. Hole, from summer 1985.

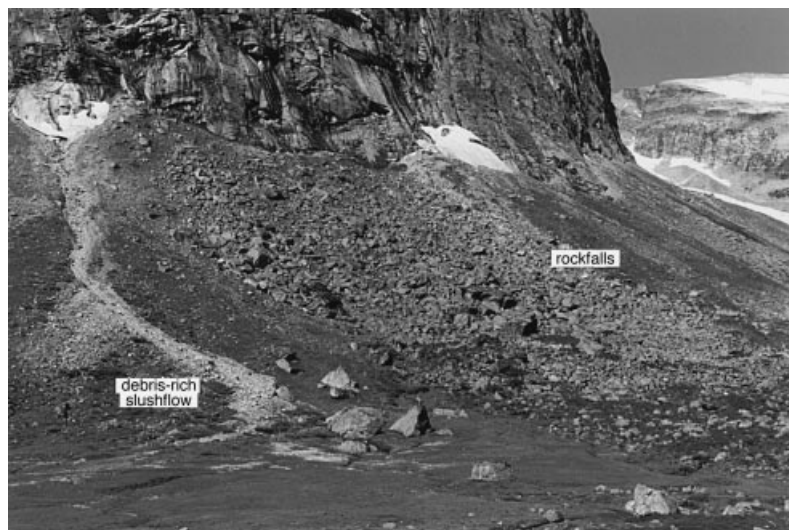




Fig. 8. Detail of a rockfall deposit in vertical outcrop section. The large basal interstices of this immature, openwork gravel have been filled with a stratified muddy sand derived by sheetwash. The lens cap (centre) is 5 cm. Colluvial fan at Midsund (locality 14 in Fig. 1).

frontal elements of an avalanche on a low-roughness slope. However, rockfall clasts generally tend to adjust their resting positions to the static slope debris, are often subject to minor secondary sliding and are vulnerable to re-orientation by subsequent avalanches. Many clasts thus show an $a(p)$ or random orientation, and the overall fabric is disorderly. The fabric in some cases may show weak downslope alignment (Statham, 1973; Pérez, 1989; Bertran *et al.*, 1997), and an aligned fabric $a(p)$ or $a(p)a(i)$ is common in the rockfall 'tails', where the collisional stresses often prevail over the free-rolling motion of the individual clasts.

A typical example of a local colluvial succession relatively rich in rockfall deposits is shown in Fig. 9.

Debrisfall avalanches

Debrisfall (Holmes, 1965) is a process mechanically analogous to rockfall, but involving an older, resedimented gravel, rather than freshly fragmented bedrock, which means debris that is relatively mature, subrounded to well-rounded (Fig. 6). Examples include fluvioglacial gravel falling from a perched kame terrace down the valley-side slope, or a river-derived gravel falling down the steep subaqueous slope of a Gilbert-type delta (Nemec, 1990b). The term 'rockfall' in such cases would be inappropriate and misleading. Although debrisfall is not a separate process category, its distinction from rockfall may be crucial to a sedimentologist, because the difference in maturity has important implications as to

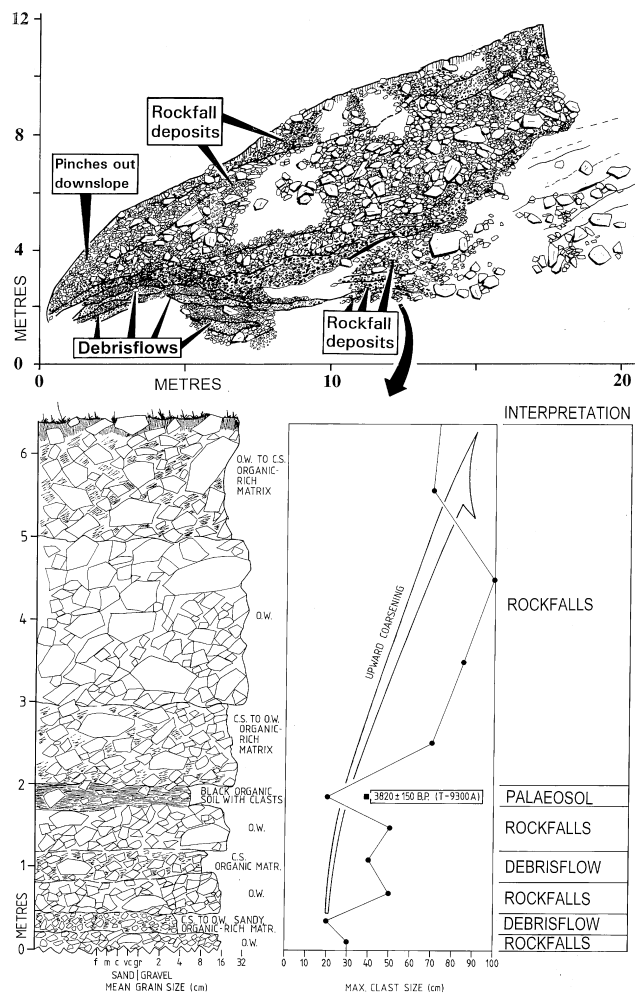


Fig. 9. Portion of outcrop section and detailed log of a colluvial fan dominated by rockfall deposits, at Stormyr (locality 14 in Fig. 1). The log is normal to the bedding. Letter code in the log: CS = clast-supported gravel texture; OW = openwork gravel texture.

the debris provenance, mobility and runoff potential.

In the present case, debrisfall processes are thought to have played a role in the resedimentation of mature glacial gravel from steep mountain slopes. However, the importance of debrisfall deposits in most of the colluvial fans and aprons is minor, compared to that of either rockfall or debrisflow deposits. The relative scarcity of debrisfalls is attributed to the matrix-rich texture of the glacial till, preventing even the coarsest gravel from rolling freely down the slope. The few debrisfall deposits that have been recognized are thought to indicate the local slope conditions where the glacial mantle included a kame terrace or has been strongly eluviated by slope wash. Apart from the roundness and high

apparent maturity of debris, the characteristics of these sporadic debrisfall deposits are similar to those of rockfall deposits (see previous section and Fig. 6).

Debrisflow avalanches

Debrisflows are a common and important agent of colluvial sedimentation in a wide range of climatic zones (Rapp, 1960, 1963, 1987; Voight, 1978; Wasson, 1979; Rapp & Nyberg, 1981, 1988; Keefer & Johnson, 1983; Eisbacher & Clague, 1984; Williams, 1984; Nyberg, 1985; Cruden & Hungr, 1986; Van Steijn, 1988, 1996; Blikra *et al.*, 1989; Brabb & Harrod, 1989; Jibson, 1989; Kotarba, 1991; Nicoletti & Sorriso-Valvo, 1991; Luckman, 1992; Rickenmann & Zimmermann, 1993; Nemec & Kazancı, 1999). In the geomorphological literature, debrisflows are referred to also as 'debris torrents', 'debris slides', 'debris streams', 'debris avalanches', 'grainflows', 'earthflows', 'flowing debris masses', 'lahars', 'landslides', 'mudflows', 'mudspates', 'rock flows', 'rocky mudflows', 'sandflows', 'sand runs' and possibly other names. Both subaerial and subaqueous debrisflows have long been a subject of laboratory and field studies, and the existing knowledge is considerable (Johnson, 1970; Hampton, 1975, 1979; Lowe, 1976, 1982; Brunsden, 1979; Lawson, 1982; McTigue, 1982; Haff, 1983; Savage, 1983; Johnson & Rodine, 1984; Nemec & Steel, 1984; Campbell & Brennen, 1985; Campbell, 1986, 1990; Pierson, 1986; Costa & Wieczorek, 1987; Van Steijn & Filippo, 1987; Van Steijn & Coutard, 1989; Savage & Hutter, 1989, 1991; Nemec, 1990b; Takahashi, 1991).

Debrisflow is a type of sediment-gravity flow, defined as a gravitational movement of a shearing, highly concentrated, yet relatively mobile, mixture of debris and water. In some climatic zones, debrisflows may involve an admixture of snow or slush, as is common on the mountain slopes in Norway. Dry debrisflows are rare in the present case, but common in other climatic settings (Melton, 1965; Oberlander, 1989; Nemec & Kazancı, 1999). A debrisflow may be turbulent, although a subaqueous turbulent massflow is to be classified as a turbidity current (Lowe, 1982).

In rheological terms, a debrisflow is a simple- to pure-shear plastic flow, which means that the granular material tends to spread, behaves like a single-phase fluid and has a finite yield strength. The shear strength derives from a combination of cohesive forces, due to the electrostatic bonds between clay particles, and frictional forces – due

to particle interlocking and the frictional resistance against interparticle slip (cohesion of clay-free silt and fine sand is very low, highly dependent upon water content and considered to be negligible; Kézdi, 1979.) Because one of the two forces usually predominates, debrisflows have been categorized as *cohesive* and *cohesionless* (frictional), respectively (Nemec & Steel, 1984), with the classic mudflow and grainflow as end-member models (Lowe, 1982). This rheological distinction corresponds with the conventional engineering classification of 'soils', or natural clastic materials, into two analogous categories (Kézdi, 1979; Keedwell, 1984).

When the shear stress, or the downslope component of the material's weight, exceeds the yield strength, the material begins to shear and flow, behaving like a dense, viscous fluid. The apparent viscosity of a debrisflow is the 'bulk' dynamic viscosity of the shearing mass, which means the dynamic resistance to shear deriving from the interparticle fluid and the sediment particles themselves. For example, a grainflow behaves like a high-viscosity fluid even when the granular material is dry (Lowe, 1976; McTigue, 1982; Melosh, 1983). In mechanical terms, the apparent viscosity is a dynamic coefficient translating the applied shear stress into the shear-strain rate, and thus controlling the mobility and internal shear regime of a debrisflow, including the possible development of turbulence.

The dynamic viscosity of a debrisflow is necessarily much higher than that of water, but may vary greatly from one flow to another; it may be as high as $c. 10^3$ Pa s (Sharp & Nobles, 1953) or as low as $c. 10$ Pa s (Pierson, 1986). The apparent viscosity of both cohesive and cohesionless debrisflows varies, depending upon the sediment texture and the content of water, or possibly snow. Further, the viscosity in some debrisflows is roughly constant and independent of the shear-strain rate, like in Newtonian fluids, whereas in others it varies with the strain rate like in non-Newtonian fluids. The former case represents the Bingham plastic category and applies reasonably well to cohesive debrisflows (Johnson, 1970; Hampton, 1975, 1979; Brunsden, 1979; Johnson & Rodine, 1984), whereas the latter case represents non-Bingham plastics and applies to cohesionless debrisflows (McTigue, 1982; Haff, 1983; Campbell, 1990), as well as to those watery debrisflows in which the collisional stresses in gravel fraction predominate despite the presence of a fluidal muddy matrix (Bagnold, 1954; Takahashi, 1991).

As the frictional debrisflow accelerates, it dilates and its apparent viscosity increases. The viscosity of such a 'shear-thickening' debrisflow increases typically as a quadratic function of the shear-strain rate (McTigue, 1982; Campbell & Brennen, 1983, 1985; Haff, 1983; Savage, 1983; Takahashi, 1991). A sandflow or sand-rich debrisflow, particularly subaqueous, may commence its movement as a 'shear-thinning' liquefied flow, in which the shear strain makes the sand expel its pore water and becomes lubricated by it, and the apparent viscosity is thus lower at higher strain rate. However, the liquefaction of loose sand is relatively rapid, and the subaqueous massflow may then: (1) cease to move after a few seconds or so; (2) accelerate and turn into a high-density turbidity current (Middleton & Southard, 1984); or (3) turn into a flowslide – a debrisflow that glides on a thin, shearing basal layer (Campbell, 1989b; Nemec, 1990b; see also Bolt *et al.*, 1975; Lang & Dent, 1983; Lang *et al.*, 1989). The undrained conditions required for sand liquefaction are rare on subaerial mountain slopes, but many of the cohesive debrisflows in our study area were probably triggered by a spontaneous liquefaction of the glacial till.

The conceptual rheological framework outlined above has been the basis for the interpretation of debrisflow deposits in the present study. Our observations indicate that the colluvial debrisflows, although derived mainly from glacial till, have shown considerable variation. The glaciogenic mantle was likely heterogeneous, and its water content probably varied greatly on both a local and temporal basis. The surficial part (*c.* 1 m) of the mantle was affected by vegetation and weathering, and the debrisflow sources also included the weathered bedrock and upper-slope colluvium, and possibly local snowpacks.

The debrisflow deposits are pebbly to bouldery gravel beds ranging from matrix- to clast-supported. Matrix varies from a muddy, poorly sorted sand to nearly arenitic sand or sandy granule gravel. The relationship between the bed thicknesses and maximum clast sizes (Fig. 10) indicates that the matrix-rich debrisflows can generally be classified as cohesive and the matrix-poor ones as cohesionless (cf. Nemec & Steel, 1984). The high apparent competence of the colluvial debrisflows (see the *b*-values in Fig. 10) can be attributed to two factors. Firstly, the debrisflows, particularly those poorer in matrix, are likely to have borne an admixture of snow. A dense snow would increase the flow competence, and as the snow melted, the gravel bed thickness would decrease, resulting in an even

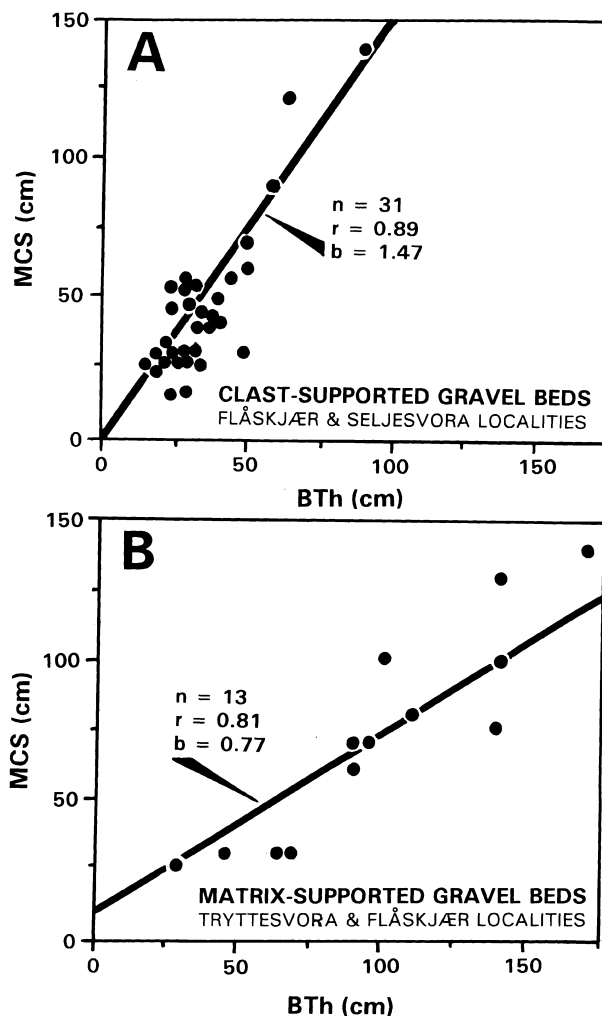


Fig. 10. Relationship between the maximum clast size (MCS) and bed thickness (BTh) of debrisflow deposits, based on data from three colluvial fans. Letter symbols: *n* = number of data; *r* = coefficient of linear correlation; *b* = regression coefficient (gradient of the least-squares regression line).

higher maximum clast size/bed thickness (MCS/BTh) ratio (the data in Fig. 10A are, in fact, from debrisflow deposits of the snowy Younger Dryas period.) Secondly, the colluvial debrisflows descended very steep slopes and were rapid. The downslope component of clast weight on a steep slope would be higher than the slope-normal component, which might effectively delay the clast settling and allow the flow to maintain relatively large clasts over the short descent time.

Furthermore, the geometry of the deposits indicates marked variation in the spreading mode of the debrisflows, even on the same colluvial fan or similar fan surfaces. Some debrisflows have spread as relatively broad lobes, whereas others

Fig. 11. Coalescing debrisflow lobes on the surface of a valley-side colluvial fan in Grasdalen. Note that some of the debrisflows have spread as relatively broad lobes, whereas others have formed elongate tongues. The slope catchment at the present time is prone to snow avalanches, to which the scattered large blocks on the fan surface are ascribed. The short dimension of the photograph is *c.* 350 m and the geographical north is downwards. Aerial photograph by Fjellanger Widerøe A/S.



have formed highly elongate tongues, passing upslope into furrows with levées (Figs 11, 12 and 13). This variation is apparently shown by both cohesive and cohesionless debrisflows, and is thought to represent flows of *high* and *low viscosity*, respectively (Fig. 6). The low-viscosity behaviour is attributed to a relatively high content of water or lubricating slush, whereas the high-viscosity behaviour is attributed to a low water content or an admixture of dense drier snow.

The rheological behaviour of a debrisflow is known to be highly sensitive to relatively minor changes in water content (Pierson, 1980, 1981, 1986; Johnson & Rodine, 1984). When a debrisflow is relatively rich in water and/or slush, its effective shear strength is considerably reduced. For example, Johnson & Rodine (1984; p. 286) noted that the strength of a debrisflow comprising

silty mud and pebble gravel had changed from *c.* 320 Pa at a water content of 14 wt.% to *c.* 40 Pa at a water content of 16.5 wt.%. The shear strength decreased by an order of magnitude with an increase of water content by merely 2.5 wt.%. The density of the mixture had changed from 2200 to 2130 kg m⁻³, respectively, which is a change of *c.* 3% only. The driving shear stress of the debrisflow on a given slope would thus have changed insignificantly, while the apparent viscosity, mobility and internal regime of the flow would be affected quite drastically. On the other hand, a significant admixture of a dry or damp snow, further densified by the load and motions of the host debris, would render the apparent viscosity of a debrisflow very high and result in high apparent cohesive strength (Tusima, 1973; Fukue, 1979; Salm, 1982).

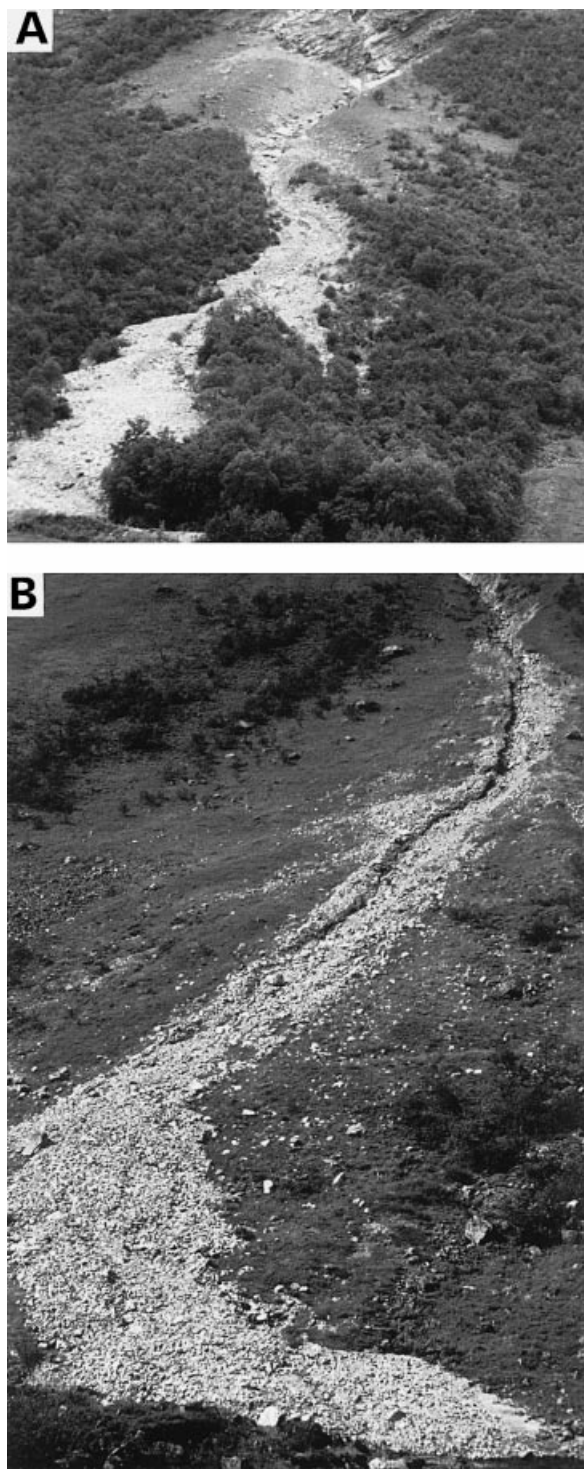


Fig. 12. Fresh deposits of low-viscosity, slush-rich debrisflows on vegetated colluvial aprons in Norangsdalen (near locality 8 in Fig. 1). **(A)** Note the 'digitated' shape of this elongate lobe, due to the lateral splays; the slope height is *c.* 100 m. **(B)** Note the elongate, tongue-like geometry of this lobe, with a relatively thick, coarser 'head' and thinner upslope 'tail'; the latter passes upslope into an erosional furrow with levées; the slope height is *c.* 50 m.

Deposits of high-viscosity debrisflows

The deposits attributed to high-viscosity debrisflows (Fig. 6) are beds of matrix-rich to clast-supported gravel, 0.4–1.7 m thick, which are relatively extensive and tabular on a gravel-pit outcrop scale. They contain 'floating' cobbles or boulders and commonly show inverse grading. The grading in matrix-supported beds is of 'coarse-tail' type, limited to the coarse gravel, and can be attributed to the presence of a 'rigid plug' above the shearing lower part of the debrisflow (Johnson, 1970; Naylor, 1980). The grading in clast-supported beds is more of a 'distribution' type, involving a wider range of clast sizes, and is attributed to clast collisions, with the upward displacement of larger clasts due to dispersive pressure (Bagnold, 1954; Lowe, 1976; Walton, 1983) combined with kinematic sieving (Middleton, 1970; Scott & Bridgwater, 1975; Savage & Lun, 1988; Jullien *et al.*, 1992). The beds of subaqueous debrisflows often show also a weak normal grading at the top (Fig. 14A), probably due to the shear at the flow/water interface (Hampton, 1972). The debrisflow beds in Gilbert-type delta foresets tend to be thinner and have more distinct boundaries (Fig. 15). The MCS/BTh data (Fig. 16) indicate that the competence of subaqueously emplaced debrisflows was generally lower, probably because these more mobile flows were more watery or incorporated water when plunging into the sea (cf. Nemec & Steel, 1984 fig. 23).

The lobate geometry of the debrisflow deposits of this category (Fig. 6) is most apparent on the fresh surfaces of many colluvial fans (Fig. 11). Some of the debrisflow lobes can be traced nearly to the fan apex, where they are thinner, much narrower and often have bouldery levées. Other lobes are more 'detached' from the apex, pinching out upslope in a mid-fan zone. The latter debrisflows have apparently bypassed the steepest fan slope with little or no deposition. Their bypass tracks are shallow scours, with or without levées. Another trace of a bypassing debrisflow are 'debris horns': cusps of debrisflow material accreted onto the upslope sides of large blocks protruding above the fan surface. The high-relief obstacles apparently cause local plastic 'freezing' of a bypassing debrisflow, if not too watery.

The clast fabric in the debrisflow beds of this category is mainly *a(p)* or *a(p)a(i)*, at least for the larger clasts (Figs 14 and 15). The steep fronts of modern debrisflow lobes commonly show an *a(t)* fabric, with large boulders that have apparently

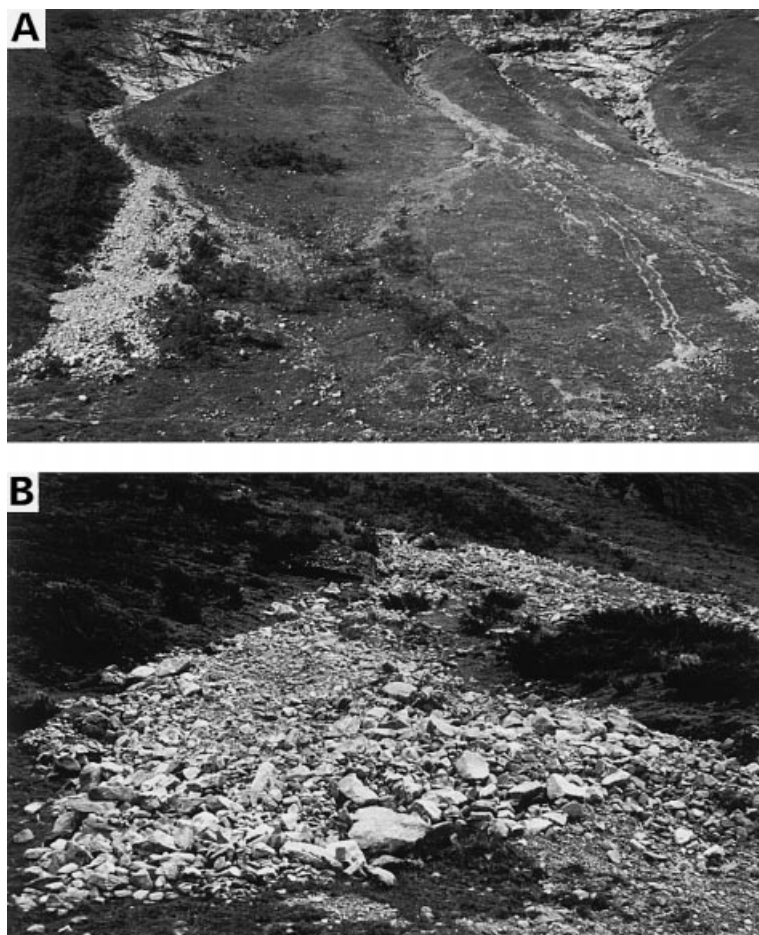


Fig. 13. Fresh deposits of slush-rich debrisflows and snowflows on vegetated colluvial aprons in Norangsdalen. (A) Note the 'digitated' lobe of a slushy debrisflow to the left; the levéed narrow tracks and small, 'digitated' debris lobes of slushflows to the right; and the scattered and 'patchy' debris deposited by snowflows in the lower middle; this colluvial apron's height is *c.* 50 m. (B) Frontal part of a lateral 'spill-over' lobe of a watery debrisflow, showing mainly 'rolling' clast fabric and common imbrication (flow towards the viewer); the main lobe has spread to the right (see in the background).

rolled down the front or been 'bulldozed' by it. These frontal features, however, are seldom recognizable in the outcrop sections of older debrisflow deposits. Likewise, the individual beds show little or no downslope change in clast size within the limits of a large gravel-pit outcrop, although the deposits of apparently similar debrisflows on modern fan surfaces often show downslope thinning and fining (Mears, 1980; Statham & Francis, 1986). It is possible that the latter trend occurs on a lateral scale larger than that of a gravel pit, for the debrisflow beds are, in fact, often thinner and finer grained (in terms of MCS) in the downfan outcrops. However, this apparent trend may reflect the greater spreading (smaller thickness) and lesser competence of the more mobile debrisflows.

Deposits of low-viscosity debrisflows

The deposits attributed to low-viscosity debrisflows (Fig. 6) typically include an erosive, furrow-like track with levées and a highly elongate,

coarse-fronted gravel lobe in the downslope depositional zone (Figs 12, 13, 14B, 17 and 18). The watery or slushy debrisflows are more sensitive to the slope topography, and their tracks often show bends. The tongue-shaped gravel lobes are characterized by a relatively thick, clast-supported, bouldery to cobbly 'head' that passes upslope into a thinner, fine cobbly to pebbly, clast- to matrix-supported 'tail'. There is little visible difference between the subaerial and subaqueous deposits of this category. In the flow-parallel outcrop sections, these debrisflow lobes are recognizable as long, but highly asymmetrical lenses, either solitary or multiple. The multiple lenses are often stacked upon one another in an 'imbricate' fashion, dipping upslope, or show a more complex style of stacking, with the successive debrisflow lobes having overridden and overstepped one another to a variable extent (Figs 6 and 14B). The head of the lobe typically shows a tractional $a(t)$ fabric (Figs 12B and 18), whereas the fabric in the tail is more varied; a 'shear' fabric $a(p)$ or $a(p)a(i)$ is common, but



Fig. 14. Debrisflow deposits in outcrop sections. **(A)** Portion of relatively thick, tabular bed of unsorted, matrix-supported gravel attributed to a high-viscosity debrisflow emplaced on the subaqueous slope of a conical colluvial-fan delta; note the coarse-tail inverse to normal grading, with 'floating' cobbles and boulders in the middle part. **(B)** 'Imbricate', lenticular gravel beds attributed to low-viscosity debrisflows emplaced on the subaqueous slope of a Gilbert-type fan delta; note that the debrisflow tongues have clast-supported, bouldery to cobbly 'heads' and a thinner, pebbly, clast-to matrix-supported 'tails'; note also the thicker, more tabular deposits of high-viscosity debrisflows in the lower part. The white ruler is 23 cm. Examples from the colluvial fan-delta complex at Tomrefjorden (locality 12 in Fig. 1).

'rolling' fabric occurs as well, particularly in gravel beds showing normal grading.

Our observations from active fans support the notion that the watery debrisflows are triggered by a rapid melting of slope snowpack (Harris & Gustafson, 1988) or episodes of heavy rainfall (Caine, 1980; Lawson, 1982). The reported velocities of such debrisflows are of the order of a few metres per second. As the watery debrisflow descends a steep slope, the flow accelerates and dilates rapidly, the dispersion of its larger clasts increases and its two component phases – the coarse gravel and the fluidal matrix – tend to behave almost independently. The dynamic regime of the avalanching debrisflow thus approaches that of a debrisfall (Campbell, 1989a;

Nemec, 1990b, fig. 9), with the clast-size distribution and the mean free distance between the large clasts becoming important controlling parameters. The large clasts tend to move downslope according to their own momentum, pushing themselves, or 'streaming' in engineering parlance, through the fluidal finer material to the front of the flow (Suwa, 1988; Nemec, 1990b). A bouldery to cobbly 'head' develops, whose growing thickness, increasing clast concentration and greater internal friction render its speed lower than that of the following 'tail'. The latter is usually turbulent, so long as it retains an abundant interstitial fluid; otherwise, the apparent viscosity rises and suppresses the turbulence. The faster-moving tail continually feeds the head

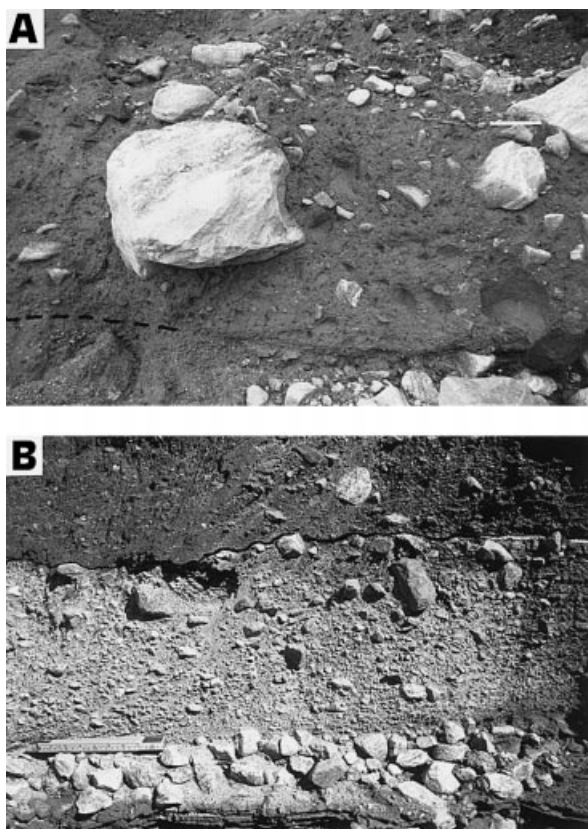


Fig. 15. Details of the subaqueous foreset of Gilbert-type fan delta, Tomrefjorden (locality 12 in Fig. 1). (A) Diamict, mud-rich bed with 'floating' cobbles and boulders, attributed to cohesive, high-viscosity debris-flow. (B) Two beds of matrix-supported gravel, attributed to high-viscosity debrisflows, underlain by a clast-supported gravel unit attributed to subaqueously emplaced, debris-rich snowflows; note the coarse-tail inverse grading in the lower (lighter-shade) debrisflow bed. Transport direction is to the left. The beds are inclined at *c.* 25°, and the photographs are parallel to bedding. The ruler is 23 cm.

with the lubricating fluid, which percolates into the frontal part due to gravity (in conditions promoting such debrisflows, the colluvial slope is usually water-logged; otherwise, the fluid would escape into the porous substratum.) The percolation rate depends upon the size distribution of debris, especially its finer fractions. If the percolation is not too rapid and the head lubrication is effective, the debrisflow may arrive on the lower slope without much change in the internal regime, and the runout may be considerable. When the head of the flow spreads and comes to a halt, its final infilling by the watery tail occurs, often with a thin sheet or multiple fingers of pebbly sand deposited in the forefront by the escaping turbid water. The fronts of slushy

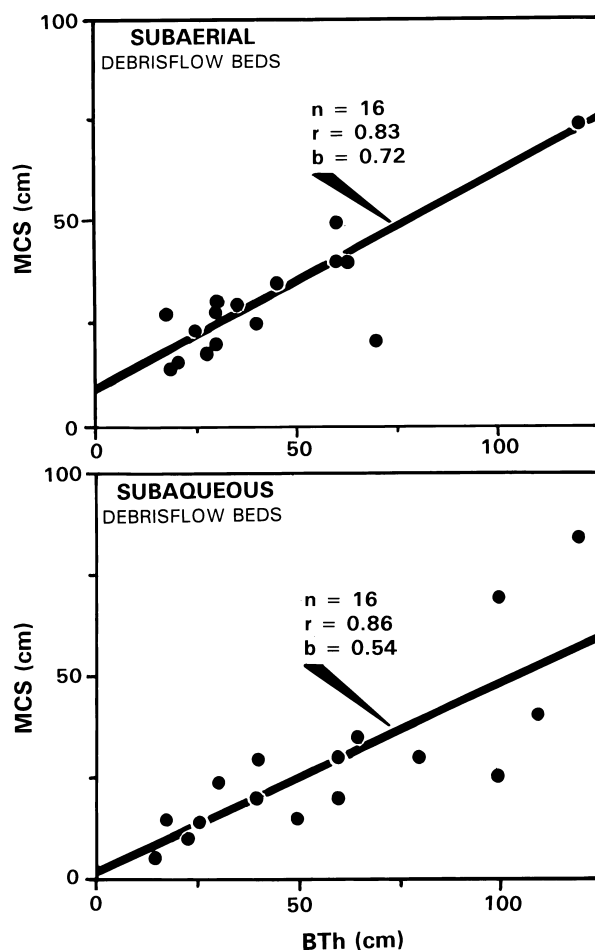


Fig. 16. Relationship between the maximum clast size (MCS) and bed thickness (BTh) of the subaerial and subaqueous debrisflow deposits in a colluvial-fan delta at Eikesdalsvatnet (locality 15 in Fig. 1). Letter symbols: *n* = number of data; *r* = coefficient of linear correlation; *b* = regression coefficient. Note that the *b*-value in the lower diagram is *c.* 25% smaller and the regression line intersects the MCS axis near the zero point, which suggests less competent and cohesionless debrisflows (for methodological details, see Nemec & Steel, 1984).

debrisflows are more 'digitated' due to the postdepositional melting and secondary mobilization (Figs 12 and 13).

The onset of turbulence in a cohesive debrisflow, approximated as a Bingham plastic, occurs when the Hampton number of the flow exceeds 1000, which may mean flow velocity in excess of *c.* 3 m s⁻¹ (Middleton & Southard, 1984). Such velocities can be attained by a debrisflow, even if briefly, on the steep colluvial slope. The more watery debrisflows have lower viscosities and become turbulent much easier, but they are also generally thinner. Vigorous turbulent churning may occur when the Froude number of the flow



Fig. 17. Elongate, tongue-shaped gravel lobes passing upslope into levéed erosive furrows, formed by watery debrisflows on a valley-side colluvial apron in Liadalsdalen (south of locality 2 in Fig. 1); the upslope extent of the avalanche tracks corresponds to the upper limit of the mountain slope's glaciogenic mantle. The width of the picture is c. 250 m. Photograph by O. Longva, from early summer 1991.



Fig. 18. Fresh deposit of a low-viscosity debrisflow on the surface of a colluvial fan in Glomsdalen (upslope view). The tongue-shaped lobe has a bouldery front with transported tree logs, and passes upslope into a narrow, gravel-lined furrow with levées. Photograph by P.A. Hole, from summer 1985.

significantly exceeds 1 (Pierson, 1986), and such supercritical conditions can easily be reached on a steep slope. However, a subaerial debrisflow is unlikely to become fully turbulent, like a New-

tonian fluid, with the large eddies breaking continually down into progressively smaller vortices. Unlike powder snowflows and some subaqueous debrisflows, the subaerial debrisflows do not burst into fully turbulent flows downslope. A watery subaerial debrisflow 1–1.5 m thick may show vigorous turbulence, but can hardly suspend clasts larger than small pebbles (Pierson, 1986), due to the limited scale and highly dissipative character of the eddies. The turbulence may be mixing the debris continuously, but the larger clasts are lifted less, settle faster and segregate from the small ones. The signatures of turbulence in a debrisflow deposit are thus normal grading and possibly a 'rolling' fabric, which are features commonly recognizable in the tails of the colluvial debrisflows. It should be noted that *subaqueous* deposits with such features are to be classified as deposits of high-density turbidity current of (Lowe, 1982).

When the fluidal matrix of the debrisflow percolates into the head and/or substratum too rapidly and the slope is very steep, the tail turns into a frictional debrisflow, possibly still slightly turbulent, where Bagnoldian dispersive stresses may prevail. The energy and frequency of clasts collisions (or the 'granular temperature' of the flow) may be high in a fast-moving, levée-confined flow, whereby the coarser clasts will tend to be pushed inwards and upwards, and be further transferred to the head of the flow in a conveyor-belt fashion (Hirano & Iwamoto, 1981; Johnson & Rodine, 1984; Pierson, 1986; Takahashi, 1991). The tail gravel will be clast-supported, inversely graded and have an $a(p)$ or $a(p)a(i)$ fabric. The head gravel will have an $a(t)$ fabric in the frontal and upper part.

Some debrisflow tails have a matrix-supported, nearly bimodal texture, though otherwise show similar characteristics as mentioned above. The matrix is a poorly sorted sand, often quite muddy. The deposit shows coarse-tail inverse grading and frontal concentration of large clasts, which has been attributed to a combination of dispersive pressure and the conveyor-belt mechanism (Johnson & Rodine, 1984; Takahashi, 1991). However, Bagnold's (1954) theory predicts that the collisions of sand grains result in relatively small dispersive pressure, and the latter also tends to be suppressed by cohesive forces. It is more likely that the large clasts in a shearing sand move away from the margins and lower boundary of the confined debrisflow due to the so-called Magnus effect: a lift force acting normal to the shear boundary and related to the rotation of the large clasts by the local shear-velocity gradient. This effect is thought to occur, for example, in some snowflow avalanches (Hopfinger, 1983).

The low-viscosity colluvial debrisflows are comparable to the watery debrisflows described from mountain ravines and narrow gorges (Okuda *et al.*, 1980; Suwa & Okuda, 1983; Johnson & Rodine, 1984; Pierson, 1980, 1986; Takahashi, 1991). However, the elongate debrisflow lobes in the present case have been deposited on open colluvial slopes of 30° to 5–15°, whereas the ravine-confined debrisflows have reportedly been turbulent and erosive on slopes as gentle as 5–8°. This difference may have two reasons: (1) the colluvial debrisflows are due to slumping of water-logged sediment, rather than to sediment entrainment by flood-water surges; and (2) the mechanism of flow-head lubrication by fluidal matrix may be less effective, or shorter-lived, on very steep, rough and porous colluvial slopes.

The debrisflow tracks are erosive furrows (Figs 12, 13, 17 and 18), widening and shallowing-out in the downslope direction. Their widths, excluding levées, are several times their depth. The depth decreases from 50 to 70 cm in the upper reaches to less than 5–10 cm in the apical part of the associated gravel lobe, which is mainly non-erosive. The furrows are probably scoured by turbulence, but their lower reaches may be ruts of nonturbulent massflow. The levées are due to the plastic 'freezing' of the lateral margins of the flow, where the shear rate is at a minimum (Johnson & Rodine, 1984). These 'dead zones' include cobbles and boulders that have been shouldered aside by the debrisflow front (Pierson, 1986).

The morphology of modern deposits shows that the turbulent tail of a low-viscosity debrisflow

may locally breach the levée and form a smaller, secondary lobe of gravel outside the main track, particularly at a local bend (Figs 6, 12 and 13). The debouching may deplete the parental debrisflow of its lubricating fluidal part and reduce the runout. Our observations further indicate that when the head of a debrisflow 'freezes' and jams the steep descent path, the tail may move sideways, develop a new head and form a secondary lobe further downslope; or the tail may override the halted head and form a new lobe directly in front of it. These secondary lobes are gravelly and their heads may be nearly as coarse as the primary ones (Fig. 13B). When formed on a lower slope, at a relatively late stage of debrisflow evolution, the secondary lobe is relatively thin, composed of sandy pebble gravel, and its head is poorly developed. These characteristics may help to distinguish between the primary and secondary lobes of debrisflows, although the distinction in outcrop sections is not easy.

The subaqueous foresets of colluvial-fan deltas abound in deposits of both high- and low-viscosity debrisflows, associated with the graded beds of sand and pebbly sand attributed to high-density turbidity currents. Turbidity currents can be generated by subaerial debrisflow avalanches plunging into the water (Hampton, 1972; Weirich, 1989). However, the turbidites are much more abundant in the foresets of Gilbert-type fan deltas, whose formation involved streamflow processes, which suggests that the latter were probably more important in generating turbidity currents, by hyperpycnal outflow or mouth-bar collapsing (Nemec, 1990b).

Some illustrative examples of local colluvial successions relatively rich in debrisflow deposits are shown in Figs 19 and 20.

Snowflow avalanches

Snowflows (Fig. 5C,D), also referred to as 'snow avalanches', have been a subject of intense research by glaciologists, geomorphologists and engineers, primarily because these avalanches are a serious hazard in mountainous terrains in many parts of the world. Surprisingly, snowflows have drawn little sedimentological interest, although they are known to carry often abundant rock debris.

The literature on snow avalanches is extensive, but widely scattered in the glaciological and technical journals, special reports and symposia volumes. There are several monographs (Mantis, 1951; Kingery, 1963; Oura, 1967; Perla &

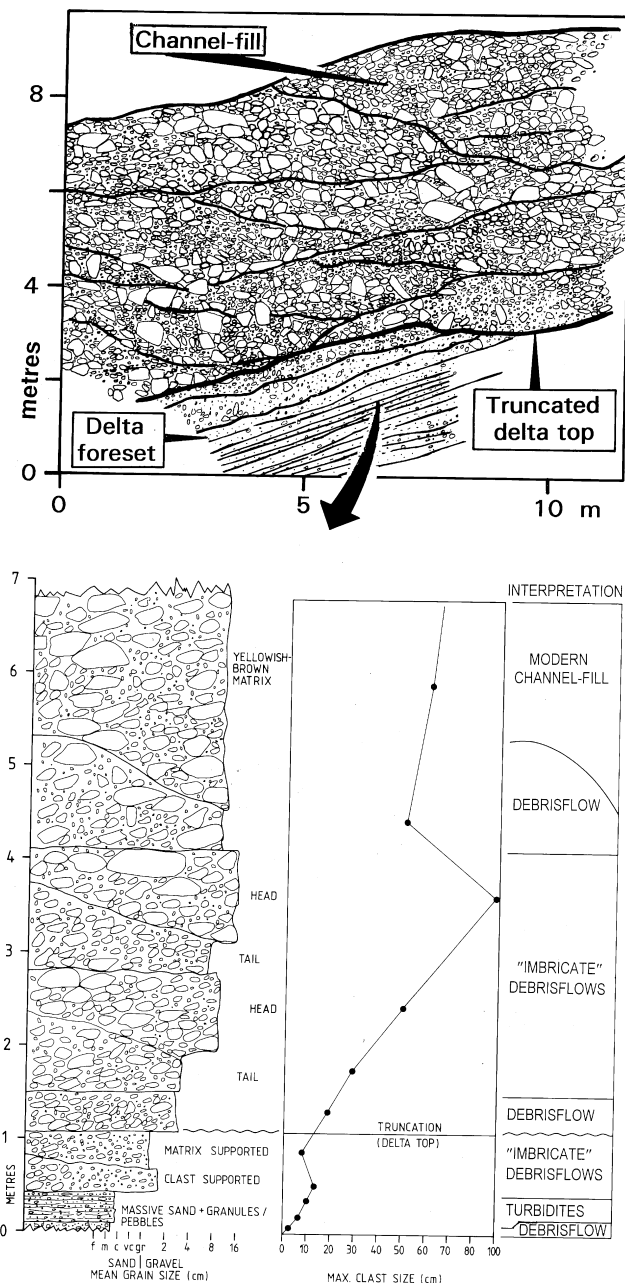


Fig. 19. Portion of an outcrop section and detailed log of the subaerial part of a fan delta rich in debrisflow deposits, Tomrefjorden (locality 12 in Fig. 1). The downslope direction is to the left, and the log is normal to bedding.

Martinelli, 1975; Voitkovskiy, 1977; Fukue, 1979; Washburn, 1979; Colbeck, 1980; Glen *et al.*, 1980; Gray & Male, 1981; Ramsli, 1981); a number of reviews (Luckman, 1971, 1977, 1978; LaChapelle, 1977; Mellor, 1978; Perla, 1980; Schaerer, 1981; Salm, 1982; Hopfinger, 1983); and a wealth of empirical studies (e.g. Dent & Lang, 1980, 1982; Lied & Bakkehøi, 1980; Mears, 1980; Narita, 1980;

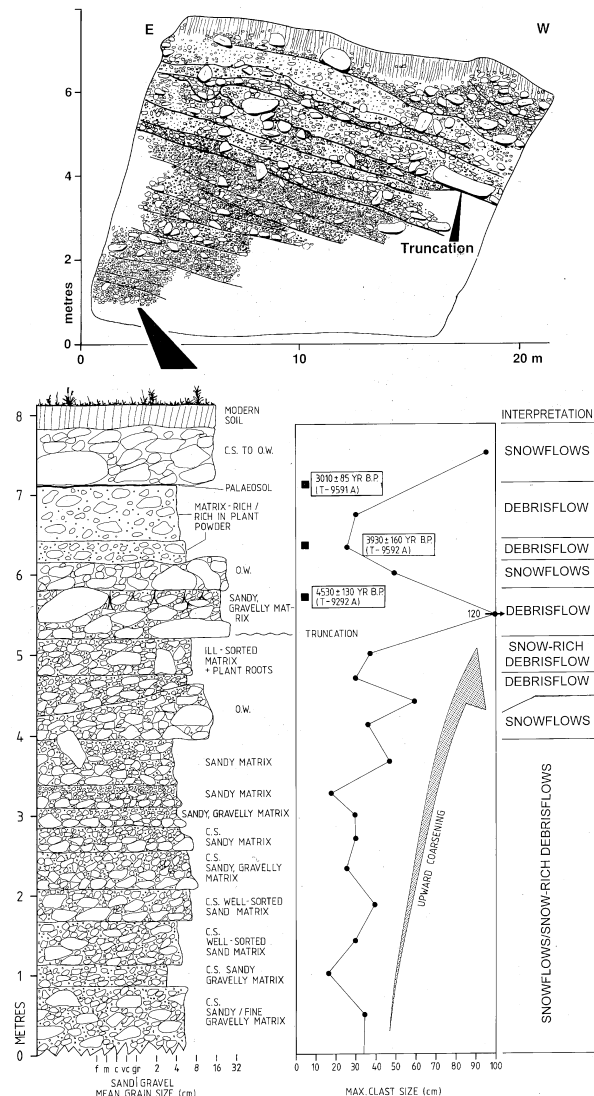


Fig. 20. Portion of an outcrop section and detailed log of the subaerial part of a colluvial-fan delta showing an alternation of debrisflow and snowflow deposits, Flåskjær (locality 2 in Fig. 1). The downslope direction is to the right, and the log is normal to bedding. Note the radiocarbon dates in the log. Texture code CS and OW as in the caption to Fig. 9.

Schaerer & Salway, 1980; Gubler, 1982; Lang & Dent, 1983; McClung & Schaerer, 1983, 1985; Lang *et al.*, 1985; Salm & Gubler, 1985; Hutter *et al.*, 1989; Hermann & Hutter, 1991; McClung & Tweedy, 1993) and various theoretical considerations (e.g. Perla *et al.*, 1980; Bakkehøi *et al.*, 1981, 1983; Dent & Lang, 1983; Norem *et al.*, 1985, 1987, 1989; McClung & Lied, 1988; Gubler, 1989; Gubler & Bader, 1989; Lackinger, 1989; Nishimura & Maeno, 1989; Nishimura *et al.*, 1989). Some publications are focused specifically on slushflows (Washburn & Goldthwaite, 1958;

Nobles, 1966; Washburn, 1979; Hestnes, 1985; Nyberg, 1985; Conway & Raymond, 1993).

The literature on snowflows seems to exceed that on debrisflows, but bears less consensus. The scientific language of the publications varies from the formal terminology of physics to the descriptive parlance of geomorphology, and there seems to be relatively little exchange of results and ideas between the two respective groups of researchers. The following short review attempts to synthesize the diverse views and classifications into a reasonably simple and coherent conceptual framework, which has been the basis of our study of colluvial snowflow deposits. The review refers to the classification in Fig. 21 and focuses on those aspects of snowflow processes that are relevant to a sedimentologist.

Snow rheology

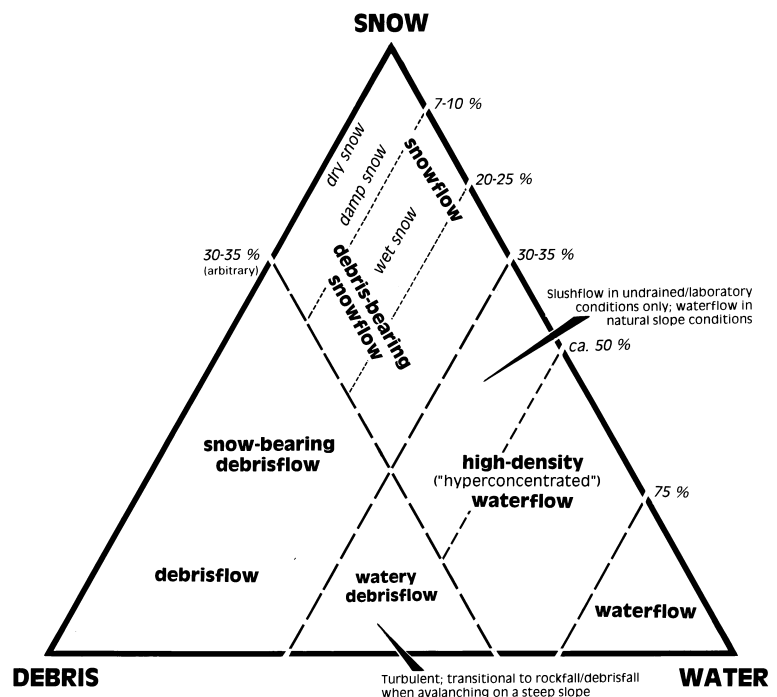
Snow is a peculiar material, with a highly complicated rheological behaviour, although snowflows are generally akin to sediment-gravity flows. On a microscopic scale, snow consists of a framework of ice particles, which may be single crystals or their larger aggregates. The mechanical properties of snow vary with the particle characteristics (size, shape, packing), interparticle bonds (number and type of contacts, pore-wall area) and the spatial arrangement of bonded particles (fabric). Snowpacks are commonly lay-

ered (bedded) and texturally heterogeneous due to their incremental accumulation under variable weather conditions. A fresh powdery snow may contain *c.* 90 vol.% air, whereas an older, compacted and recrystallized snow may be nearly as dense as ice.

In broad terms, snow can be regarded as a plastic material, whose shear strength ranges from mainly frictional to mainly cohesive. However, snow has a high and irreversible compressibility and an equally high thermodynamic instability. The shear deformation of snow is volumetric, rather than purely deviatoric (Salm, 1982), and the content of free water depends on the ambient temperature (Ambach & Howorka, 1966), which renders snow rheologically quite different from all natural clastic materials.

Snow has a high capacity to dissipate stress, by densification. For example, the compaction of snow from an initial density of 300 kg m^{-3} to a density of 900 kg m^{-3} absorbs three times as much energy as its compaction from 600 to 900 kg m^{-3} (Brown, 1980a). Further, the content of water is very important. The free water spreads through the pores by capillary forces, but may begin to percolate through the snow, due to gravity, when the saturation exceeds *c.* 1 vol.% (Langham, 1981). At low, 'pendular' saturations (< *c.* 7 vol.%), the interparticle water film is discontinuous, the snow abounds in air bubbles and is relatively strong, as is common with early

Fig. 21. Tentative classification of the relevant flowing media in terms of the relative proportion of rock debris, snow and water involved. The terminology pertains to subaerial flows. For subaqueous conditions, the solid-laden, high-density waterflow and the turbulent watery debrisflow would be classified as turbidity currents. The class boundaries are based partly on Beverage & Culbertson (1964) and Fukue (1979).



spring snowpacks (Male, 1980). At higher, 'funicular' saturations ($> c. 7\text{--}12 \text{ vol.}\%$), the water film becomes continuous and the snow is relatively weak. When the water saturation exceeds $c. 25 \text{ vol.}\%$, the snow turns into slush (Fig. 21). Saturations of up to $35\text{--}50 \text{ vol.}\%$ have been reported from watery slushflows (Nobles, 1966; Mellor, 1978). In undrained laboratory tests, slush reaches a maximum water saturation of $58 \text{ vol.}\%$ (Nyberg, 1985).

Frictional interparticle forces dominate in fresh *powdery snow* and dry *granular snow*, although cohesive forces are also active in the former: down to a temperature of -5°C in dry conditions and down to -30°C in regelational 'wet' conditions; below these temperatures, a granular snow develops in either case. Cohesive forces predominate in *damp/wet snow*, due to the adhesive effect of free water; in *semibonded snow*, due to the interparticle water films and crystalline bonds; and in *bonded (sintered) snow*, due to the crystalline bonds alone. Sintering occurs at temperatures below the melting point, but the bonds form faster as the temperature nears the latter (Fukue, 1979). The shear strength varies greatly with the snow density, from $c. 10^2 \text{ Pa}$ for a very low-density snow ($\rho \leq 100 \text{ kg m}^{-3}$) to $c. 10^6 \text{ Pa}$ for a high-density snow ($\rho \approx 600 \text{ kg m}^{-3}$). The density of a slushy or densified snow may reach $c. 700 \text{ kg m}^{-3}$, and a strongly sintered snow approaches the density of ice (917 kg m^{-3}). However, a high water content renders snow weaker (Salm, 1982), hence the strength of slush is very low.

As the cohesive strength prevails in some snow varieties and the frictional strength dominates in others, it has been suggested that snowflows be classified into *cohesive* and *cohesionless* (or *frictional*) (Nyberg, 1985). Notably, this rheological distinction is similar to the classification suggested for debrisflows (Nemec & Steel, 1984).

The static angle of internal friction for snow is high, typically in the range of $35\text{--}46^\circ$, and also the dynamic angle of friction for a flowing loose snow is high, $25\text{--}32^\circ$ (Fukue, 1979), comparable to the angle for classic grainflows (Bagnold, 1954). However, the dynamic angle depends strongly upon the shear-strain rate (Fukue, 1979). The dynamic viscosity increases almost exponentially with the density, much stronger for dry than for damp or wet snow (Salm, 1982, fig. 15). For example, laboratory tests show that the dynamic viscosity of a wet snow increases from $c. 10^3$ to $c. 10^6 \text{ Pa s}$ due to a change in density from 700 to 900 kg m^{-3} , whereas a dry snow shows a similar

change in viscosity due to a density increase of less than 10 kg m^{-3} . Rapid rebonding of particles occurs in the failing framework of dry snow, whereas extensive bond slips and particle growth occur in wet snow. The rate of particle growth at an ambient temperature of $+20^\circ\text{C}$ is nearly 50% higher than at 0°C , and the increasing size and decreasing number of the particles and bonds render wet snow considerably weaker (Salm, 1982). Further, the effective stress at the particle contacts in wet snow is significantly reduced by the repulsive electrostatic forces due to the double-charged layers at each solid-liquid interface of the water film separating the particles. These repulsive forces are stronger at low water salinities (Colbeck *et al.*, 1978).

The constitutive relationship between the shear stress and shear-strain rate for snow is generally considered to be nonlinear, with a rate-dependent apparent viscosity, but depends strongly upon the strain rate itself (Mellor, 1978; Fukue, 1979; Salm & Gubler, 1985). The relationship is nearly linear at very high rates (Fukue, 1979), particularly for powdery and granular snows, which is probably why turbulent snowflows are akin to turbidity currents. A dry loose snow at high strain rate shows shear-softening and strong dilation, after the initial collapse of the particle framework (McClung, 1979; Narita, 1980). At lower strain rates, the relationship varies. At a very low rate, snow creeps due to the rupture of interparticle bonds and the localized melting and slip within the ice crystals and their aggregates. The creep is often approximated as a linear viscous deformation (Brown & Lang, 1973; Salm, 1982), although the strain rate decreases with depth, roughly linearly, as the viscosity increases linearly with the normal stress (Desrues *et al.*, 1980; McClung, 1980; Watanabe, 1980). The constitutive relationship is nonlinear once the snow mass has detached itself and flows at a low rate. The viscosity then increases almost exponentially with the strain rate, much faster than the snow's Young modulus, whose increase is nearly linear (Kry, 1975). This is the state of 'brittle' flowage (Fukue, 1979), with the strain breaking and thoroughly reworking the particle framework. Importantly, the shear strain does not dilate the loose snow, but rather increases its density. The snow thus densifies, yet its rheological behaviour is similar to that of dilational grainflow (LaChapelle, 1977). The shear stress/rate relationship has been modelled as a third-order dilation, proportional to the cube of the rate (Brown & Lang, 1973).

The apparent viscosity increases with the strain rate until the microstructure of the snow has been pervasively reworked. The viscosity then shifts to a lower level and remains approximately constant, almost like in a Newtonian fluid. This is the state of 'ductile' flowage (Fukue, 1979), which causes snow hardening in laboratory shear-box tests. On a mountain slope, the flowing snow mass at this point accelerates and its further behaviour may be quite different. For example, turbulence may be ignited in a dry snowflow, which will then rapidly dilate into suspension. Unfortunately, the available empirical data are sparse and often inconclusive, and the existing constitutive models show large discrepancies (Voellmy, 1955; Mellor, 1978; Salm & Gubler, 1985).

For example, Mellor (1978) reported that the shear rate in a purely deviatoric (nonvolumetric) snowflow increased rapidly with the shear stress, which would imply a decreasing viscosity and thus a contractional non-Newtonian behaviour. However, the velocity profiles measured by Salm & Gubler (1985) and Nishimura & Maeno (1989) indicate that the apparent viscosity of relatively dense snowflows remains constant, as in a Bingham plastic flow, but increases (proportionally to the second power or so of the shear rate) in faster flows with greater particle dispersion. This dilational non-Newtonian behaviour would be akin to that of a grainflow.

It would thus appear that the rheological behaviour of snow varies greatly, depending on the snow type and the shear stress level. There is no universal constitutive equation for snow, but rather equations for its behaviour under particular conditions (Salm, 1982). As a convenient simplification, the flow of a relatively dense snow ($> 300 \text{ kg m}^{-3}$) is often considered to be contractional ('shear-thinning'), and the flow of a lower-density snow to be dilational ('shear-thickening'), although these behaviours may change or combine in an evolving snowflow (Brown, 1979, 1980b).

Snowflow types

As snow accumulates on a mountain slope, the normal stress in the snowpack increases with the increasing thickness, or load. Concurrently, the yield strength of the snowpack increases, due to densification. Strong winds may increase the snowpack density, and a wind-blown snow is almost invariably denser than one deposited by freefall. When the stress increases faster than the strength, a gravitational failure occurs. Other

triggering mechanisms include falling cornices and snowpack destabilization by creep. The wind drift of snow is very important, for it affects the snowpack thickness, builds cornices on the lee side of mountain ridges, and fills the mountain ravines and gullies with thick snowpacks that may later obstruct runoff.

Snow typically fails on slopes of $30\text{--}40^\circ$, but a wet snow can fail on a surface of 10° , if relatively smooth or icy. The snowpack may slough by a series of small retrogressive failures, or collapse *en masse* as an avalanche (Perla, 1978). Two types of snowflow avalanche can be distinguished, with possible intermediate varieties (Hopfinger, 1983).

Dense snowflows. Cohesive or other dense snow is usually subject to a line failure, leading to a translational slide. A broad slab of shearing snow then descends the slope, leaving well-defined crown and flank scarps in the snowpack. The result is a dense snowflow, also called 'flowing avalanche [Ger. *Fliesslawine*]' or 'granular-snow gravity flow' (Hopfinger, 1983). These snowflows may be cohesive or cohesionless, and range from pseudolaminar to turbulent. The snow involved may be a dry granular or sintered snow, a damp granular or semibonded snow, a wet granular snow, or a slush. A hard snow slab (sintered or semibonded) may resist fragmentation, and the avalanche may carry large snow blocks to the depositional area (Fig. 22C). If fully fragmented, the avalanche will consist of gravel-sized hard clods mixed with a granular or powdery snow (Fig. 22B, 3A). Cohesive snow allows 'snowrollers' (snow balls) to form and break repeatedly.

Dense snowflows are comparable to debrisflows, and are rheologically modelled as cohesive or cohesionless plastics (Salm & Gubler, 1985; Lang *et al.*, 1989; Nishimura & Maeno, 1989), or a viscoelastic material (Voellmy, 1955; Mellor, 1978; Salm, 1982) in the case of very slow movement. Their steep-fronted depositional lobes and levéed tracks (Figs 22A & B, 23A and 24) are similar to those of debrisflows. In fact, slushflow was originally defined as 'a mudflow-like flowage of water-saturated snow' (Washburn & Goldthwaite, 1958). However, the snowflows have shear-dependent viscosity and behave more like non-Bingham plastics (Lang & Dent, 1983; Lang *et al.*, 1985). In a flow of roughly constant density (say, $c. 400 \text{ kg m}^{-3}$), the snow hardness may range over an order of magnitude and the kinematic viscosity may vary from $c. 400$ to $c. 2500 \text{ m}^2 \text{ s}^{-1}$ (Maeno *et al.*, 1980; Lang *et al.*, 1985).

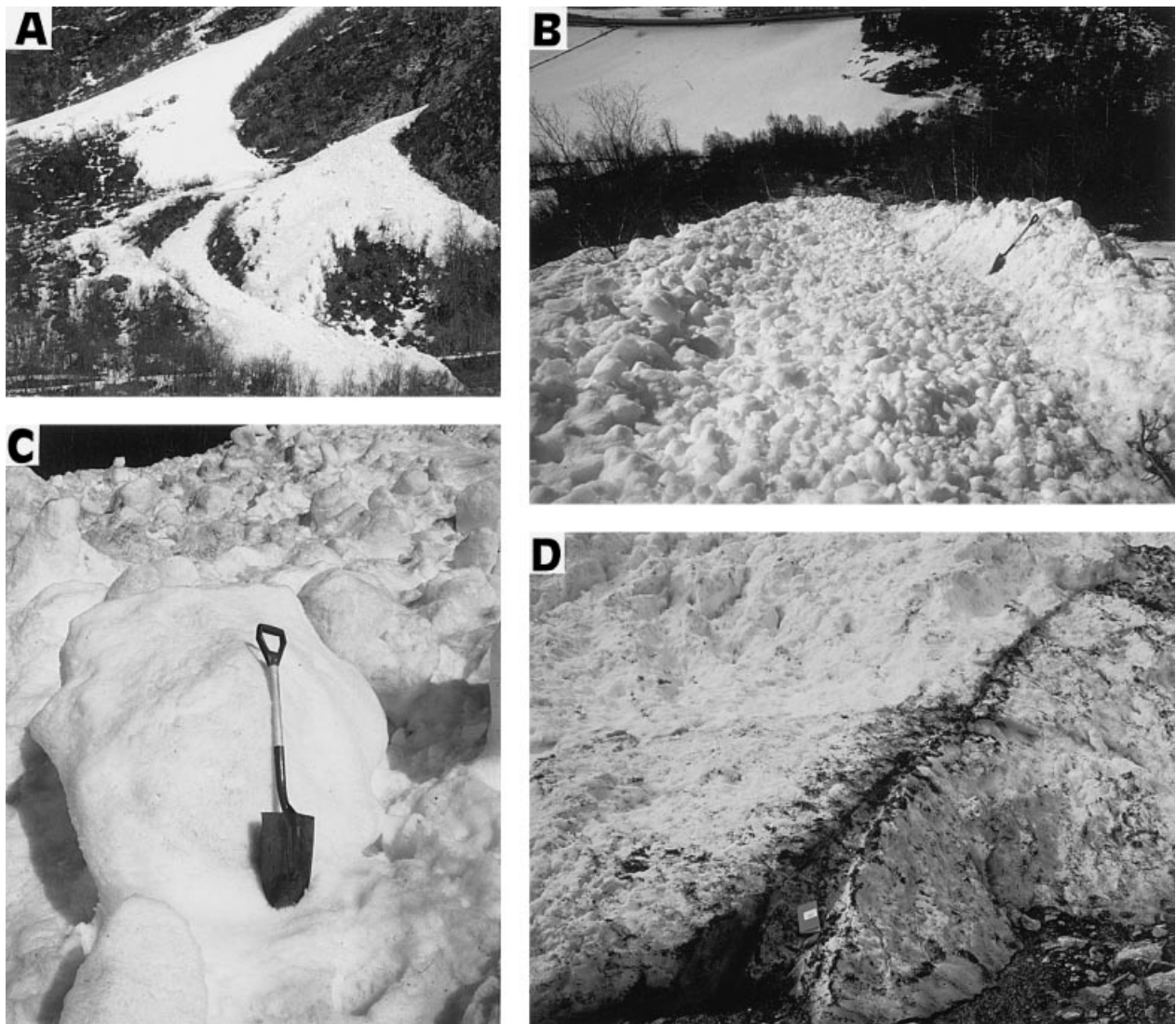


Fig. 22. Features of fresh snowflow deposits. (A) Dense snowflow lobes on a colluvial fan at Gravem (locality 17 in Fig. 1), spring 1993. (B) Snowflow deposit composed of pebble- to boulder-sized, hard snow clods mixed with a powdery snow entrained *en route* by the avalanche; note the levée to the right (downslope view, shovel for scale); Gravem, spring 1993. (C) Large, hard snowballs at the surface of a melting snowflow lobe; Gravem, spring 1993. (D) Longitudinal shear zone, rich in meltout debris, in the lateral part of a dense snowflow lobe; Hjørundfjorden (locality 6 in Fig. 1), spring 1988.

The dense snowflows on mountain slopes have typical velocities of $10\text{--}30\text{ m s}^{-1}$ and are mainly supercritical ($Fr > 1$). The mean density ranges from $c. 150\text{ kg m}^{-3}$ for damp snow to $c. 350\text{ kg m}^{-3}$ for wet or hard snow (Mellor, 1978), and the snow particle concentration is typically in the range of 33–44 vol.%. These snowflows are ‘ground avalanches’ (Hopfinger, 1983), with the lower boundary cut at the ground surface or deeply in the snowpack.

Dense snowflows often arrive on the lower slope by turning into flowslides: the flow ‘freezes’ plastically from the top downwards, but

keeps gliding on a thin, shearing basal layer; and when the front brakes, the snow mass deforms by means of discrete listric thrusts and longitudinal shear zones (Salm & Gubler, 1985). The resulting longitudinal and transverse shears/ridges (Fig. 22D, 23A; Mears, 1980, figs 6, 7 & 8) resemble those observed in debrisflows that have completed their movement in a sliding fashion (Nemec, 1990b, figs 28, 29 & 30). Slushflow can move on a smooth slope of less than 2° (Nobles, 1966), but stop on a rough, bouldery slope of more than 70° (Luckman, 1971) (Fig. 24).

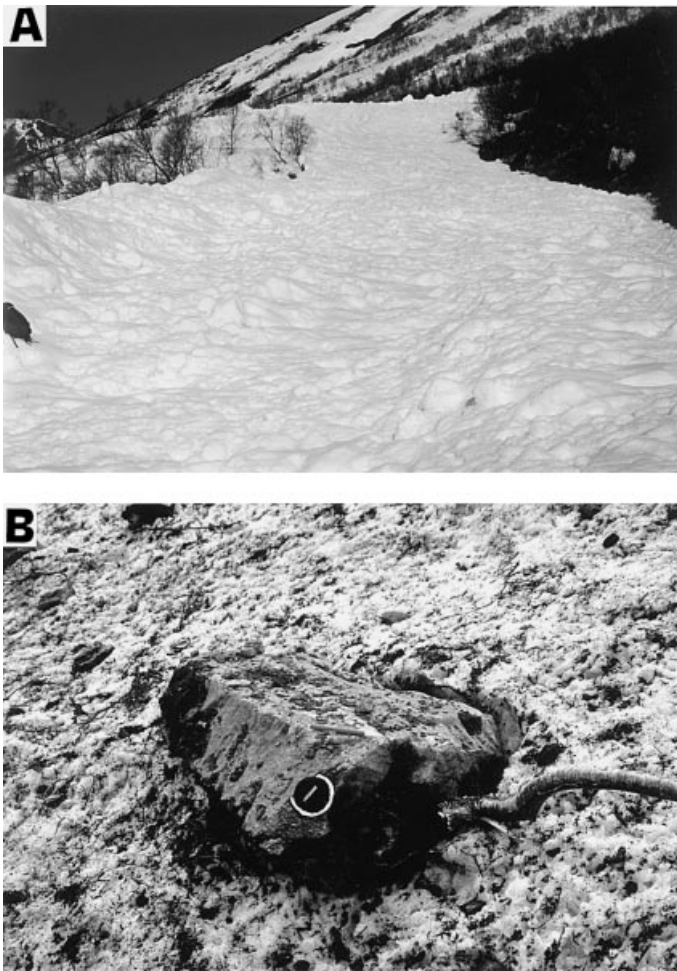


Fig. 23. Features of fresh snowflow deposits on a colluvial fan at Bøndergerde, Skorgedalen (locality 13 in Fig. 1). (A) Upslope view of the upper part of a dense snowflow lobe, showing large axial furrow, levées and transverse listric shears; the furrow was scoured by younger, bypassing snowflows. The backpack to the left is *c.* 50 cm long. (B) Rock boulders, an uprooted birch tree, numerous broken branches and abundant finer debris melting out at the surface of a dense snowflow lobe; the lobe at this stage is still *c.* 3 m thick. The lens cap is 5 cm. Photographs from late spring 1993.

Powder snowflows. A fresh, powdery snow or a loose older snow that has lost cohesion (dry granular snow) is usually subject to a point failure, which quickly expands. The term 'powder snowflow' is used here broadly for such low-density snowflows, composed partly or entirely of powdery snow and most often turbulent. These snowflows come to rest on slopes ranging from 34° to horizontal, but most commonly on those of 17–28° (McClung & Schaerer, 1983). The turbulent snowflows, also referred to as 'airborne snow avalanches' (Hopfinger, 1983), have generally longer runouts.

A turbulent cloud typically develops at the top of a powder snowflow and grows at the expense of the latter. The entrainment of dry snow by the ambient air begins when their relative velocity reaches *c.* 7 m s⁻¹, and the turbulent cloud becomes fully developed when the velocity exceeds *c.* 10 m s⁻¹. The trailing cloud accelerates and turns into an overriding surge, which may attain speeds of 30–70 m s⁻¹, possibly up to 125 m s⁻¹, thus outrunning and overtaking the depleted parental flow. The thickness of the resulting turbulent avalanche may vary from less than 10 m to more than 100 m, depending on the snow volume involved and the travel distance. The density may vary from *c.* 10–20 kg m⁻³ in the lower part to little more than 1–2 kg m⁻³ at the top of the flow (Mellor, 1978).

Many powder snowflows burst into a ground-hugging, highly turbulent cloud shortly after their release, probably due to an internal shock wave (Hopfinger, 1983). For a snowflow with mean velocity *U* and thickness *h*, the kinematic wave that travels through the flow has a celerity $u_k = 1.5 U$, whereas the corresponding long dynamic wave has a celerity $u_d = (\rho h)^{1/2}$ and effectively propagates with a velocity $u_d^* = U + (\rho h)^{1/2}$ where ρ is the acceleration due to gravity. When the Froude number of a flow, $Fr = U/(\rho h)^{1/2}$, exceeds 2, the kinematic wave moves faster than the dynamic wave, which may generate a 'roll-wave', or growing shock bore. A velocity of 10 m s⁻¹, to which an avalanche can accelerate very quickly on a steep slope, corresponds to $Fr > 2$. Ultra-rapid flow regime, with Froude numbers as high as 6–8.5, can be reached by large powder snowflows on very steep slopes (Schaerer & Salway, 1980).

A turbulent powder snowflow is typically a 'surface avalanche' (Hopfinger, 1983), whose lower boundary is cut shallowly in the snowpack, rather than at the ground surface. These flows are akin to turbidity currents (Hopfinger, 1983, fig. 4), and are often modelled as such. They have mean frontal velocities of 12–60 m s⁻¹, more typically 20–40 m s⁻¹, and mean densities of 50–300 kg m⁻³ (Mellor, 1978; McClung & Schaerer, 1983). The density in the basal part may be 2–4 times greater than the mean. The maximum velocity is near the base, at a height of roughly 1/10 of the flow thickness. For a flow thickness *h* and a typical range of slope inclinations of 60° to 30°, the maximum velocity zone is theoretically at a height of $2.1h^{1/2}$ above the base (McClung & Schaerer, 1983, 1985). The maximum velocity of the flow body is 2–2.5 times the frontal velocity. The concentration of snow is low,



Fig. 24. Multiple tongues of debris-rich slushflows on a colluvial fan in Skjerdingsdalen, late spring 1988. Note that the narrow tracks of snowflows to the left have cobbly levées, one-clast thick, but show little debris deposition at the terminus; the snowflows were nonerosive (vegetation not removed), carried little debris and formed the levées mainly by shouldering aside the pre-existing slope debris. The large blocks and smaller debris scattered in the forefront are attributed to large powder snowflows.

typically 5–25 vol.%, which renders internal friction very low. For example, the dynamic angle of friction for a concentration of 5 vol.% is less than 1° , and such a snowflow will behave like a Newtonian fluid.

Some powder snowflows are non-turbulent. They are typically mixtures of powdery snow and an older granular snow, and are akin to cohesionless debrisflows. Gubler (1989) has compared the existing models for dry non-turbulent snowflows and concluded that the Salm & Gubler (1985) model of 'partly fluidized' snowflow predicts the observed velocities and runouts most correctly. The model invokes a lower 'fluidized' layer (liquidized by the basal shear), with an exponentially convex velocity profile, overlain by a nonshearing 'rigid plug'. Their relative thicknesses depend on the total flow thickness and the gradient and roughness of the slope surface, as the latter factors control the flow speed and runout. The convex velocity profile, resembling that of a grainflow (Middleton & Southard, 1984), suggests a concentration gradient and is attributed to the snow texture, considered to be a mixture of powder snow and granular snow rich in hard clods of fine pebble size. The powder snow and air, incorporated *en route* by the flow, act as an interstitial fluid in the basal part. The energy dissipation in the lower layer is mainly due to pseudolaminar shear, so long as the slope roughness elements have a relief/spacing ratio smaller than 0.03, but is more due to the snow-clod collisions (Bagnoldian 'viscous regime') when the slope roughness is greater. The constitutive relationship used in this model invokes a non-Newtonian behaviour with the power coefficient

for the strain rate taken to be 0.6 (contractional flow).

Snowflow avalanches have an enormous impact force and high transport competence, which renders them capable of carrying huge and heavy objects. Published measurements indicate that the impact force may vary from 10 to 20 kPa for turbulent powder snowflows to 1000–2000 kPa for some large denser snowflows, with a reported maximum of 3900 kPa. For example, Voellmy (1955) calculated an impact force of 8.3 kPa for a snowflow that displaced a 120-t locomotive by 20 m. Hopfinger (1983) reported a large avalanche that detached a three-storey barracks from its concrete basement and carried it across topographic ridges and gorges over a distance of 1.5 km.

Snowflow deposits

Snowflow avalanches are capable of transporting large amounts of rock debris, including huge

Fig. 25. Features of modern snowflow deposits. (A–B) Longitudinal grooves, interpreted as tool-marks formed by the dragging of large, angular clasts in snowflow traction; note the 'rolling' *a(t)* fabric of scattered pebbles and cobbles. (C) Upslope view of a 'patchy' lobe of coarse gravel, one-clast thick, showing clast imbrication and both *a(t)* and *a(p)* fabric; the 'mixed' fabric indicates clast reorientation by subsequent snowflow avalanches. (D) Close-up view of *a(p)a(i)* clast fabric (depicted by the notebook, 20-cm long) in a 'patchy' gravel lobe deposited by dense snowflow. (E) Large boulders and finer debris concentrated at the surface of a melting lobe of dense snowflow; the snow deposit at this stage is still c. 4.5 m thick. (F) Rock debris and humic soil material rich in uprooted plants, at the surface of a melting lobe of dense snowflow, which is still c. 4 m thick here.

boulders. Some snowflows bear little or no debris, as is the case with many powder snowflows in the mid-winter time, whereas others are very rich in

clastic material (Figs 23B, 25E & F). The content of debris in a single flow may be extremely variable (Fig. 22D; Luckman, 1971). Snowflows



transport debris that has accumulated on the snowpack due to rockfalls and related processes, including wind-blown fines; debris that has been removed from the mountain slope/ravine and incorporated *en route* by the flow; and debris that has been swept by the flow from the apical part of a colluvial fan.

Dense snowflows have high shear strength, and their 'rigid plugs' can support rock clasts as large as boulders. Non-turbulent powder snowflows can carry cobbles in a similar way. These denser snowflows thus carry rock debris in much the same way as debrisflows do, with the important difference that the snow 'matrix' here melts out shortly after deposition and all the debris settles to the ground. The turbulent powder snowflows carry debris similarly to rapid turbidity currents: granules, sand and finer grains are carried in turbulent suspension, and the coarser debris in bedload traction. On a steep and relatively smooth or snow-covered slope, the bedload may easily include cobbles and boulders.

The sedimentary deposits of snowflows, as observed on modern colluvial slopes, range from blankets of scattered, unsegregated debris to irregular, 'patchy' lobes of unsorted debris, no more than one-cobble or -boulder thick (Figs 6, 24 and 25C). The clasts are occasionally found resting upon one another in precarious positions, due to the passive settling from the melting snow mass. The debris is surrounded by a blanket of waterlain sand (Fig. 24), usually rich in fine gravel, but is seldom fully illuviated or buried (Fig. 26B). The sand blanket, derived by meltwater runoff, has low-relief internal scours and commonly shows planar stratification and ripple cross-lamination, even within the larger interstices of the buried gravel patches (Fig. 26A). When emplaced on a subaqueous slope and soon buried by a debrisflow, the 'patchy' debris lobe may retain its openwork texture (Fig. 26C). Otherwise, it is filled with silt and fine sand from nearshore suspension (Fig. 15B), occasionally bearing fauna shells.

The deposits of successive snowflows, when emplaced directly after one another, are amalgamated and the indistinct boundaries render the individual avalanche events difficult to recognize in an outcrop section. Although the discontinuous horizons of large clasts within a thicker blanket of waterlain sand (Fig. 6) almost certainly represent separate avalanches, the actual number of snowflow events recorded by such a composite unit is likely to be larger, because not every snowflow might necessarily carry coarse debris or

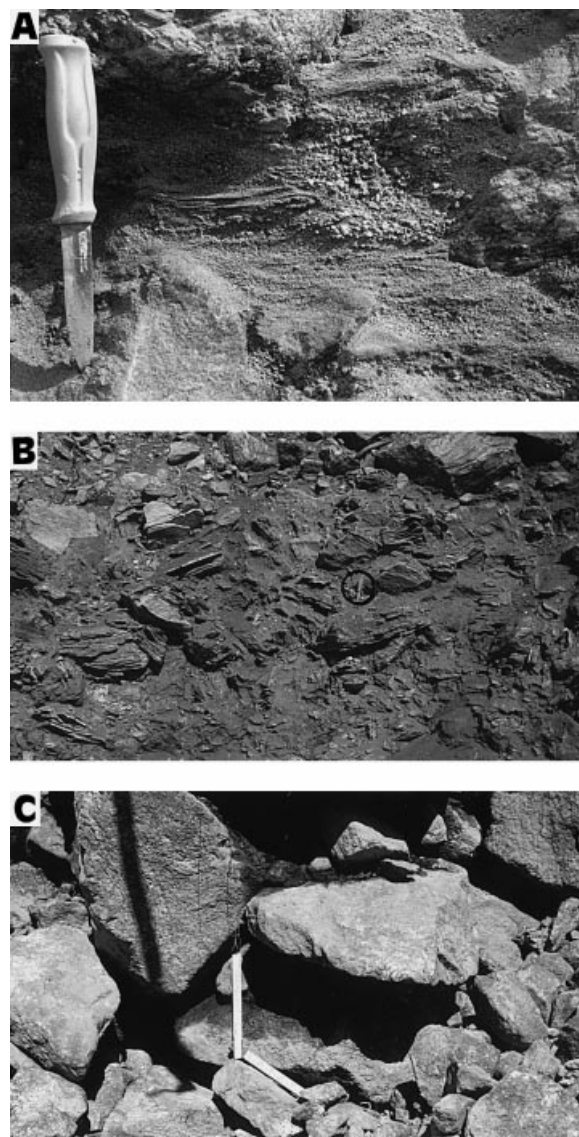


Fig. 26. Details of snowflow deposits in outcrop sections. (A) Bouldery, clast-supported gravel whose large interstices have been filled with ripple cross-laminated sand and poorer-stratified granule gravel; the knife is 17 cm. (B) Debris deposited by a larger number of snowflows in an intertidal backbeach zone, illuviated with fines and heavily shattered by frost action (note the open fractures in the foliated gneiss fragments); outcrop of the Younger Dryas palaeobeach in a colluvial-fan delta; the knife (encircled) is 17 cm. (C) Openwork gravel deposited by snowflows that have descended onto the subaqueous slope of a fan delta; the ruler's arms are 23 cm each. Photographs from the colluvial successions at Gardvik and Fiksdalstrand (localities 1 & 11 in Fig. 1).

the large clasts may be few and unexposed in a particular section. A sedimentary unit little more than one-cobble thick may represent 5–15 consecutive snowflows.

The clast fabric of snowflow deposits varies on a local scale, and is disorderly when measured more systematically. Boulders and cobbles deposited from turbulent powder snowflows may originally have tractional $a(t)$ fabric (Fig. 27A), but the scattered clasts on a steep and sand-filled substratum are highly vulnerable to reorientation by the subsequent avalanches and meltwater flow (Fig. 25C & D). The nonturbulent dense snowflows and slushflows may create an internal $a(p)$ fabric of clasts, due to laminar shear, but the fabric loses order when the debris melts out and settles to the ground (Fig. 25E & F).

Among the characteristic features formed by snowflows on colluvial slopes are low-relief longitudinal grooves (Fig. 25A & B) and ribs (Fig. 27A). The occasional presence of a cobble or boulder stuck at the downslope end of a groove suggests that these furrows are tool-marks formed by the snowflow's dragging of large angular clasts. The ribs are due to a linear accumulation of debris, rather than erosion (Fig. 27A), but their

formation mechanism is unclear. These longitudinal ribs are merely one-boulder or -cobble thick and their width/height ratio is in the range of 2–5. Where coupled, they may be levées made of the surficial debris that has been shouldered aside by a dense, highly elongate snowflow (Figs 13A and 24). Where multiple (Fig. 27A), they may still be levées of a series of such snowflows, or may reflect some peculiar, helicoidal pattern of secondary flow in the turbulent boundary layer of a large powder snowflow (cf. Allen, 1984, chapt. 1). Snowflows in western Norway often alternate with heavy rainfalls, and it cannot be precluded that the longitudinal ribs are due to strong runoff, with the sheetflow power maximized by the steep slope and a frozen or water-logged substratum.

Snowflows occasionally leave 'debris horns' on the upslope sides of large, immobile obstacles (Fig. 6), which is attributed to the local plastic 'freezing' of a dense snowflow rich in rock debris. A disorderly 'meltout' fabric and an openwork texture with waterlain basal sandy infill help to

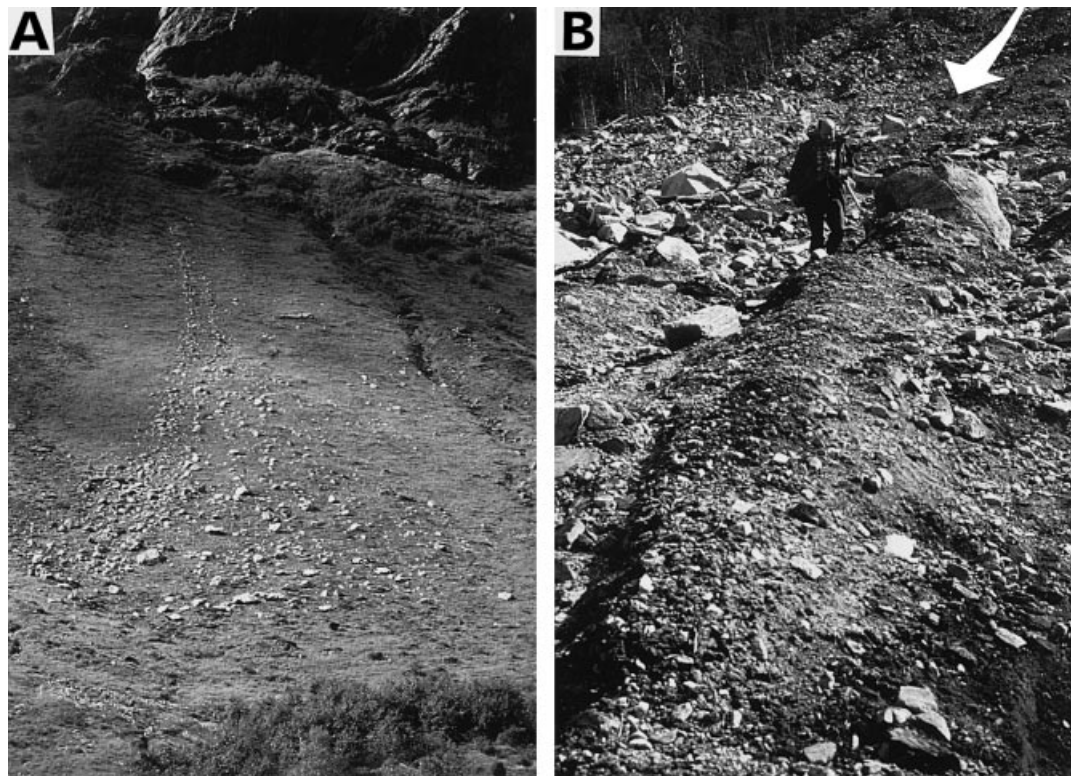


Fig. 27. (A) 'Patchy' gravel lobe deposited by a turbulent, powder snowflow on the grass-covered surface of a colluvial fan's flank; Sunnylvsmoldskreddalen (locality 8 in Fig. 1), spring 1993. Note the 'rolling' fabric of large clasts, the longitudinal 'debris ribs', one-clast thick, and the overall scatter of debris. The slope's height is c. 60 m. (B) 'Debris shadow' on the lee side of large block, left by an erosive slushflow; this short ridge is a relict of the upper part of a pre-existing debrisflow deposit. (A large, bouldery debrisflow descended the adjoining, till-covered mountain slope of c. 40° during a heavy rainfall in the early spring 1991, and is thought to have been followed by a turbulent slushflow derived from the higher slope; the latter avalanche scoured the deposit of its predecessor.) Fiksdal (locality 10 in Fig. 1); photograph taken a few days after the event.

distinguish these 'debris horns' from the similar features formed by debrisflows (see earlier section).

Snowflows may also form 'debris shadows' on the downslope sides of large boulders (Fig. 6). Some of these features are depositional, comprising coarse debris that has apparently been dropped from a turbulent, debris-laden snow avalanche in the flow-separation zone on the obstacle's lee side. Other 'debris shadows' are clearly erosional, representing the lee-side relicts of a surficial layer of colluvium that has elsewhere been wiped out by an erosive snowflow (Fig. 27B). The obstacle in either case must have been deeply grounded, or its height was much less than 1/10 of the flow thickness (see previous section).

The extreme hydraulic jump at the foot of a cliff may cause a virtual crash-landing of snowflow avalanches, with the snow mass splashing out and ejecting substratum debris in a blast-like fashion. A result of the powerful impacts is a characteristic impact crater, referred to also as 'plunge pool/pit' (Liestøl, 1974; Corner, 1980). These oval depressions are 1–5 m deep and 20–100 m in diameter, are often filled with meltwater (pond) and have a distinct outer rim of debris ejecta (Fig. 28). No such craters are found to be related to the other avalanche types, although their impact on the foot-zone substratum, combined with the powerful thrust, can be enormous. For example, a georadar (GPR) survey in Romsdalen indicates that some large debrisflow avalanches have deformed the postglacial valley-floor alluvium to a depth of *c.* 30 m, forming hydroplastic folds, thrusts and surficial 'pressure ridges'.

Some illustrative examples of colluvial successions rich in snowflow deposits are shown in Figs 20 and 29. Importantly, these deposits often contain plant fragments (Fig. 25D, E & F), and also their waterlain infill commonly includes accumulations of humic soil rich in plant detritus, derived by contemporaneous slopewash. This plant material and the marine shells from subaqueous facies have been used for the radio-carbon dating of the colluvial deposits.

Waterflow processes

Waterlain deposits are of minor volumetric importance in most of the colluvial systems, whose slope catchments are typically small. However, the role played by waterflow is often quite significant, as is shown particularly well by the colluvial-fan deltas.

The flow of water, whether due to snow-melt or rainfall, occurs generally in two modes: as a shallow, unconfined or poorly confined *sheetflow*, and as a channelized *streamflow*. Sheetflow washes the colluvial slope and hence is often referred to as 'sheetwash' by geomorphologists. The flowing water winnows mud and sand from the upper slope and deposits this sediment further downslope, mainly by percolating through the coarse surficial colluvium and filling its interstices. Sheetflow is more powerful when the surficial colluvium is frozen or water-logged. The shallow waterflow in such conditions is supercritical, capable of transporting pebbles and dislodging isolated larger clasts. In short, sheetflow transfers the finer surficial sediment from the fan apex to the lower slope, alters the



Fig. 28. An impact crater formed by snowflow avalanches that have crash-landed at the foot of a very steep colluvial slope; Valldalen (west of locality 15 in Fig. 1), August 1996. Note the crescentic rim of ejected debris at the outer margin of the crater pond (*c.* 25 m in diameter).

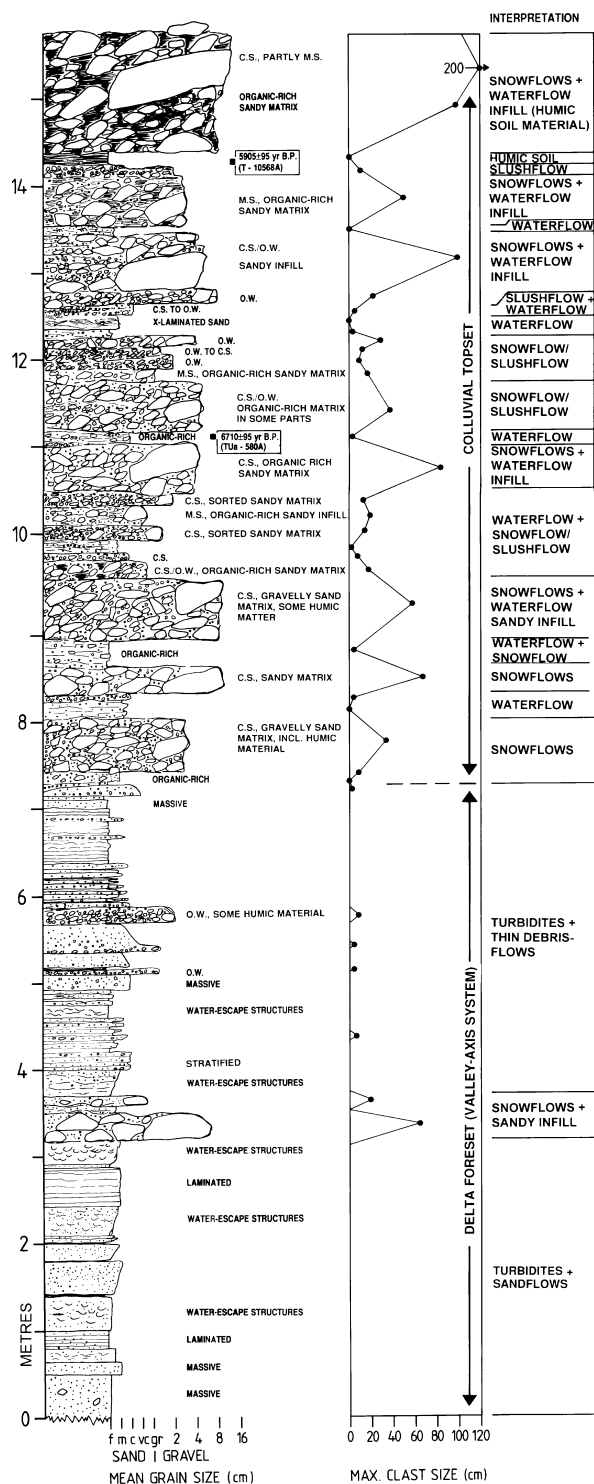


Fig. 29. Detailed log from a valley-side colluvial apron dominated by snowflow avalanches, Korsbrette (locality 9 in Fig. 1). The colluvial system has prograded, obliquely, onto the submarine front of a Gilbert-type delta formed by the valley-axis river system, supplying debris to the delta slope and forming the delta topset. Note the radiocarbon dates. Texture code CS and OW as in the caption to Fig. 9; MS= matrix-supported texture.

primary texture of the surficial colluvium and tends to bury the openwork or scattered debris of preceding rockfalls and snowflows (Fig. 29). An analogous process, more often called 'slopewash', occurs on the adjoining mountain slope, where the flowing water removes fine debris, including contemporaneous soil material, and deposits it on the colluvial slope below.

Streamflow is a more pronounced mode of waterflow (Fig. 6). There is seldom more than one channel active on a colluvial fan (Figs 3 and 5D), and the channel shifts due to infilling and avulsion, rather than lateral migration. These channels are typically narrow gullies, developed from the ruts of earlier avalanches, whose tracks have been overtaken and modified by waterflow. The channels are up to 1–1.5 m deep, have V-shaped cross-sections and generally lack levées. Some channels have levées formed by earlier and/or contemporaneous debrisflows, but the only waterlain overbank deposits are thin splays of sand and fine gravel. The modern channels are mainly ephemeral, carrying the seasonal meltwater discharge and the runoff from heavy autumn rains. The isolated palaeochannels found in the colluvial successions suggest that similar conditions occurred also in the past.

The waterflow in the gullies is often slushy, carrying heavy sediment load and rapidly losing competence in the middle to lower reaches. The sediment concentration is high, and the water may also bear slush at the beginning of a snow-melt season. A 'hyperconcentrated', high-density waterflow (Fig. 21) is thought to be characterized by high apparent viscosity and a rheological behaviour intermediate between plastic and Newtonian fluid flow (Beverage & Culbertson, 1964; Nemec & Muszyński, 1982; Rickenmann, 1990, 1991); this would mean a non-Newtonian pseudoplastic fluid, which has no limiting plastic strength, but whose viscosity coefficient increases rapidly with the decreasing turbulent shear stresses. The turbulence in such conditions tends to be suppressed and the deposition of debris occurs mainly by rapid dumping, with little or no tractional segregation.

Where the slope catchment involves a glacier or semipermanent snowpack and the water discharge is relatively high and more perennial, the streamflow on a colluvial fan assumes the form of a relatively wide and shallow channel, often braided (Fig. 30). These channels may be a few metres wide, less than 0.5 m deep, and show medial gravel bars. The flow is rapid and the sediment transport is mainly tractional. The bars

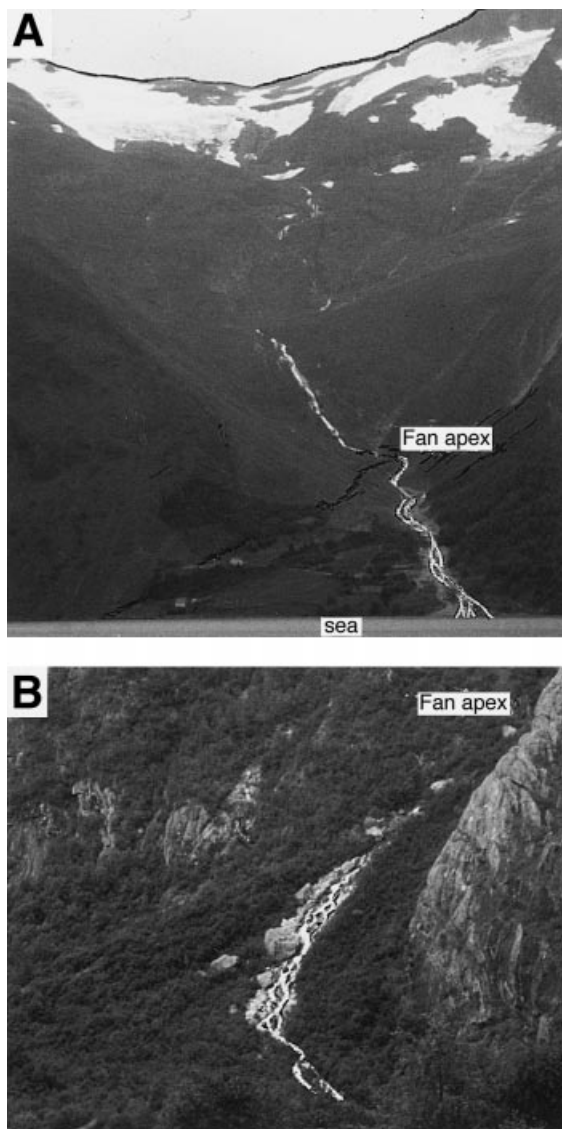


Fig. 30. Shallow braided streams on a colluvial-fan delta at Skår (A) and a vegetated colluvial fan in Romsdalen (B). Photographs taken in August 1996, after the main phase of meltwater discharge.

are small, no more than 15–20 cm in relief, lack slipfaces and emerge as rhomboidal islands at low stages. They form mainly as pebbly ‘shadows’ on the lee sides of cobble/boulder clusters, but there are seldom more than 1 or 2 such bars per channel width. The stream is very effective in transferring sand and fine gravel to the fan toe. In the case of a fan delta, the stream builds a secondary deltaic lobe, or underwater mouth-bar, on the subaqueous slope. Conditions of such pronounced streamflow activity occurred periodically in the past, when many of the colluvial-fan deltas turned into stream-dominated Gilbertian systems (see subsequent section).

Streamflow has a natural tendency to scour and transfer sediment to the lowest part of a fan, but this does not necessarily mean that the process is purely ‘destructive’. Stream channels often play the role of a distributary that causes marked progradation of the depositional system. The channels on colluvial fans shift less frequently than on common alluvial fans, and hence the build-out is more localized.

Deposits. The channel-fill deposits in the colluvial successions are bedded gravels with interlayers of stratified sand, very coarse to medium grained. The beds are 10–30 cm thick, pebbly to cobbly, with a clast-supported texture and sporadic boulders. Some beds are crudely stratified, but most are massive and normally graded (Fig. 31). Most of the gullies are thought to have been filled by episodes of high-density streamflow, commonly followed by the tractional deposition of stratified sand and fine gravel (Fig. 31). The smaller gullies often show a simple fining-upward infill, with little or no internal bedding. Many gullies have apparently been plugged by debrisflow and slushflow avalanches.

The wider and shallower colluvial channels show tractional clast fabric and gravel segregation into lenses (low-relief transient bars). These channel-fill deposits show internal scours and greater textural variation, with common planar stratification and isolated sets of low-angle cross-strata.

Debris creep

The knowledge on colluvial creep processes has advanced quite recently. For example, Kirkby (1967, p. 359), only three decades ago, felt still compelled to assert that ‘the role of creep in slope evolution is largely a matter of speculation ..., unsupported by evidence’.

Debris creep, also referred to as ‘soil creep’ by geomorphologists and engineers, is a very slow gravitational movement of the surficial mantle of slope debris, which involves no basal detachment plane of sliding and is perceptible only over relatively long periods of time (Bryan, 1922; Sharpe, 1938; Kirkby, 1967). Creep is a cumulative effect of the innumerable tiny displacements, or discrete interparticle slips, driven by the distributed load stress of the colluvial mantle. The percolation of water through the debris mantle, the heaving of clasts by frost action and the biological activity of plant-roots and animals are the most important physical agents of colluvial creep (Schumm, 1956; Kirkby, 1967; Emery,

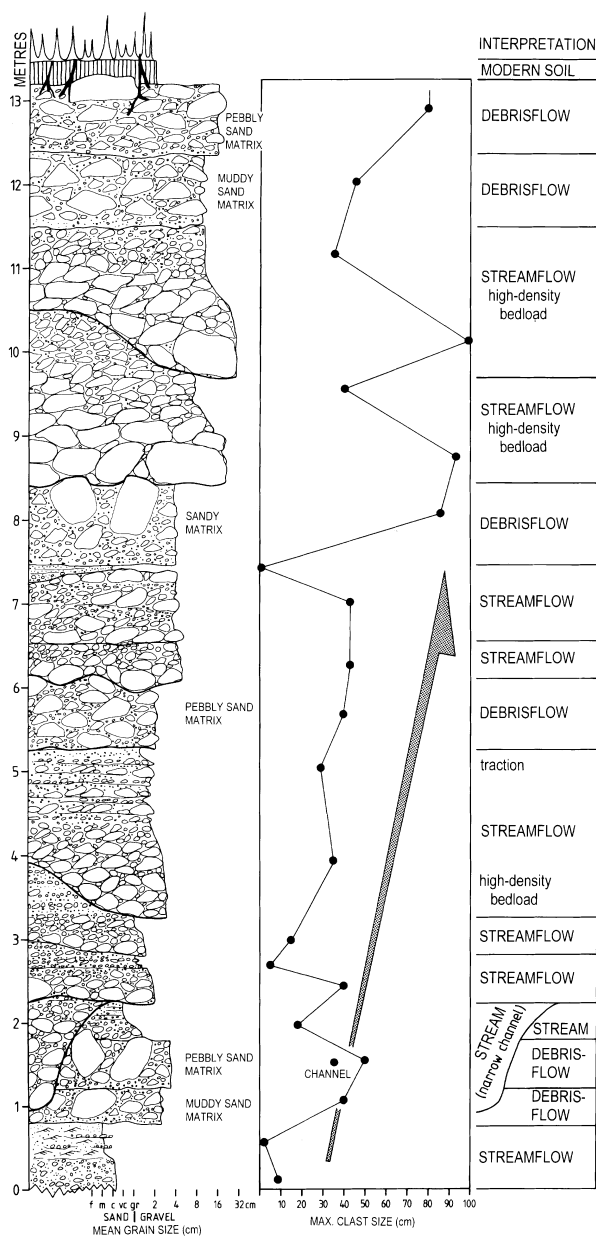


Fig. 31. Detailed log from a colluvial fan formed by alternating debrisflow and streamflow processes; Bars-taddalen (locality 4 in Fig. 1). The mountain slope here is 23–35° and the channel of the feeder stream, Tverrelva, has an inclination of 20–24°, but the depositional surface of the fan is inclined at 13° (apex) to 10° (toe), which renders it transitional to a common alluvial fan.

1978; Finlayson, 1985; Feda, 1992). The interparticle slips occur at random and the creep process is highly incremental, with discrete and relatively brief episodes of activity. Longer-term measurements indicate rates ranging from a few millimetres to a few centimetres per year, depending on climate and material type (Fleming & Johnson, 1975; Young, 1978a,b; Selby, 1982; Goudie *et al.*,

1985; Jahn, 1989; Lautridou *et al.*, 1992; Auzet & Ambroise, 1996). In warm arid regions, significant creep may occur only after a series of heavy rainfalls have saturated the colluvium (Schumm, 1956). In humid regions, creep is more common and may reach speeds as high as 20 cm day⁻¹ (Radbruch-Hall, 1978).

Although commonly defined as ‘a very slow, more or less continuous flow’ (Bolt *et al.*, 1975; Emery, 1978), creep in reality is highly discontinuous, and is not a flow in the strict terms of low-velocity friction dynamics (Baumberger *et al.*, 1994). Creep, even when driven at a constant rate, involves a multitude of interparticle ‘stick’ and ‘slip’ states, or localized jerky movements, due to the build-up and random release of interparticle frictional stresses. Creep is thus characterized by marked velocity fluctuations, which disappear when the strain rate increases and a slow frictional flow begins. The higher strain rate eliminates the stick-slip mode of particle movements and renders them increasingly continual, although the transition from creep to slow inertial flow is hardly discernable to an observer’s eye, even when the flow rate is of the order of 1 $\mu\text{m s}^{-1}$ (or *c.* 30 m yr⁻¹). Further, the kinetic friction coefficient (defined as the tangential stress normalized to the material weight) in creep is ‘rate-weakening’, which means decreasing with the increasing strain rate, typically in a logarithmic fashion. In a frictional flow, the coefficient is ‘rate-strengthening’, increasing with the strain rate, no matter if the flow rate is high (McTigue, 1982; Haff, 1983; Campbell, 1990) or very low (Baumberger *et al.*, 1994).

In rheological terms, creep is considered simply as an increase of permanent strain with time under a constant stress (Lubahn & Felgar, 1961; Coates, 1967). Interestingly, the strain in creep may be episodically reversible (Kirkby, 1967; Finlayson, 1981; Auzet & Ambroise, 1996), hence the constitutive models include an elastic component (Emery, 1978, fig. 3). It is now widely agreed that the creep of clastic materials is a nonlinear, elasticoviscous Maxwell-type phenomenon, whereas their flow is a nonlinear or linear, plasticoviscous Coulomb-type phenomenon. In contrast to massflow, there is also no true steady-state creep of clastic materials (Emery, 1978). Under a constant deviatoric stress, the strain rate either declines or increases exponentially with time. The increase often leads to *en masse* sliding failure (Emery, 1978, fig. 1) and possibly massflow (Holmes, 1978).

The velocity profile of a creeping debris layer, as predicted by Davison's (1889) theory and confirmed by field studies (Auzet & Ambroise, 1996), is characteristically concave, with the downslope velocity component declining exponentially with depth, but dependent upon the sediment properties (represented by the Davison 'soil constant'). Kirkby's (1967) theory predicts the exponential velocity decline to occur below a surficial rigid-plug zone, which means maximum shear strain at some depth, rather than near the surface. This condition would more readily promote sliding failure.

When driven by frost and thaw action, the colluvial creep is called *solifluction* (or 'soil flow'). Many authors distinguish 'solifluction' from 'soil creep', although there is little physical difference, apart from the sawtooth pattern of clast movement due to the frost-heave and thaw-collapse of larger clasts (Washburn, 1979). In fact, the concept and first quantitative theory of colluvial creep were introduced, by Davison (1889), in the context of freeze-thaw cycles. However, solifluction is due to specific conditions and is the most pronounced variety of colluvial creep, involving a good deal of slow frictional flowage. Solifluction contributes to the smooth, 'flowing' profile of periglacial colluvial slopes and has been a subject of extensive field studies (Frenzel *et al.*, 1993). The studies show, for example, that a surficial colluvial mantle can creep over a frozen substratum on slopes as gentle as 2–3°.

The colluvium in permafrost regions is often permanently cemented with ice, except for a shallow summer thaw. With the continuous replenishment by debris from upper slope, the increasing load stress may cause the interstitial ice to yield and flow in a plastic fashion. A *rock-glacier* then creeps down the slope and spreads slowly in the foot zone (Giardino *et al.*, 1987; Barsch, 1988; Whalley & Martin, 1992; Leliwa-Kopystynski & Maeno, 1993).

Deposits. A pronounced colluvial creep, such as solifluction, involves lobes or broader sheets of surficial debris, ranging from *c.* 1 m to 50–80 m in width. Colluvial deposits attributed to solifluction include well-bedded to poorly bedded gravels, fine pebbly to cobbly, as well as some crudely bedded diamictons (Bertran *et al.*, 1995). This wide range of deposits suggests that their characteristics may be far more related to the primary slope material, or the local mode of debris production, than to the creep process itself. In short, the products of creep in ancient

colluvial successions are difficult to recognize due to the lack of diagnostic criteria, or an established concept for the sedimentary signatures of creep.

An exception may be the concept of 'stone-banked' solifluction lobes and sheets (Bertran *et al.*, 1994, 1995; Van Steijn *et al.*, 1995), invoked for the alternating layers of openwork coarse-pebble gravel and matrix-supported finer gravel of *grèzes-litées* type. In this model, a lobe or sheet of surficial debris creeps downslope, at a rate of 2–5 cm to 20–30 cm yr⁻¹. Frost action makes the coarsest clasts reach the surface, where they further creep downslope, due to needle-ice growth, at a rate of up to 1 m yr⁻¹. This coarse debris accumulates at the front of the lobe or sheet, and the resulting 'stone bank' is progressively buried, in a caterpillar fashion, by the slow-creeping parental layer of matrix-rich debris. As the process continues and the front is replenished with coarse clasts, an undulatory layer of coarse openwork gravel forms and is covered by a flat-topped layer of finer, matrix-rich gravel. The stony pavement that creeps over the top may develop an upward coarsening due to the frost segregation of clast sizes, whereas the progressive burial of the frontal 'bank' results in an upward fining, with a matrix-rich upper part. When significant illuviation occurs, the layer may be covered with a thin sand or silty mud capping. The successive lobes or sheets lead to a repetition of this bedding motif, with the bed geometry ranging from lenticular (lobes) to more tabular (sheets) in outcrop sections parallel to the slope strike.

However, the model should be applied with caution if used as a possible guide for the recognition of solifluctional deposits in colluvial successions. Firstly, the 'matrix-rich' layers in the reported type sections are mainly clast-supported, though matrix-filled (Bertran *et al.*, 1994, 1995; Van Steijn *et al.*, 1995), which renders the bedded gravel similar to some other colluvial facies, for which a solifluctional origin is unlikely (see deposits of low-viscosity debrisflows earlier in the text) or can outrightly be precluded (see colluvium D of Nemec & Kazancı, 1999). Secondly, many solifluctional deposits reported in the literature are quite unlike those implied by the 'stone-bank' model (Flint, 1971; Washburn, 1979; Frenzel *et al.*, 1993). Thirdly, solifluctional deposits are widely reported to have an *a(p)* fabric (Nelson, 1985; Bertran *et al.*, 1997), which may not be the case with the 'stone banks' (Van Steijn *et al.*, 1995).

The style of creep-related deformation on a colluvial slope may vary from extensional, with a pronounced downslope spreading of the debris mantle (as lobes or sheets) and possible formation of transverse 'gulls' (open cracks), to distinctly compressional, with a surficial buckling or more localized bulging of the mantle. The creep of colluvium is liable to sudden acceleration after an episode of heavy rainfall or snow melting, when the bulk weight of the mantle increases and interparticle friction is reduced. Many debris-flows are thought to be generated in this way on mountain slopes (Holmes, 1978; Radbruch-Hall, 1978). Likewise, the deposits of colluvial slides and debrisflows often tend to creep after the emplacement (Bolt *et al.*, 1975; Van Asch, 1984), and this secondary creep may strengthen the $a(p)$ clast fabric of a debrisflow deposit.

In short, most colluvial slopes are probably subject to creep processes, and there is little doubt that these processes have played a role on the colluvial slopes in western Norway. Creep was probably important in triggering debrisflows, or in displacing the fragmented bedrock into unstable positions and causing rockfalls (Haefeli, 1966; Hausen, 1971; Wyroll, 1977). However, any direct evidence of creep processes in a colluvial system dominated by avalanches is rather difficult to recognize.

SEDIMENTARY SUCCESSIONS

This discussion of colluvial successions is focused on coastal depositional systems, which

include both subaerial and subaqueous facies and thus bear also the record of relative sea-level changes (Fig. 32). These depositional systems are *colluvial-fan deltas* (Blikra & Nemec, 1993b): coastal accumulations of land-derived sediment formed by the progradation of colluvial fans directly into the sea (Figs 3 and 5D). The steep morphometry and the predominance of avalanche processes, from the subaerial apex to the subaqueous toe, render these gravelly systems a specific end-member category of the spectrum of deltas observed in nature (Nemec & Steel, 1988; Nemec, 1990a; Reading & Collinson, 1996).

The colluvial-fan deltas have relatively large subaqueous parts and small, short subaerial apices (Fig. 32), which pass upslope into distinct avalanche tracks, often stemming from bedrock gullies or mountain ravines. The deposits are slope-waste gravels, poorly sorted and often poorly bedded, as is typical of a colluvium. However, much of the material here has been derived by the resedimentation of glacial till and possibly kame terraces, which renders the colluvium somewhat unusual: the gravel is commonly subrounded to rounded, and does not necessarily correspond to the local bedrock.

The colluvial successions at first glance look 'chaotic' and very poorly organized. However, they are clearly heterogeneous, and a close examination of the stratigraphic sections almost invariably reveals distinct changes in the component facies assemblages (depositional processes) and their bedding architecture (fan-delta physiography).

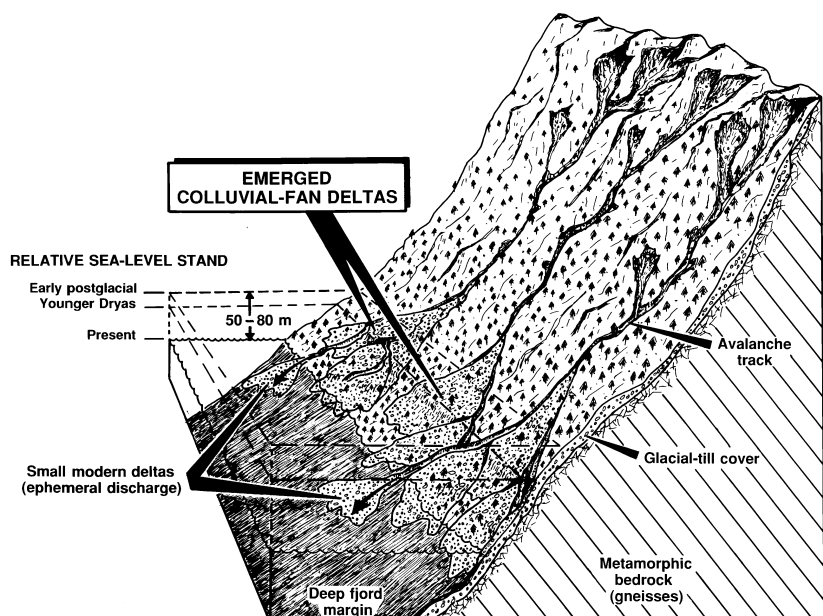


Fig. 32. The depositional setting of colluvial-fan deltas at a steep fjord margin affected by the postglacial regional isostatic uplift; schematic diagram pertaining to the study area in western Norway.

The ensuing review focuses on three fan-delta types, which are representative of the general range of colluvial systems in the region. They show the varying role of different avalanche processes, reflecting the variable responses of the local mountain slopes to the postglacial climate and its changes. The emphasis is on the facies anatomy and depositional history of the colluvial systems, and the developmental 'stages' distinguished in the local successions are chronostratigraphically correlative, as indicated by radiocarbon data.

Debrisflow-dominated colluvial systems

An example of this type of colluvial system is the array of coalescent colluvial fans that have prograded into the sea at the western margin of Tomrefjorden (locality 12 in Fig. 1). The adjoining mountain slope has a thick glacial-till mantle resting on gneissic bedrock. The fans are steep accumulations of coarse debris at the termini of distinct avalanche tracks scoured in the till mantle. The tracks reach an altitude of *c.* 600 m, and the main source zone for the colluvium is at the height of 200–600 m, where the mountain slope is steeper than 30° and its till cover has been markedly depleted. The slope has a low potential for snow-drift accumulation under the prevailing pattern of westerly winds. Snow avalanches here are very rare and have played a negligible role in the postglacial sedimentation.

Our analysis of this coastal apron, now emerged, is based on one of its component fan deltas, well-exposed in a large gravel pit (Figs. 19, 33 and 34). The colluvial facies assemblages and their depositional architecture indicate five main stages of the fan-delta development (Fig. 35).

Stage 1. The oldest part of the sedimentary succession, or the fan delta's 'core' (Fig. 35), consists of bouldery to cobbly debrisflow deposits rich in fine-grained matrix (log 4 in Fig. 33). They represent mainly high-viscosity debrisflows, some apparently accompanied by a watery, low-viscosity trailing flow. The trailing massflows, carrying pebble gravel and coarse sand, were turbulent, capable of accreting backsets of up-slope-dipping cross-strata onto the debrisflow lobes. This trailing flow was probably generated when the debrisflow plunged into the water on the steep fjord-margin slope. The debrisflow beds often show normal grading at the top (Fig. 14A), which suggests subaqueous emplacement with strong shearing against the ambient water. Ungraded debrisflow beds tend to be amalgamated,

due to the lack of visible textural differences between two or more successive deposits. Some beds are separated by thin interlayers of well-sorted, fine-grained sand, which show normal grading and are thought to have been deposited from wave-derived nearshore suspension. The wave base in Norwegian fjords is seldom deeper than 2 m, and the steep nearshore slopes tend to be draped with storm-derived suspension fines. The sand layers are often strongly deformed by loading.

This earliest colluvial sedimentation probably followed directly the deglaciation of the area (*c.* 12 700 years BP), when the till-covered, non-vegetated mountain slope was highly unstable. The regional data on postglacial relative sea levels (Mangerud *et al.*, 1979; Svendsen & Mangerud, 1987, 1990) and the stratigraphic position of this facies assemblage beneath a younger Gilbert-type delta (Figs 33 and 35) indicate that the deposits must be subaqueous. The sedimentary facies support this interpretation.

The colluvial system at this early stage was apparently a steep cone, whose depositional slope extended directly into the deep water, with little or no change in gradient (Fig. 35). Many modern fjord-margin systems have such a physiography. The debrisflows, derived from the slope till, were thus emplaced mainly subaqueously. The relative sea level at this stage was high (Fig. 35), and the subaerial apex of the cone was probably small and might not even be preserved. If preserved, it would now be buried beneath the younger colluvium at an altitude higher than the gravel-pit outcrop.

Stage 2. The overlying facies assemblage consists of moderately thick beds of clast-to matrix-supported, pebble to cobble gravel (Figs 14B and 15), intercalated with thinner beds of fine-pebble gravel and pebbly sand, mainly normally graded or graded-stratified (logs in Fig. 33). Their deposition is attributed to subaqueous debrisflows and high-density turbidity currents, respectively. These steeper-inclined deposits represent the foreset of a Gilbert-type fan delta that has downlapped the pre-existing subaqueous cone. The foreset deposits show extensive internal truncations and also local angular disconformities marked by downlap bedding (Figs 33 and 34). The erosional features are attributed to the falling of the relative sea level with the onset of the postglacial isostatic uplift, whereas the episodes of delta-slope downlap indicate lateral shifts of the axis of sediment dispersal of the fan.

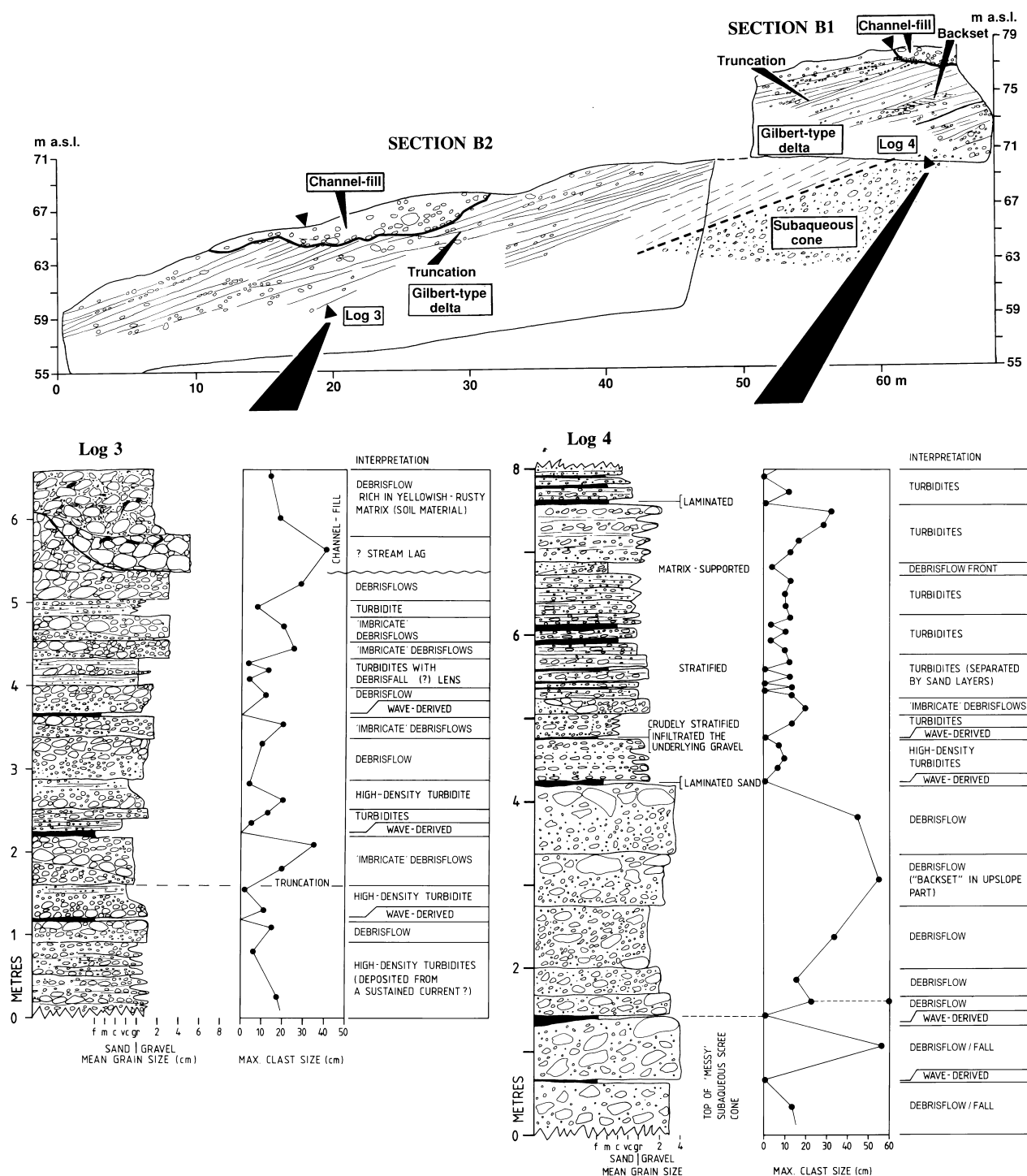


Fig. 33. Outcrop section and detailed logs of the colluvial fan-delta complex at Tomrefjorden (locality 12 in Fig. 1). The cross-section is approximately normal to the palaeoshoreline.

The predominance of clast-supported deposits of low-viscosity debrisflows and the abundance of turbidites suggest relatively 'wet' conditions on the adjoining mountain slope, with a greater role of flowing water. There is evidence of stream palaeochannels and mouth-bar cross-strata at the

top of the foreset (Fig. 34). The pre-existing avalanche tracks on the mountain slope were probably overtaken by flushy, ephemeral streams carrying meltwater and/or rainwater, and the predominance of streamflow promoted the development of a Gilbert-type system. The fan delta

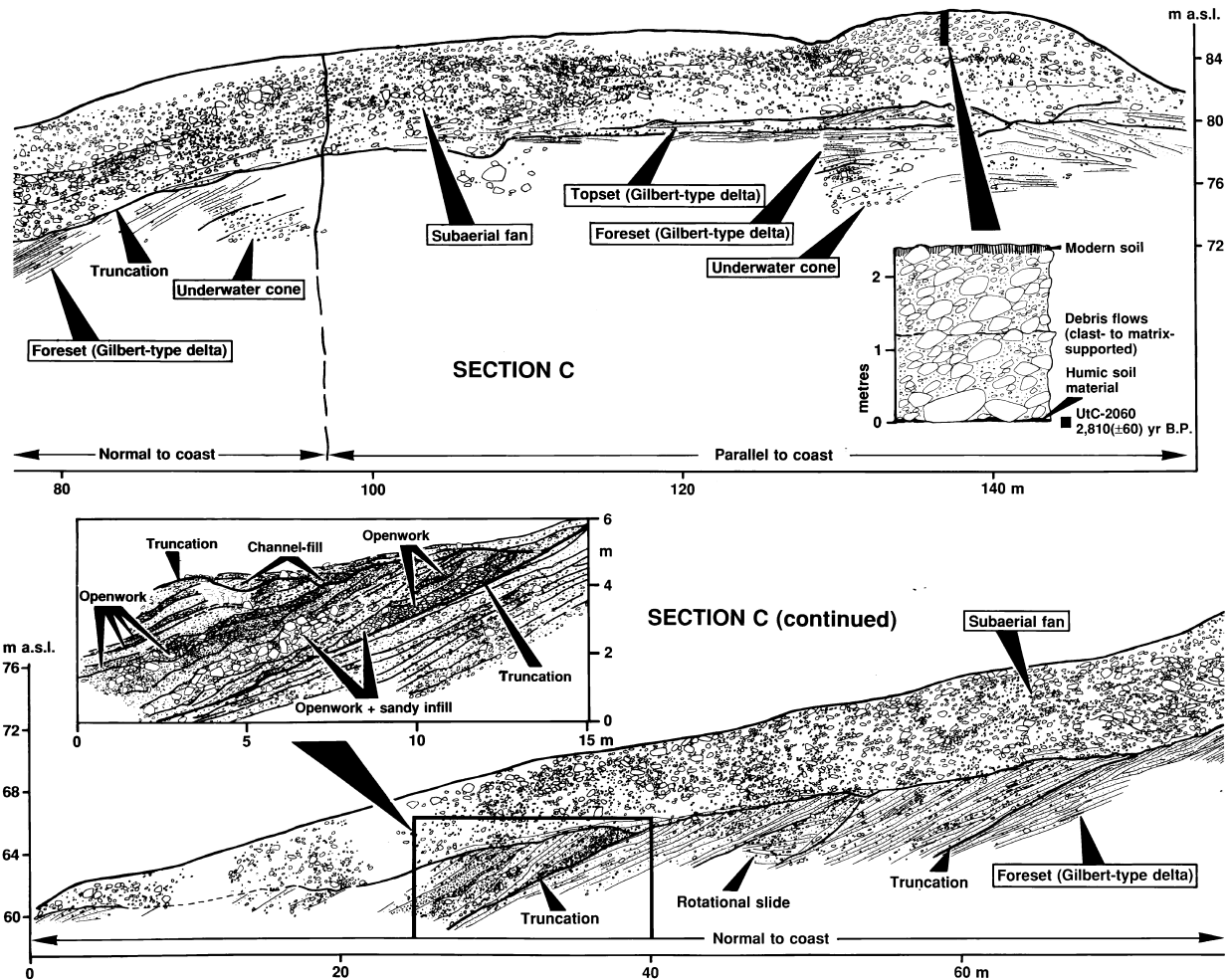


Fig. 34. Outcrop section of the colluvial fan-delta complex at Tomrefjorden (locality 12 in Fig. 1). Note that the upper right-hand part of the cross-section is parallel to the palaeoshoreline, whereas the rest of the section is roughly normal to the latter.

had a steep and short subaerial plain, allowing debrisflow avalanches to pass directly onto the subaqueous slope.

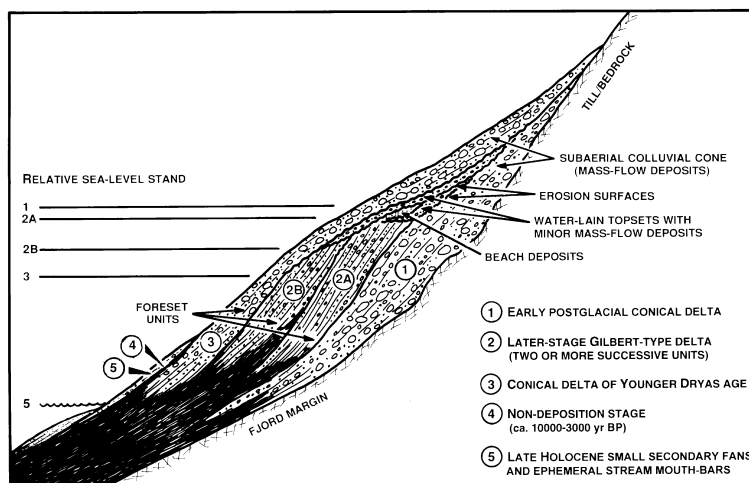
The foreset facies assemblage is internally varied, but shows two packages of mainly coarse-gravel beds separated by a thinner package of mainly sandy and fine-pebbly turbidites (Fig. 33; the younger part is to the lower-left in Fig. 34). The bipartition suggests two phases of slope wastage dominated by watery debrisflows, separated by a phase dominated by streamflow (stages 2A & 2B in Fig. 35). A narrow belt of erosive beach deposits occurs at the top of foreset lobe 2A, covered erosively by the waterlain topset of lobe 2B (Fig. 35). The altitude of this palaeobeach (*c.* 80 m) corresponds to the sea-level stand shortly after the deglaciation, which means that the sedimentation of stage 1 was relatively brief and was followed directly by development of the delta lobe 2A. Lobe 2B extends to an altitude of *c.*

76 m, which suggests that its deposition commenced *c.* 12500 years BP.

Stage 3. The colluvial system subsequently resumed the simple conical physiography that characterized stage 1, although the relative sea level had fallen considerably by that time (Fig. 35). The emerged part of the Gilbert-type delta of stage 2 had been strongly truncated by erosion and overlain by a succession of clast-supported, subaerial debrisflow deposits (Figs 19 and 34). They are poorly bedded and commonly amalgamated, but the consecutive debrisflow events are recognizable (Fig. 19). Some gravel beds show features suggesting deposition from slushy debrisflows or dense snowflows.

The slope of the colluvial fan at this stage extended 'smoothly' into the sea (Fig. 35), with a narrow, aggradational beach zone that was easily bypassed by many avalanches. The palaeobeach unit is a relatively thick succession of coarse,

Fig. 35. Stratigraphic anatomy of the colluvial fan-delta complex at Tomrefjorden. Schematic diagram; the frame's length is *c.* 850 m and height *c.* 200 m; the total relative sea-level fall (1–5) is *c.* 80 m.



clast-supported gravel that has been severely shattered by frost action, probably in an intertidal backbeach zone (Blikra & Longva, 1995). The altitude of the palaeobeach corresponds to the relative sea-level stand the Younger Dryas time (11 000–10 000 years BP).

Stage 3 indicates a dramatic increase in slope-waste processes, apparently due to the climatic deterioration of the Younger Dryas time. The colder climate, with a decreased and more seasonal rainfall, probably reduced slopewash and rendered the mountain slope prone to mass failures. Solifluctional creep and the effects of slush and seasonal snow-melt might be important in triggering the debrisflows.

Stage 4. The sediment yield then considerably decreased, probably due to reduced snowfall and depletion of the mountain-slope source by the preceding phase of intense wastage. This stage of minimal sedimentation and no record of avalanche deposits is attributed to the phase of regional climatic warming, known as the Holocene climatic optimum (*c.* 10 000–5000 years BP). The hiatus is regional.

Stage 5. The intensity of slope-waste processes subsequently increased, although the late Holocene colluvium is thin, more local, and due mainly to the redeposition of the older colluvium. The radiocarbon date of soil material separating the levées of these younger debrisflows from the deposits of stage 3, at the margin of an avalanche track, indicates avalanches younger than *c.* 2800 years BP. This suggests a relatively long break between the Younger Dryas sedimentation of stage 3 and the onset of the Holocene sedimentation. A few gullies have more recently been incised in the apron surface. The streams carry mainly the spring meltwater runoff from the fan

apices to the shoreline, where underwater mouth-bars have formed on the steep subaqueous slope (Fig. 35).

The relative sea level is known to have fallen strongly after the Younger Dryas time, and this factor is likely reflected in the redeposition of colluvium and the incision of stream gullies. Streamflow processes suggest an increase in seasonal runoff. Some of the gullies have been plugged with debrisflow and/or slushflow deposits and subsequently rejuvenated by waterflow, with the avalanche deposits preserved as levées. The plugging of channels probably reflects a younger phase of climatic deterioration, when the gullies became pathways for massflow avalanches. The radiocarbon date of a palaeosol buried beneath one of the levées indicates debrisflows younger than *c.* 1500 years BP. Several debrisflows have also descended the colluvial slope along the stream gullies in the historical times (Blikra, 1994).

'Mixed-type' colluvial systems

The two colluvial-fan deltas near Gardvik (Fig. 3), at the eastern margin of Ørstafjorden, afford an example of colluvial systems formed by alternating debrisflow and snowflow avalanches. The fans are steep accumulations of coarse debris at the termini of two distinct avalanche tracts that can be traced to an altitude of *c.* 900 m on the mountain slope (Fig. 3, top). As in the previous case, the gneissic bedrock here is covered with a thick glacial till, but the mountain slope faces the south-west and has a relatively high potential to accumulate snow, drifted by winds from the north and north-east. The fan surfaces show clear evidence of recent snow avalanches, including

damaged trees/bushes and the occurrence of scattered bouldery gravel and 'patchy' debris lobes on grass-covered slopes. There are also some relatively fresh gravel lobes deposited by watery or slushy debrisflows (Fig. 3, bottom).

The two fan deltas are very similar, although the stratigraphic analysis is based on the northern one, well-exposed in a large gravel pit (Figs 3 and 36). The sedimentary facies assemblages and their depositional architecture indicate the following developmental stages (Fig. 37), correlative with those of the Tomrefjord fan-delta complex (Fig. 35).

Stage 1. The oldest part of the colluvium consists of bouldery to cobbly, matrix-supported debrisflow deposits, similar to those in the Tomrefjord fan delta (previous section). They represent the subaqueous part of a steep colluvial cone, which probably had a very small subaerial apex (unexposed or unpreserved) and was built

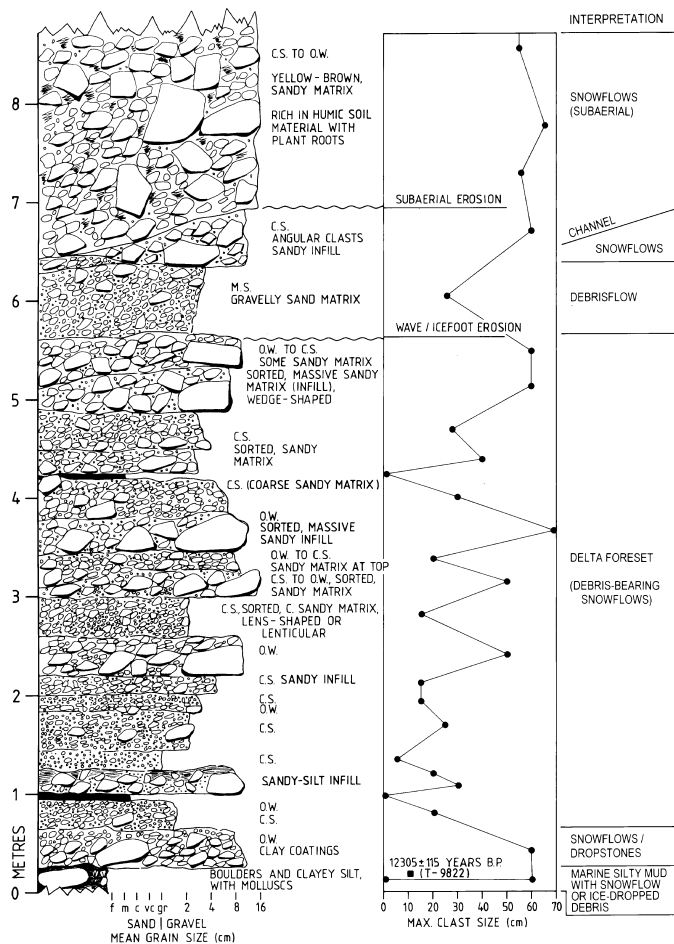


Fig. 36. Detailed log from the colluvial-fan delta at Gardvik (from outcrop section C in Fig. 3, bottom). Texture code CS and OW as in the captions to Fig. 9 & 29. The succession corresponds to stage 3 in Fig. 37.

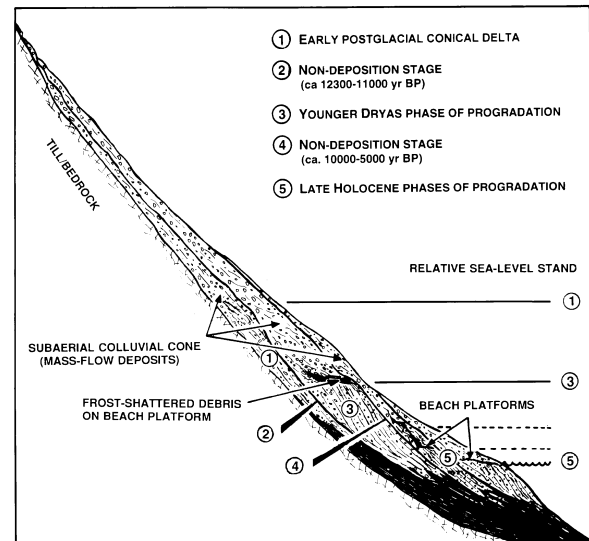


Fig. 37. Stratigraphic anatomy of the colluvial-fan delta at Gardvik (Fig. 3). Schematic diagram; the frame's length is *c.* 450 m and height *c.* 175 m; the total relative sea-level fall (1–5) is *c.* 50 m.

chiefly by high-viscosity debrisflows that descended from the mountain slope directly into the fjord. The oldest radiocarbon date from mollusc shells found at the stratigraphic top of this steeply bedded facies assemblage is 12400 years BP, which indicates deposition directly after the deglaciation. This early stage would thus be coeval with stage 1 of the Tomrefjord fan delta.

Stage 2. Deposits correlative with stage 2 of the latter fan delta are negligible here. A thin layer of shell-bearing, well-sorted fine sand, dated to *c.* 12300 years BP, indicates a period of marked decrease in slope-waste processes. Scattered cobbles and boulders with pebbly sand 'patches' (thin lenses) suggest sporadic snow avalanches, possibly powder snowflows, reaching the subaqueous slope. Some of the coarse debris could be derived by snowflow avalanches and further shed from a shoreline ice-foot. The marine sand layer is covered by a heterogeneous unit of chaotic, cobbly to bouldery gravel, whose clasts show clayey coatings and the interstices are partly filled with fine, silty sand. This composite unit suggests deposition from a series of snowflow avalanches slightly younger than 12300 years BP. The pause in colluvial sedimentation was probably due to the temporal depletion of the slope source by the preceding phase of mass wastage and possibly a local climatic effect (e.g. change of prevalent wind direction).

Stage 3. The overlying succession of cobbly to bouldery gravel beds (Figs 36 and 37) indicates an

alternation of subaqueously emplaced debris-flows and snowflows. This dramatic increase in slope-waste processes represents the Younger Dryas climatic cooling, as is indicated by the associated palaeobeach, rich in frost-shattered gravel, at an altitude of 25–30 m (Figs 26B and 37). Some snowflows were apparently halted in the beach zone, but most of the avalanches bypassed the latter, causing considerable accretion and progradation on the subaqueous slope. The subaerial part of this facies assemblage is dominated by bouldery deposits attributed to dense snowflows (Figs 26A and 36).

Stage 4. No deposits from the first half of the Holocene epoch are found in this colluvial system, which indicates a relatively long break between the Younger Dryas sedimentation and the onset of the Holocene slope-waste processes. This hiatus is regionally correlative.

Stage 5. The overlying subaerial deposits (Fig. 37), covering also the emerged slope of the fan delta, represent mainly debris-laden snowflows. Radiocarbon dates indicate that this stage of deposition commenced not much earlier than 4300 years BP (Blikra, 1994). The facies characteristics and intervening palaeosol horizons suggest several pulses of snow-avalanche activity separated by periods of slopewash, with the redeposition of contemporaneous soil. The available radiocarbon dates from this facies assemblage suggest a high incidence of snow avalanches shortly after *c.* 4300 years BP, then from slightly before 3500 until *c.* 3200 years BP, and two more pulses after 3200 and *c.* 3100 years BP, respectively.

More recently, a stream channel has been incised in the emerged colluvial system (Fig. 3). This phase of waterflow activity is probably younger than *c.* 3000 years BP and indicates an increase in seasonal rainfall and surficial runoff. The gully carries mainly water from the spring snow-melt and heavy autumn rains, causing vigorous redeposition of the colluvium. The streamflow and gully-conveyed avalanches, mainly snowflows, have built a small, secondary delta lobe at sea level (Fig. 37).

Rockfall-dominated colluvial systems

Colluvial fans and aprons dominated by rockfall avalanches are generally the steepest, and are sourced by very steep, weathered bedrock cliffs with little capacity for snow accumulation. Systems of this type are more common in the outer coastal zone (Fig. 1), where the mountain slopes

have lesser altitudes (Fig. 5A). The stratigraphic sections of these colluvial systems are not well-exposed, and also the radiocarbon dates on rockfall deposits are relatively few. Therefore, the stratigraphic model of a rockfall-dominated fan delta (Fig. 38) is a tentative compilation from several localities, including the colluvial systems at Midsund and Stormyr, Oterøya (localities 14 in Fig. 1). The recognizable depositional stages (Fig. 38) are correlative with those distinguished in the other fan deltas (Figs 35 and 37).

Stage 1. The oldest part of a rockfall-dominated fan delta is typically an assemblage of matrix-rich gravel beds resting directly on the mountain slope, with a marked backlap (Fig. 38). These are mainly deposits of high-viscosity debrisflows. This early stage of deposition is attributed to the vigorous resedimentation of glacial till almost concurrently with the deglaciation, for the glaciogenic mantle on a cliff-like slope must have been extremely prone to gravitational failures.

Stage 2. There is little record of rockfall avalanches at the early postglacial stage, whereas the overlying colluvial deposits apparently represent the Younger Dryas. A phase of nondeposition and weathering is thought to have occurred, which is hardly recognizable in a sedimentary succession, apart from a possible

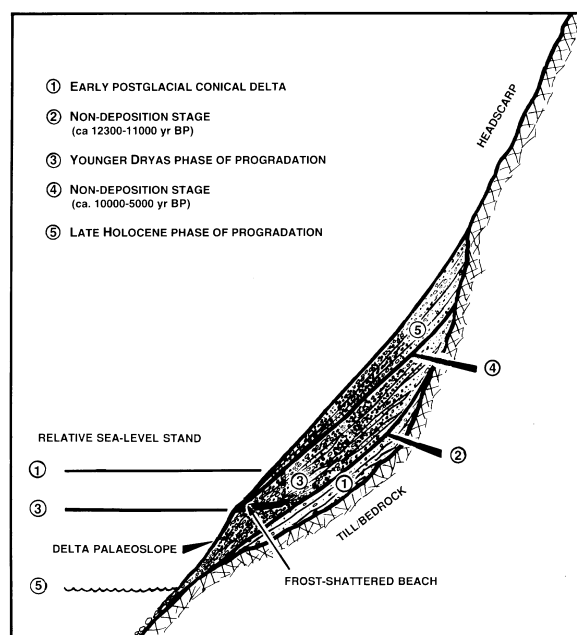


Fig. 38. Stratigraphic anatomy of a postglacial colluvial-fan delta dominated by rockfall avalanches. Schematic compilation from several localities; the frame's length is *c.* 360 m and height *c.* 250 m; the total relative sea-level fall (1–5) is *c.* 50 m.

drape of marine fines on the subaqueous slope of a fan delta. We have few radiocarbon data to assess the time-span of stage 2 in rockfall-dominated systems, but the resedimentation of glacial till in these cases was probably very early and relatively fast, and the following hiatus in slope-waste processes was thus likely longer than in the other systems.

Stage 3. The overlying deposits are bouldery to cobbly, openwork rockfall gravels alternating with the clast-supported, cobbly to pebbly deposits of low-viscosity debrisflows. The lack of any intervening palaeosols and the occurrence of frost-shattered gravelly palaeobeach facies at the altitude of Younger Dryas palaeoshoreline indicate that this stage of slope wastage represents the well-known phase of regional climatic cooling, dated elsewhere to *c.* 11 000–10 000 years BP.

Stage 4. There is no record of rockfall processes from the first half of the Holocene epoch, which indicates another major hiatus in the rockfall-dominated colluvial systems.

Stage 5. The younger colluvium is dominated by rockfall deposits, commonly separated by interlayers of humic soil material derived by contemporaneous slopewash (Fig. 9). The radiocarbon dates from these palaeosols indicate deposition in the second half of the Holocene epoch. This wedge-shaped facies assemblage is slightly steeper and has a lesser downdip extent, pinching out near the slope break of the Younger Dryas palaeoshoreline (Fig. 38). The limited downslope extent probably reflects the decreased volume and/or free-fall height of rockfall ava-

lanches, due to the source depletion and the progressive backlap of the mountain cliff. Only some exceptionally large rockfalls occasionally reach the low-lying modern shoreline and come to rest on the steep underwater slope (Fig. 38).

PALAEOCLIMATIC RECORD

The stratigraphic analysis of the postglacial colluvium in western Norway has shown that the local sedimentary successions bear an important record of climatic changes (Blikra & Nemec, 1993a; Blikra, 1994; Blikra & Longva, 1995; Blikra & Nesje, 1997; Blikra & Selvik, 1998). More than 100 radiocarbon (^{14}C) dates of humic palaeosols, wood fragments, mollusc shells and organic carbon-rich mud have been derived from over 20 localities. The colluvial successions show a consistent, regionally correlative record indicating periods of pronounced slope wastage and periods of relative stagnation. The regional data are compiled in Fig. 39 in terms of the main avalanche categories, and are discussed further below.

Avalanches and climate

The avalanche processes in mountainous terrains are generally controlled by both climate and the local slope conditions (topographic gradient, altitude range, orientation relative to main winds, and debris source type). Colluvial systems are characterized by highly episodic sedimentation

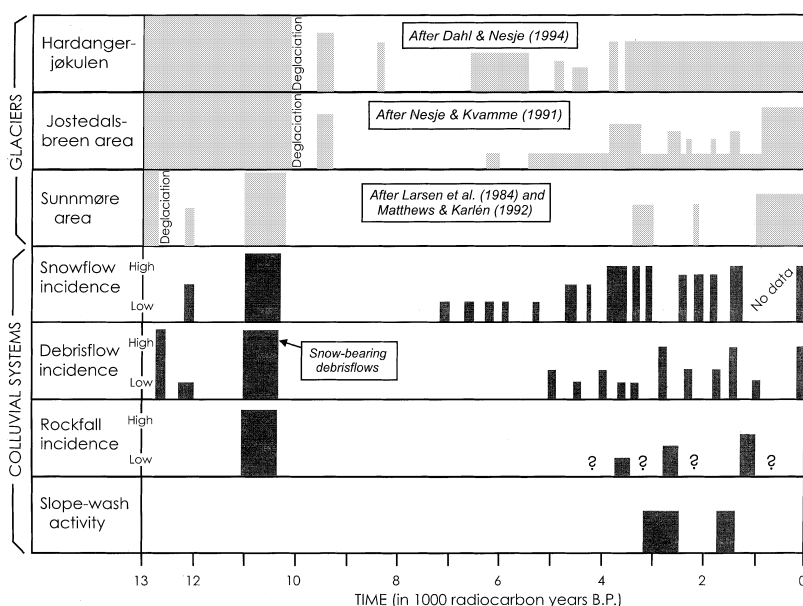


Fig. 39. The chronostratigraphy and intensity of the main colluvial processes, based on a compilation of data from more than 20 local successions, compared with the record of glacier development and ice-front oscillations in Sunnmøre area (Larsen *et al.*, 1984; Matthews & Karlén, 1992), Jostedal-breen area (Nesje & Kvamme, 1991) and Hardangerjøkulen area (Dahl & Nesje, 1994). The activity of particular processes has been estimated qualitatively on the basis of the abundance of their deposits.

and are thus more likely to respond to major climatic changes than to minor fluctuations. For example, a climatic change must bring sufficient cooling, or enough rainfall, to be 'recognized' by the dynamics of a colluvial system. Further, the local slopes may have different thresholds of response to a particular climatic change, and this variation may cause 'random noise' in the regional record. It is therefore very meaningful that the climatic record shown in the postglacial colluvium in Norway is legible and regionally correlative.

Climate is widely recognized to be the principal control on colluvial sedimentation, with different processes generally related to somewhat different conditions (Campbell, 1975; Caine, 1980; Rapp & Nyberg, 1981, 1988; Eisbacher & Clague, 1984; Fitzharris & Bakkehøi, 1989; Jibson, 1989; Kortarba, 1991; Luckman, 1992; González Díez *et al.*, 1996; Wieczorek & Jäger, 1996). The incidence of snow avalanches is generally related to cold winters and depends on snowfall intensity, prevalent wind direction and snow-drift rate. This relationship is thought to be reflected, for example, in the high incidence of snow avalanches during the cold Younger Dryas (Blikra & Nemec, 1993a; Blikra & Nesje, 1997) and the Little Ice Age, AD 1450–1920 (Grove, 1972). Rockfalls, although directly related to bedrock weathering, are likely here to have been triggered mainly by the air temperature variations (freeze-thaw cycles) and the effects of rainstorms and snowpack. The incidence of debrisflows might depend on a wider range of factors, including local slope conditions and the more recent anthropogenic activity (Innes, 1983). Some debrisflows could be triggered by the impact of rockfalls and snowflows on fan apices. Debrisflow deposits predominate at some localities but are sparse or absent at others, which suggests an important role of local conditions. However, the main cause of debrisflows was the slumping of glacial deposits and upper colluvium, probably due to heavy rainfall or meltwater runoff and thus related mainly to climate. For example, the increase in debrisflow processes at the end of the Little Ice Age has been attributed to permafrost degradation and the higher proportion of rainfall in annual precipitation (Van Steijn, 1996).

The following discussion puts special emphasis on the regional record of snowflow avalanches, because these processes are more closely related to climate and also because the radiocarbon dates on snowflow deposits are more abundant.

Snowflow record

There is a good regional evidence of abundant snow avalanches around 12 300–12 000 years BP (Fig. 39), when the climate is thought to have been cold, but fluctuating (Karpuz & Jansen, 1992). This earliest record of snow avalanches and the frost-shattered coeval palaeobeaches (Blikra & Longva, 1995) lend strong support to the notion of cold climatic conditions in the Older Dryas time, contrary to the opinion of some other authors (Broecker, 1992). The majority of the colluvial systems further show a distinct pulse of snowflow processes corresponding to the Younger Dryas phase of climatic cooling, *c.* 11 000–10 000 years BP (Fig. 39). A major hiatus separates these early postglacial phases of pronounced snow-avalanche activity from the phase that followed the Holocene climatic optimum. A similar hiatus has been recognized in the adjacent Jostedalsbreen area, where the available radiocarbon dates from the palaeosols and peat layers separating avalanche deposits from the underlying glacial till are consistently younger than the Holocene optimum (Nesje *et al.*, 1991, 1994).

The Holocene regional record of snow avalanches indicates a progressive climatic deterioration and increasingly colder winter conditions since at least *c.* 4700 years BP. Shorter-term climatic fluctuations are indicated by the intervening debrisflow and waterlain deposits, including local peat layers and common occurrences of humic soil redeposited by contemporaneous slope wash. A regional climatic deterioration since at least *c.* 5000 years BP is indicated also by the published dates and palynological data on palaeosols (Matthews & Dresser, 1983; Matthews & Caseldine, 1987).

Some of the local colluvial systems, with catchments at high altitudes or particularly prone to snow-drift accumulation, show the first evidence of Holocene snow avalanches as early as *c.* 7000 years BP. Other localities show the onset of Holocene avalanche sedimentation as late as *c.* 4700 years BP, with at least two consecutive pulses of pronounced slope wastage. This apparent diachroneity of the initiation of slope-waste processes after the Holocene climatic optimum is meaningful, as it probably reflects the varied response threshold of the local mountain slopes to the regional climatic deterioration.

An increase in snow avalanches occurred between *c.* 3800 and *c.* 3000 years BP, although the intervening local palaeosols indicate phases

of nondeposition and slope stability. The subsequent decline in snowflows was followed by at least three marked pulses between *c.* 2500 and *c.* 1800 years BP, separated by phases of mainly waterflow processes. The youngest prehistorical record of snow avalanches indicates a regional pulse around 1400 years BP. Historical evidence (Grove, 1972) and lichenometric data (McCarroll, 1993) indicate an increase in snow avalanches during the Little Ice Age.

Debrisflow record

The colluvial successions at some localities indicate a pulse of debrisflows directly after the deglaciation, around 13 000 years BP, prior to the onset of the Holocene sedimentation *c.* 10 000 years BP (Blikra & Nesje, 1997). However, the main activity of these processes dates to the late Holocene (Fig. 39). Some mid-Holocene debrisflows, dated as younger than *c.* 5000 years BP, accompanied snow avalanches on several fans or were roughly coeval with such avalanches on other fans. The association of the two processes, although not a rule, is recognizable more often in the younger Holocene colluvium. The deteriorating climate was probably seasonal, with sharper winters, and the increase in snowfall might have caused snow avalanches in the winter and early spring, and debrisflows during the snow-melt season and summer/autumn rains (Rapp & Nyberg, 1981, 1988). Jonasson (1991) has recognized an increase in colluvial processes, particularly debrisflows, in other parts of Scandinavia from *c.* 4600 until *c.* 3800 years BP.

Our radiocarbon data on the Holocene debrisflow deposits are quite limited, but the dates are consistently younger than 5000 years BP and indicate several pulses of debrisflow processes (Fig. 39). The dates are mainly from the local palaeosols that separate debrisflow lobes or levées from the underlying colluvium or glacial till. The greater abundance of younger debrisflow deposits suggests that some kind of geomorphic threshold has been reached by the mountain slopes around 3000 years BP, possibly due to the climatic deterioration, creep processes, slope-stripping by snow avalanches and anthropogenic deforestation. Soil erosion and the increased weathering of the glacial mantle, enhanced by vegetation, are likely to have caused the more recent debrisflows on slopes of quite modest gradients. The crystalline bedrock renders plant-root growth a destabilizing agent for the mantle. A similar increase in debrisflow processes around 3000–2500 and 500–

300 years BP has been recognized in other parts of Europe (Selby, 1982; Innes, 1983; Brazier & Ballantyne, 1989; González Díez *et al.*, 1996). Kotarba (1991) has noted an increase in debrisflows in the Polish Tatra Mountains at the end of the Little Ice Age.

The late Holocene increase in debrisflow processes correlates with an increase in waterflow activity on the colluvial slopes (Blikra & Nesje, 1997). Likewise, the dating of solifluction lobes in the Jostedalsgreen area (Nesje *et al.*, 1989) indicates that the creep processes there commenced *c.* 3200–2800 years BP. In Jotunheimen area, Matthews *et al.* (1986) have recognized an increase in slopewash processes from *c.* 3000 years BP and an increase in solifluction rate from *c.* 1000 years BP.

Although some debrisflows have apparently been associated or coeval with snowflows, the regional compilation of data suggests that the pronounced pulses of the two processes tended to *alternate* with each other, rather than be coeval (Fig. 39). The climatic conditions conducive to debrisflows were probably different from those causing snow avalanches. The record of snow avalanches is thought to reflect an increase in snowstorm frequency, whereas the record of debrisflows, as well as solifluction, reflects milder climatic conditions and an increase in high-intensity rainfall (Sandersen *et al.*, 1996). The latter suggestion is supported by the record of waterflow processes (Blikra & Nesje, 1997); local palaeobotanical data indicate a warmer climate and forestation by abundant deciduous trees during periods with few or no snow avalanches (Blikra, 1994; Blikra & Selvik, 1998); and radiocarbon data support the onset of peat formation in the outer coastal zone of the Sunnmøre area (Solem, 1989).

Rockfall record

The radiocarbon data on rockfall deposits are relatively few (Blikra & Nesje, 1997), but some periods of pronounced rockfall processes can tentatively be recognized (Fig. 39). The oldest rockfall deposits correspond to the Younger Dryas phase of climatic cooling, and are separated by a regional hiatus from the rockfall deposits of middle to late Holocene age. Rockfall avalanches in the middle Holocene were infrequent and occurred probably as a seasonal phenomenon related to the early phase of climatic deterioration and/or increased precipitation. Nesje, Blikra & Anda (1994) have used the Schmidt-hammer

method to estimate the age of the deposits of two large rockfalls in Norangsdalen, western Norway, and concluded that these were younger than *c.* 6000 years BP.

The Holocene colluvial record in the study area suggests an increase in rockfall processes since *c.* 3800 years BP, which probably reflects the late Holocene climatic deterioration, with sharper, colder winters and more rainy summers. The rockfall deposits are locally separated by palaeosols, which indicate climatic fluctuations and relatively long phases of nondeposition and slope stability. Rockfall processes are enhanced by freeze-thaw cycles, but often triggered by thunderstorms, heavy rainfall and/or snowpack melting (Sandersen *et al.*, 1996).

DISCUSSION

The colluvial record has further been compared with the proxy record of atmospheric temperature variations based on the mountain glacier fluctuations in the Sunnmøre, Jostedalsbreen and Jotunheimen areas (Nesje & Kvamme, 1991; Matthews & Karlén, 1992; Nesje & Dahl, 1993) and the Hardangerjøkulen area further to the south (Dahl & Nesje, 1994). The two types of palaeoclimatic record, although based on quite different criteria, show a remarkably good agreement (Fig. 39). The glacier-derived record indicates an overall climatic deterioration from at least 6000 years BP, and the pattern of ice-front oscillations corresponds quite well with the colluvial record. The Holocene phases of pronounced snow-avalanche activity can readily be correlated with the neoglacial stages; except, perhaps, for the phase of climatic cooling around 9000 years BP, for which no avalanche record has been recognized in the colluvial successions. The record from Jostedalsbreen indicates neoglacial stages dated to *c.* 6000, 3700–3100, 2600–2100, *c.* 1800 and < 1400 years BP. The Jotunheimen record shows a neoglacial stage around 6400–5900 years BP, whereas the record from Sunnmøre indicates neoglacial stages around 3400–3000, 2200–2100, < 1600 and < 1000 years BP (Matthews & Karlén, 1992). The record from Hardangerjøkulen indicates neoglacial stages around 6300–5200, 4750–3900 (several phases) and < 3800 years BP. Based on the radiometric data on peat growth and humification, Matthews (1991) has inferred periods of pronounced climatic deterioration around 5700, 4300–3200 and 1750–1300 years BP. All these data correspond rather well with the colluvial

record. It is worth noting also that the resolution of the colluvial record is, in fact, significantly higher than that of the other data types.

Nevertheless, the correspondence of the colluvial and glacial records is by no means perfect, and the discrepancies require a comment. Firstly, one must be aware that a glacier-derived record has a limited resolution, bears many uncertainties and necessarily reflects the local conditions only. Notably, there are many discrepancies between the records from the different glaciers (Fig. 39). For comparison, snow avalanches are seasonal phenomena, and their dependence on local conditions is far less critical when the overall record from a larger number of localities is compiled. Secondly, the climatic aspects reflected in the glacier dynamics and the colluvial-slope dynamics may not be the same, and also the response thresholds of glaciers and colluvial systems with respect to climatic changes may be different. Arguably, the record of ice-front oscillations reflects the net rate of snow accumulation, which means both the winter snowfall rate and the summer air temperatures. The record of snow avalanches, in contrast, is likely to reflect the snowfall rate and the occurrence of snowstorms, which means the winter conditions alone.

If the latter notion is correct, the relatively good correspondence between the two types of palaeoclimatic record may indicate that the glacier oscillations in western Norway have been controlled mainly by the winter conditions. Furthermore, the discrepancy between the records from Hardangerjøkulen and Jostedalsbreen for 6300–4000 years BP may suggest that the glacier dynamics in the former area were more related to the snowfall rate, whereas the effect of annual temperature variations was more important in the latter area. In short, it is crucial to compare different types of climatic proxy record, because their correspondence and discrepancies may be quite meaningful.

CONCLUSIONS

Colluvial depositional systems are one of the unexplored frontiers of clastic sedimentology. *Colluvium*, in striking contrast to its sister *alluvium*, is hardly mentioned in sedimentological textbooks and has virtually been ignored in the recent development of clastic facies models. Modern colluvial deposits, due to their unsorted and seemingly chaotic nature, have commonly been regarded as nearly intractable 'slope breccias', and

the colluvial systems have thus drawn little sedimentological interest. Relatively few ancient colluvial successions have been reported (see review in Nemec & Kazancı, 1999), although their preservation potential should not necessarily be much lower than that of 'footwall' alluvial fans or valley-fill alluvium, which have commonly been recognized in the ancient record. One may reasonably suspect that colluvial deposits in basinal studies were often lumped as proximal fanglomerates, simply because the sedimentological criteria for their distinction were not available.

The postglacial colluvium in western Norway, related to the steep mountain slopes of valley sides and fjord margins, comprises deposits of slope-waste avalanches ranging from rockfalls/debrisfalls to debrisflows and snowflows, with some role played also by waterflow and debris-creep processes. The sediment provenance here is specific, involving gneissic bedrock and its glacial mantle, and the colluvial facies assemblages range from subaerial to subaqueous. The study has focused on the processes of sediment movement and their depositional products, with special emphasis on snow avalanches, whose role as a depositional agent was unexplored by sedimentologists.

The chronostratigraphic analysis of the local colluvial successions indicates that these deposits bear an important proxy record of regional palaeoclimatic changes. This aspect is particularly well-shown by the colluvial-fan deltas, whose varied facies assemblages and bedding architecture reflect the combined record of climate and relative sea-level changes.

Although it is true that colluvial systems depend upon the local slope conditions and that a particular genetic facies may not be a reliable palaeoclimatic indicator (Van Steijn *et al.*, 1995), our field studies lead us to contend that the stratigraphic changes in colluvial facies assemblages reflect significant climatic changes. This notion is supported by the regional correlation of local facies changes and their good correspondence with other types of regional palaeoclimatic data (see also Nemec & Kazancı, 1999).

The palaeoclimatic record deciphered from the colluvial successions corresponds quite well with the record of alpine glacier fluctuations in western Norway, and seems to have, in fact, a much higher resolution than the latter type of climatic proxy data. Therefore, it may be concluded that the colluvial systems have acted as sensitive recorders of regional climatic changes. However, it should be emphasized that colluvial systems

are also highly dependent upon local slope conditions, and the palaeoclimatic record is thus most legible when facies data from a larger number of localities are compiled in chronostratigraphic terms.

The study demonstrates that colluvial fans and aprons, with their specific range of processes and high sensitivity to changes in climatic conditions, are a fascinating type of depositional system. Comparative studies should show how the signal of Quaternary climatic changes has been recorded in colluvial successions in other regions, in a wider range of climatic zones (Nemec & Kazancı, 1999).

ACKNOWLEDGMENTS

The study was sponsored by the Geological Survey of Norway (NGU), with additional financial support from the Norwegian Research Council (NFR) and the University of Bergen. Einar Anda, Oddvar Longva and Dag Ottesen are thanked for helpful discussions and field assistance. The radiocarbon dating of samples was done by S. Gulliksen at the Radiological Dating Laboratory in Trondheim. Figures were drafted by B. Svendgård and I. Lundquist (NGU). The manuscript was critically reviewed by Björn Andersen, Brian Jones, Eiliv Larsen, George Postma and Henk Van Steijn. This project represents activities of the Norwegian Research Group for Quaternary Sedimentology (NFKS).

REFERENCES

- Aanstad, K.M., Gabrielsen, R.H., Hagevang, T., Ramberg, I.B. and Torvanger, O. (1981) Correlation of offshore and onshore structural features between 62°N and 68°N, Norway. In: *Proc. 11th Symp. Norwegian Sea Exploration*, pp. 1–24. Norwegian Petroleum Society, Stavanger.
- Allen, J.R.L. (1984) *Sedimentary Structures – Their Character and Physical Basis*, Vol. II. Elsevier, Amsterdam.
- Ambach, W. and Howorka, F. (1966) Avalanche activity and free water content of snow at Obergurgl (1980 m a.s.l., spring 1962). In: *Proc. Int. Symp. Scientific Aspects of Snow and Ice Avalanches* (Davos 1965). *Int. Assoc. Sci. Hydrol. Publ.*, **69**, 65–72.
- Auzet, A.-V. and Ambroise, B. (1996) Soil creep dynamics, soil moisture and temperature conditions on a forested slope in the granitic Vosges Mountains, France. *Earth Surf. Proc. Landf.*, **21**, 531–542.
- Bagnold, R.A. (1954) Experiments on a gravity-free dispersion of large solid spheres in a Newtonian fluid under shear. *Proc. R. Soc. London*, **A255**, 49–63.

- Bakkehøi, S., Cheng, T., Domaas, U., Lied, K., Perla, R. and Schieldrop, B. (1981) On the computation of parameters that model snow avalanche motion. *Can. Geotech. J.*, **18**, 1–10.
- Bakkehøi, S., Domaas, U. and Lied, K. (1983) Calculation of snow-avalanche runout distance. *Ann. Glaciol.*, **4**, 24–29.
- Barsch, A. (1988) Rock glaciers. In: *Advances in Periglacial Geomorphology* (Ed. by M.J. Clark), pp. 69–90. John Wiley & Sons, Chichester.
- Bates, R.L. and Jackson, J.A. (eds) (1987) *Glossary of Geology*. 3rd ed., American Geological Institute, Fall Church (Virginia).
- Baumberger, T., Heslot, F. and Perrin, B. (1994) Cross-over from creep to inertial motion in friction dynamics. *Nature*, **367**, 544–546.
- Bertran, P., Coutard, J.-P., Francou, B., Ozouf, J.-C. and Texier, J.-P. (1994) New data on grèzes bedding and their palaeoclimatic implications. In: *Cold Climate Landforms* (Ed. by D.J.A. Evans), pp. 437–455. John Wiley & Sons, Chichester.
- Bertran, P., Francou, B. and Texier, J.-P. (1995) Stratified slope deposits: the stone-banked sheets and lobes model. In: *Steepland Geomorphology* (Ed. by O. Slaymaker), pp. 147–169. John Wiley & Sons, Chichester.
- Bertran, P., Hétu, B., Texier, J.-P. and van Steijn, H. (1997) Fabric characteristics of subaerial slope deposits. *Sedimentology*, **44**, 1–16.
- Beverage, J.P. and Culbertson, J.K. (1964) Hyperconcentration of suspended sediment. *Proc. Am. Soc. Civ. Engrs., J. Hydraul. Div.*, **90**, 117–128.
- Bjerrum, L. and Jørstad, F. (1968) Stability of rock slopes in Norway. *Norw. Geotech. Inst. Publ.*, **79**, 1–11.
- Blikra, L.H. (1994) *Postglacial Colluvium in Western Norway: Sedimentology, Geomorphology and Palaeoclimatic Record*. Unpubl. Dr.Scient. thesis, University of Bergen.
- Blikra, L.H., Hole, P.A. and Rye, N. (1989) Rapid mass movements and related deposits in alpine areas, Indre Nordfjord, western Norway. *Nor. Geol. Unders. Skrift.*, **92**, 1–17. (In Norwegian, with an English abstract).
- Blikra, L.H. and Longva, O. (1995) Frost-shattered debris facies of Younger Dryas age in the coastal sedimentary successions in western Norway. *Palaeogeogr. Palaeoclim. Palaeoecol.*, **118**, 89–110.
- Blikra, L.H. and Nemec, W. (1993a) Postglacial avalanche activity in western Norway: depositional facies sequences, chronostratigraphy and palaeoclimatic implications. *Paläoklimaforsch.*, **11**, 143–162.
- Blikra, L.H. and Nemec, W. (1993b) Postglacial fan deltas in western Norway: a case study of snow avalanche-dominated, colluvial fans prograding into deep fjords. In: *Abstr. 3rd Int. Workshop on Fan Deltas*, pp. 1–4. University of Seoul.
- Blikra, L.H. and Nesje, A. (1997) Holocene avalanche activity in western Norway: chronostratigraphy and palaeoclimatic implications. *Paläoklimaforsch.*, **19**, 299–312.
- Blikra, L.H. and Selvik, S. (1998) Palaeoclimatic signals recorded in snow avalanche-dominated colluvium, western Norway: depositional facies successions, chronostratigraphy and pollen records. *The Holocene*, in press.
- Bolt, B.A., Horn, W.L., Macdonald, G.A. and Scott, R.F. (1975) *Geological Hazards*. Springer-Verlag, Berlin.
- Brabb, E.E. and Harrod, B.L. (eds) (1989) *Landslides: Extent and Economic Significance*. A.A. Balkema, Rotterdam.
- Brazier, V. and Ballantyne, C.K. (1989) Late Holocene debris cone evolution in Glen Feshie, western Cairngorm Mountains, Scotland. *Trans. R. Soc. Edinburgh, Earth Sci.*, **80**, 17–24.
- Broecker, W.S. (1992) Defining the boundaries of the late glacial isotope episodes. *Quater. Res.*, **38**, 135–138.
- Brown, R.L. (1979) A volumetric constitutive law for snow subjected to large strains and strain rates. *U.S. Army cold Reg. Res. Engin. Lab. Rep. (Hanover, N.H.)*, **79-20**, 13 pp.
- Brown, R.L. (1980a) Pressure waves in snow. *J. Glaciol.*, **25**, 99–107.
- Brown, R.L. (1980b) A volumetric constitutive law for snow based on a neck growth model. *J. Appl. Phys.*, **51**, 161–165.
- Brown, R.L. and Lang, T.E. (1973) On the mechanical properties of snow and relation to the snow avalanche. In: *Proc. 11th Ann. Symp. Engineering Geology and Soil Engineering*, pp. 19–36. University of Washington, Seattle.
- Brunsdon, D. (1979) Mass movements. In: *Process in Geomorphology* (Ed. by C. Embleton & J. Thornes), pp. 130–186. Edward Arnold, London.
- Bryan, K. (1922) Erosion and sedimentation in the Papago country, Arizona. *U.S. Geol. Surv. Bull.*, **730**, 19–90.
- Caine, N. (1980) The rainfall intensity-duration control of shallow landslides and debris flows. *Geogr. Ann.*, **62A**, 23–27.
- Campbell, R.H. (1975) Soil slips, debris flow, and rainstorms in the Santa Monica Mountains and vicinity, southern California. *Prof. Pap. U.S. Geol. Surv.*, **851**, 1–51.
- Campbell, C.S. (1986) The effect of microstructure development on the collisional stress tensor in a granular flow. *Acta Mech.*, **63**, 61–72.
- Campbell, C.S. (1989a) The stress tensor for simple shear flows of a granular material. *J. Fluid Mech.*, **203**, 449–473.
- Campbell, C.S. (1989b) Self-lubrication of long runout landslides. *J. Geol.*, **97**, 653–665.
- Campbell, C.S. (1990) Rapid granular flows. *Ann. Rev. Fluid Mech.*, **22**, 57–92.
- Campbell, C.S. and Brennen, C.E. (1983) Computer simulation of shear flows of granular material. In: *Mechanics of Granular Material: New Models and Constitutive Relations* (Ed. by J.T. Jenkins and M. Satake), pp. 313–326. Elsevier, Amsterdam.
- Campbell, C.S. and Brennen, C.E. (1985) Computer simulation of granular shear flows. *J. Fluid Mech.*, **151**, 167–188.

- Campbell, C.S. and Gong, A. (1986) The stress tensor in a two-dimensional granular shear flow. *J. Fluid Mech.*, **164**, 107–125.
- Carson, M.A. and Kirkby, M.J. (1972) *Hillslope Form and Processes*. Cambridge University Press, Cambridge.
- Cas, R.A.F. and Wright, J.V. (1987) *Volcaniclastic Successions – Modern and Ancient*. Allen and Unwin, Boston.
- Coates, D.F. (1967) Rock Mechanics Principles. *Can. Dept. Energy, Mines Resour., Mines Branch Monogr.*, **874**, 216 pp.
- Colbeck, S.C. (Ed.) (1980) *Dynamics of Snow and Ice Masses*. Academic Press, New York.
- Colbeck, B.D., Shaw, K.A. and Lemieux, G. (1978) The compression of wet snow. *U.S. Army Cold Reg. Res. Engin. Lab. Rep. (Hanover, N.H.)*, **79–20**, 13 pp.
- Collinson, J.D. and Thompson, D.B. (1982) *Sedimentary Structures*. George Allen & Unwin, London.
- Conway, H. and Raymond, C.R. (1993) Snow stability during rain. *J. Glaciol.*, **39**, 635–642.
- Corner, G.D. (1980) Avalanche impact landforms in Troms, North Norway. *Geogr. Ann.*, **62A**, 1–10.
- Costa, J.E. and Wieczorek, G.F. (eds) (1987) Debris Flows/Avalanches. *Process, Recognition, Mitigation. Geol. Soc. Am., Rev. Engin. Geol.*, **7**, 239 pp.
- Cruden, D.M. and Hungr, O. (1986) The debris of the Frank Slide and theories of rockslide-avalanche mobility. *Can. J. Earth Sci.*, **23**, 425–432.
- Dahl, S.O. and Nesje, A. (1994) Holocene glacier fluctuations at Hardangerjøkulen, central-southern Norway: a high-resolution composite chronology from lacustrine and terrestrial deposits. *The Holocene*, **4**, 269–277.
- Davison, C. (1889) On the creeping of the soil cap through the action of frost. *Geol. Mag.*, **6**, 255.
- Dent, J.D. and Lang, T.E. (1980) Modeling of snow flow. *J. Glaciol.*, **26**, 131–140.
- Dent, J.D. and Lang, T.E. (1982) Experiments on mechanics of flowing snow. *Cold Reg. Sci. Technol.*, **5**, 253–258.
- Dent, J.D. and Lang, T.E. (1983) A biviscous modified Bingham model of snow avalanche motion. *Ann. Glaciol.*, **4**, 42–46.
- Desrués, J.-F., Darve, F., Flavigny, E., Navarre, J.-P. and Taillefer, A. (1980) An incremental formulation of constitutive equations for deposited snow. *J. Glaciol.*, **25**, 289–307.
- Eisbacher, G.H. and Clague, J.J. (1984) Destructive mass movements in high mountains: hazard and management. *Pap. Geol. Surv. Can.*, **84–16**, 230 pp.
- Emery, J.J. (1978) Simulation of slope creep. In: *Rockslides and Avalanches, 1. Natural Phenomena* (Ed. by B. Voight), pp. 669–691. Elsevier, Amsterdam.
- Fareth, O.W. (1987) Glacial geology of Middle and Inner Nordfjord, western Norway. *Nor. Geol. Unders.*, **408**, 1–55.
- Feda, J. (1992) *Creep of Soils and Related Phenomena*. Elsevier, Amsterdam.
- Finlayson, B.L. (1981) Field measurements of soil creep. *Earth Surf. Proc. Landf.*, **6**, 35–48.
- Finlayson, B.L. (1985) Soil creep: a formidable fossil of misconception. In: *Geomorphology and Soils* (Ed. by K.S. Richards, R.R. Arnett and S. Ellis), pp. 141–158. Allen and Unwin, London.
- Fitzharris, B.B. and Bakkehøi, S. (1989) A synoptic climatology of major avalanche winters in Norway. *Publ. Nor. Geotech. Inst.*, **178**, 1–15.
- Fleming, R.W. and Johnson, A.M. (1975) Rates of seasonal creep of silty clay soil. *Quart. J. Engin. Geol.*, **8**, 1–29.
- Flint, R.F. (1971) *Glacial and Quaternary Geology*. John Wiley & Sons, New York.
- Follestad, F. (1990) Block fields, ice-flow directions and the Pleistocene ice sheet in Nordmøre and Romsdal, West Norway. *Nor. Geol. Tidsskr.*, **70**, 27–33.
- Frenzel, B., Matthews, J.A. and Gläser, B. (eds) (1993) Solifluction and Climatic Variation in the Holocene. *Paläoklimaforsch.*, **11**. Gustav Fischer Verlag, Stuttgart.
- Fukue, M. (1979) *Mechanical Performance of Snow Under Loading*. Tokai University Press, Tokyo.
- Gabrielsen, R.H., Førseth, R., Hamar, G. and Rønnevik, H. (1984) Nomenclature of the main structural features on the Norwegian Continental Shelf north of the 62nd parallel. In: *Petroleum Geology of the North European Margin* (Ed. by A.M. Spencer), pp. 41–60. Graham and Trotman, London.
- Giardino, J.R., Shroder, J.F. and Vitek, J.D. (eds) (1987) *Rock Glaciers*. Allen and Unwin, London.
- Glen, J.W., Adie, R.J., Johnson, D.M. and Homer, D.R. (eds) (1980) Symposium on Snow in Motion. *J. Glaciol.*, **26**, spec. issue 94, 526 pp.
- González Díez, A., Salas, L., Díaz de Terán, J.R. and Cendrero, A. (1996) Late Quaternary climate changes and mass movement frequency and magnitude in the Cantabrian region, Spain. *Geomorphology*, **15**, 291–309.
- Goudie, A., Atkinson, B.W., Gregory, K.J., Simmons, I.G., Stoddart, D.R. and Sugden, D. (1985) *The Encyclopedic Dictionary of Physical Geography*. Blackwell, Oxford.
- Gray, D.M. and Male, D.H. (eds) (1981) *Handbook of Snow*. Pergamon Press, Toronto.
- Grimstad, E. and Nesdal, S. (1991) The Loen rockslides — a historical review. *Publ. Norw. Geotech. Inst.*, **182**, 1–6.
- Grove, J.M. (1972) The incidence of landslides, avalanches, and floods in western Norway during the Little Ice Age. *Arct. Alp. Res.*, **4**, 131–138.
- Gubler, H. (1982) Strength of bonds between ice grains after short contact times. *J. Glaciol.*, **28**, 457–473.
- Gubler, H. (1989) Comparison of three models of avalanche dynamics. *Ann. Glaciol.*, **13**, 82–89.
- Gubler, H. and Bader, H.-P. (1989) A model of initial failure in slab-avalanche release. *Ann. Glaciol.*, **13**, 90–95.
- Haefeli, W.B. (1966) Creep and progressive failure in snow, soil, rock and ice. In: *Proc. 6th Int. Confer. Soil Mechanics Foundation Engineering*, **1**, 134–138.
- Haff, P.K. (1983) Grain flow as a fluid-mechanical phenomenon. *J. Fluid Mech.*, **134**, 401–430.

- Hampton, M.A. (1972) The role of subaqueous debris flows in generating turbidity currents. *J. Sedim. Petrol.*, **42**, 775–793.
- Hampton, M.A. (1975) Competence of fine-grained debris flows. *J. Sedim. Petrol.*, **45**, 834–844.
- Hampton, M.A. (1979) Buoyancy in debris flows. *J. Sedim. Petrol.*, **49**, 753–758.
- Harms, J.C., Southard, J.B., Spearing, D.R. and Walker, R.G. (1975) *Depositional Environments as Interpreted from Primary Sedimentary Structures and Stratification Sequences*. Short Course Lecture Notes no. 2, Society of Economic Paleontologists and Mineralogists, Tulsa.
- Harris, S. and Gustafson, C.A. (1988) Retrogressive slumps, debris flows and river valley development in icy, unconsolidated sediment on hills and mountains. *Z. Geomorph., N.F.*, **32**, 441–455.
- Hausen, H. (1971) Rockfalls, landslides and creep in the Canaries. *Acta Geogr.*, **23**, 1–42.
- Hermann, F. and Hutter, K. (1991) Laboratory experiments on the dynamics of powder-snow avalanches in the run-out zone. *J. Glaciol.*, **37**, 281–295.
- Hestnes, E. (1985) A contribution to the prediction of slush avalanches. *Ann. Glaciol.*, **6**, 1–4.
- Hirano, M. and Iwamoto, M. (1981) Measurement of debris flow and sediment-laden flow using a conveyor-belt flume in a laboratory. *Publ. Int. Assoc. Hyrdol. Sci.*, **133**, 225–230.
- Holmes, A. (1965) *Principles of Physical Geology*. 2nd edn. Thomas Nelson, London.
- Holmes, A. (1978) *Holmes Principles of Physical Geology*. 3rd edn. (Rev. by D.L. Holmes). Nelson, London.
- Hopfner, E.J. (1983) Snow avalanche motion and related phenomena. *Ann. Rev. Fluid Mech.*, **5**, 47–76.
- Hsü, K.J. (1975) Catastrophic debris streams (stürzströms) generated by rockfalls. *Bull. Geol. Soc. Am.*, **86**, 129–140.
- Hutter, K., Savage, S.B. and Nohguchi, Y. (1989) Numerical, analytical, and laboratory experimental studies of granular avalanche flows. *Ann. Glaciol.*, **13**, 109–116.
- Innes, J.L. (1983) Lichenometric dating of debris-flow deposits in the Scottish Highlands. *Earth Surf. Proc. Landf.*, **8**, 579–588.
- Jahn, A. (1989) The soil creep on slopes in different altitudinal and ecological zones of Sudetes Mountains. *Geogr. Ann.*, **71**, 161–170.
- Jibson, R.W. (1989) Debris flows in southern Puerto Rico. In: *Landslide Processes of the Eastern United States and Puerto Rico* (Ed. by A.P. Schultz and R.W. Jibson). *Spec. Pap. Geol. Soc. Am.*, **236**, 21–55.
- Johnson, A.M. (1970) *Physical Processes in Geology*. Freeman, Cooper & Co., San Francisco.
- Johnson, A.M. and Rodine, J.R. (1984) Debris flow. In: *Slope Instability* (Ed. by D. Brunsten and D.B. Prior), pp. 257–361. John Wiley & Sons, Chichester.
- Jonasson, J. (1991) *Holocene Slope Processes of Periglacial Mountain Areas in Scandinavia and Poland*. Doctoral thesis, UNGI Rapport **79**, University of Uppsala.
- Jullien, R., Meakin, P. and Pavlovitch, A. (1992) Three-dimensional model for particle-size segregation by shaking. *Phys. Rev. Lett.*, **69**, 640–643.
- Karpuz, N.K. and Jansen, E. (1992) A high-resolution diatom record of the last deglaciation from the SE Norwegian Sea: documentation of rapid climatic changes. *Paleoceanography*, **7**, 499–520.
- Keedwell, M.J. (1984) *Rheology and Soil Mechanics*. Elsevier Applied Science Publ., London.
- Keefer, D.K. and Johnson, A.M. (1983) Earth flows: morphology, mobilization, and movement. *Prof. Pap. U.S. Geol. Surv.*, **1264**, 1–56.
- Kent, P.E. (1965) The transport mechanism in catastrophic rockfalls. *J. Geol.*, **74**, 79–83.
- Kézdi, A. (1979) *Soil Physics*. Elsevier, Amsterdam.
- Kingery, D. (ed.) (1963) *Ice and Snow: Properties, Processes and Applications*. M.I.T. Press, Cambridge (Mass.).
- Kirkby, M.J. (1967) Measurement and theory of soil creep. *J. Geol.*, **75**, 359–378.
- Kotarba, A. (1991) On the ages and magnitude of debris flows in the Polish Tatra Mountains. *Bull. Pol. Acad. Sci., Earth Sci.*, **39**, 129–135.
- Kry, P.R. (1975) The relationship between the viscoelastic and structural properties of fine-grained snow. *J. Glaciol.*, **14**, 479–500.
- LaChapelle, E.R. (1977) Snow avalanches: a review of current research and applications. *J. Glaciol.*, **19**, 313–324.
- Lackinger, B. (1989) Supporting forces and stability of snow-slab avalanches: a parameter study. *Ann. Glaciol.*, **13**, 140–145.
- Lang, T.E. and Dent, J.D. (1983) Basal surface-layer properties in flowing snow. *Ann. Glaciol.*, **4**, 158–162.
- Lang, R.M., Leo, B.R. and Hutter, K. (1989) Flow characteristics of an unconstrained, non-cohesive, granular medium down an inclined, curved surface: preliminary experimental results. *Ann. Glaciol.*, **13**, 146–153.
- Lang, T.E., Nakamura, T., Dent, J.D. and Martinelli, M. Jr (1985) Avalanche flow dynamics with material locking. *Ann. Glaciol.*, **6**, 5–8.
- Langham, E.J. (1981) Physics and properties of snow-cover. In: *Handbook of Snow* (Ed. by D.M. Gray and D.H. Male), pp. 275–337. Pergamon Press, Toronto.
- Larsen, E., Eide, F., Longva, O. and Mangerud, J. (1984) Allerød-Younger Dryas climatic inferences from cirque glaciers and vegetational development in the Nordfjord area, western Norway. *Arct. Alp. Res.*, **16**, 137–160.
- Larsen, E., Longva, L. and Follestad, B. (1991) Formation of De Geer moraines and implications for deglaciation dynamics. *J. Quat. Sci.*, **6**, 263–277.
- Larsen, E., Sandven, R., Heyerdahl, H. and Hernes, S. (1995) Glacial geological implications of preconsolidation values in sub-till sediments at Skorgenes, western Norway. *Boreas*, **24**, 37–46.
- Lautridou, J.-P., Francou, B. and Hall, K. (1992) Present-day periglacial processes and landforms in mountain areas. *Permafr. Periglac. Proc.*, **3**, 93–101.

- Lawson, D.E. (1982) Mobilization, movement and deposition of active subaerial sediment flows, Matanuska Glacier, Alaska. *J. Geol.*, **90**, 279–300.
- Leliwa-Kopystynski, J. and Maeno, N. (1993) Ice/rock porous mixtures: compaction experiments and interpretation. *J. Glaciol.*, **39**, 643–652.
- Lied, K. (1989) The avalanche accident at Vassdalen, Norway, 5 March 1986. *Publ. Norw. Geotech. Inst.*, **178**, 1–14.
- Lied, K. and Bakkehøi, S. (1980) Empirical calculations of snow-avalanche run-out distance based on topographic parameters. *J. Glaciol.*, **26**, 165–177.
- Liestøl, O. (1974) Avalanche plunge-pool effect. *Norsk Polarinst. Årbok*, **1972**, 179–181.
- Lowe, D.R. (1976) Grain flow and grain flow deposits. *J. Sedim. Petrol.*, **46**, 188–199.
- Lowe, D.R. (1982) Sediment gravity flows, II. Depositional models with special reference to the deposits of high-density turbidity currents. *J. Sedim. Petrol.*, **52**, 279–297.
- Lubahn, J.D. and Felgar, R.P. (1961) *Plasticity and Creep of Metals*. John Wiley & Sons, New York.
- Luckman, B.H. (1971) The role of snow avalanches in the evolution of alpine talus slopes. In: *Slopes – Form and Process. Spec. Publ. Inst. Br. Geogr.*, **3**, 93–109.
- Luckman, B.H. (1977) The geomorphic activity of snow avalanches. *Geogr. Ann.*, **59A**, 31–48.
- Luckman, B.H. (1978) Geomorphic work of snow avalanches in the Canadian Rocky Mountains. *Arct. Alp. Res.*, **10**, 261–276.
- Luckman, B.H. (1992) Debris flows and snow avalanche landforms in the Lairig Ghru, Cairngorm Mountains, Scotland. *Geogr. Ann.*, **74A**, 109–121.
- Maeno, N., Nishimura, K. and Kaneda, Y. (1980) Viscosity and heat transfer in fluidized snow. *J. Glaciol.*, **26**, 263–274.
- Male, D.H. (1980) The seasonal snowcover. In: *Dynamics of Snow and Ice Masses* (Ed. by S.C. Colbeck), pp. 305–395. Academic Press, New York.
- Mangerud, J. (1980) Ice-front variations of different parts of the Scandinavian ice sheet, 13,000–10,000 years BP. In: *Studies in the Lateglacial of North-West Europe* (Ed. by W.H. Berger and J.E. Robinson), pp. 23–30. Pergamon Press, New York.
- Mangerud, J., Larsen, E., Longva, E. and Sønstegaard, E. (1979) Glacial history of western Norway 15,000–10,000 yr BP. *Boreas*, **8**, 179–187.
- Mantis, H.T. (Ed.) (1951) *Review of the Properties of Snow and Ice*. SIPRE Report, **4**, 174, pp. University of Minnesota, Minneapolis.
- Matthews, J.A. (1991) The late neoglacial ('Little Ice Age') glacier maximum in southern Norway: new ¹⁴C-dating evidence and climatic implications. *The Holocene*, **1**, 219–233.
- Matthews, J.A. and Caseldine, C.J. (1987) Arctic-alpine brown soils as a source of palaeoenvironmental information: further ¹⁴C dating and palynological evidence from Vestre Memurubreen, Jotunheimen, Norway. *J. Quat. Sci.*, **2**, 59–71.
- Matthews, J.A. and Dresser, P.Q. (1983) Intensive ¹⁴C dating of a buried palaeosol horizon. *Geol. Fören. Stockholm Förhandl.*, **105**, 59–63.
- Matthews, J.A., Harris, C. and Ballantyne, C.K. (1986) Studies on a gelifluction lobe, Jotunheimen, Norway: ¹⁴C chronology, stratigraphy, sedimentology and palaeoenvironment. *Geogr. Ann.*, **68**, 345–360.
- Matthews, J.A. and Karlén, W. (1992) Asynchronous neoglaciation and Holocene climatic change reconstructed from Norwegian glaciolacustrine sedimentary sequences. *Geology*, **20**, 991–994.
- McCarrol, D. (1993) Lichenometric and weathering-based dating of arctic-alpine slope processes and associated landforms. *Paläoklimaforsch.*, **11**, 325–337.
- McClung, D.M. (1979) Shear fracture precipitated by strain softening as a mechanism of dry slab avalanche release. *J. Geophys. Res.*, **84** (B7), 3519–3526.
- McClung, D.M. (1980) Creep and glide processes in mountain snowpacks. *Pap. Nation. Hydrol. Res. Inst. (Ottawa)*, **6**, 66 pp.
- McClung, D.M. and Lied, K. (1988) Statistical and geometrical definition of snow avalanche runout. *Publ. Nor. Geotech. Inst.*, **170**, 1–13.
- McClung, D.M. and Schaerer, P.A. (1983) Determination of avalanche dynamics friction coefficients from measured speeds. *Ann. Glaciol.*, **4**, 170–173.
- McClung, D.M. and Schaerer, P.A. (1985) Characteristics of flowing snow and avalanche impact pressures. *Ann. Glaciol.*, **6**, 9–14.
- McClung, D.M. and Tweedy, J. (1993) Characteristics of avalanching: Kootenay Pass, British Columbia, Canada. *J. Glaciol.*, **39**, 316–322.
- McTigue, D.F. (1982) A nonlinear constitutive model for granular materials: applications to gravity flows. *J. Appl. Mech.*, **49**, 291–296.
- Mears, A.I. (1980) A fragment-flow model of dry-snow avalanches. *J. Glaciol.*, **26**, 153–163.
- Mellor, M. (1978) Dynamics of snow avalanches. In: *Rockslides and Avalanches, 1. Natural Phenomena* (Ed. by B. Voight), pp. 753–792. Elsevier, Amsterdam.
- Melosh, H.J. (1983) Acoustic fluidization. *Am. Scient.*, **71**, 158–165.
- Melton, M.A. (1965) Debris-covered hillslopes of the southern Arizona desert – consideration of their stability and sediment contributions. *J. Geol.*, **73**, 715–729.
- Middleton, G.V. (1970) Experimental studies related to flysch sedimentation. In: *Flysch Sedimentology in North America* (Ed. by J. Lajoie). *Spec. Pap. Geol. Assoc. Can.*, **7**, 253–272.
- Middleton, G.V. and Southard, J.B. (1978) *Mechanics of Sediment Movement*. Short Course Lecture Notes no. 3, Society of Economic Paleontologists and Mineralogists, Eastern Section, Binghamton.
- Middleton, G.V. and Southard, J.B. (1984) *Mechanics of Sediment Movement*. Short Course Lecture Notes no. 3, 2nd ed., Society of Economic Paleontologists and Mineralogists, Tulsa.
- Narita, H. (1980) Mechanical behaviour and structure of snow under uniaxial tensile stress. *J. Glaciol.*, **26**, 275–282.
- Naylor, M.A. (1980) The origin of inverse grading in muddy debris flow deposits – a review. *J. Sedim. Petrol.*, **50**, 1111–1116.

- Nelson, F.E. (1985) A preliminary investigation of solifluction macrofabrics. *Catena*, **12**, 23–33.
- Nemec, W. (1990a) Deltas – remarks on terminology and classification. In: *Coarse-Grained Deltas* (Ed. by A. Colella and D.B. Prior). *Spec. Publ. Int. Ass. Sediment.*, **10**, 3–12.
- Nemec, W. (1990b) Aspects of sediment movement on steep delta slopes. In: *Coarse-Grained Deltas* (Ed. by A. Colella and D.B. Prior). *Spec. Publ. Int. Ass. Sediment.*, **10**, 29–73.
- Nemec, W. and Kazancı, N. (1999) Quaternary colluvium in west-central Anatolia: sedimentary facies and palaeoclimatic significance. *Sedimentology*, in press.
- Nemec, W. and Muszyński, A. (1982) Volcaniclastic alluvial aprons in the Tertiary of Sofia district (Bulgaria). *Ann. Geol. Soc. Polon.*, **52**, 239–303.
- Nemec, W. and Steel, R.J. (1984) Alluvial and coastal conglomerates: their significant features and some comments on gravelly mass-flow deposits. In: *Sedimentology of Gravels and Conglomerates* (Ed. by E.H. Koster and R.J. Steel). *Mem. Can. Soc. Petrol. Geol.*, **10**, 1–30.
- Nemec, W. and Steel, R.J. (eds) (1988) *Fan Deltas – Sedimentology and Tectonic Settings*. Blackie, London.
- Nesje, A., Aa, A.R., Kvamme, M. and Sønstegeard, E. (1994a) A record of late Holocene avalanche activity in Frudalen, Sogndalsdalen, western Norway. *Nor. Geol. Tidsskr.*, **74**, 71–76.
- Nesje, A., Anda, E., Rye, N., Lien, R., Hole, P.A. and Blikra, L.H. (1987) The vertical extent of the Late Weichselian ice sheet in the Nordfjord-Møre area, western Norway. *Nor. Geol. Tidsskr.*, **67**, 125–141.
- Nesje, A., Blikra, L.H. and Anda, E. (1994b) Dating rock-avalanche deposits from degree of rock-surface weathering by Schmidt-hammer tests: a study from Norangsdalen, Sunnmøre, Norway. *Nor. Geol. Tidsskr.*, **74**, 108–113.
- Nesje, A. and Dahl, S.O. (1993) Lateglacial and Holocene glacier fluctuations and climate variations in western Norway: a review. *Quat. Sci. Rev.*, **12**, 255–261.
- Nesje, A., Dahl, S.O. and Løvlie, R. (1995) Late Holocene glaciers and avalanche activity in the Ålfotbreen area, western Norway: evidence from a lacustrine sedimentary record. *Nor. Geol. Tidsskr.*, **75**, 120–126.
- Nesje, A. and Kvamme, M. (1991) Holocene glacier and climate variations in western Norway: evidence for early Holocene glacier demise and multiple Neoglacial events. *Geology*, **9**, 610–612.
- Nesje, A., Kvamme, M. and Rye, N. (1989) Neoglacial gelifluction in the Jostedalsbreen region, western Norway: evidence from dated buried paleopodsols. *Earth Surf. Proc. Landf.*, **14**, 259–270.
- Nesje, A., Kvamme, M., Rye, N. and Løvlie, R. (1991) Holocene glacial and climate history of the Jostedalsbreen region, western Norway; evidence from lake sediments and terrestrial deposits. *Quat. Sci. Rev.*, **10**, 87–114.
- Nicoletti, P.G. and Sorriso-Valvo, M. (1991) Geomorphic controls of the shape and mobility of rock avalanches. *Bull. Geol. Soc. Am.*, **103**, 1365–1373.
- Nishimura, K. and Maeno, N. (1989) Contribution of viscous forces to avalanche dynamics. *Ann. Glaciol.*, **13**, 202–206.
- Nishimura, K., Narita, H., Maeno, N. and Kawada, K. (1989) The internal structure of powder-snow avalanches. *Ann. Glaciol.*, **13**, 207–210.
- Nobles, L.H. (1966) Slush avalanches in Northern Greenland and the classification of rapid mass movements. *Publ. Assoc. Int. Hydrol. Scient.*, **69**, 267–272.
- Norem, H., Irgens, F. and Schieldrop, B. (1987) A continuum model for calculating snow avalanche velocities. *Rep. Norw. Geotech. Inst.*, **58120–9**, 16 pp.
- Norem, H., Irgens, F. and Schieldrop, B. (1989) Simulation of snow-avalanche flow in run-out zones. *Ann. Glaciol.*, **13**, 218–225.
- Norem, H., Kvisterøy, T. and Evensen, B.D. (1985) Measurement of avalanche speed and forces: instrumentation and preliminary results of the Ryggfonn project. *Ann. Glaciol.*, **6**, 19–22.
- Nyberg, R. (1985) Debris flows and slush avalanches in northern Swedish Lapland: distribution and geomorphological significance. *Meddel. Lunds University Geogr. Inst. Avhandl.*, **97**, 222 pp.
- Oberlander, T.M. (1989) Slope and pediment systems. In: *Arid Zone Geomorphology* (Ed. by D.S.G. Thomas), pp. 56–84. Belhaven/Halsted Press, London.
- Okuda, S., Suwa, H., Okunishi, K., Yokoyama, K. and Nakano, M. (1980) Observations on the motion of a debris flow and geomorphological effects. *Z. Geomorph., N.F.*, **35**, 142–163.
- Oura, H. (ed.) (1967) *Physics of Snow and Ice*. Proc. int. Confer. Low Temperature Science, 495, pp. Hokkaido University of Press, Hakodate.
- Parsons, A.J. and Abrahams, A.D. (1987) Gradient-particle size relations on quartz monzonite debris slopes in the Mojave Desert. *J. Geol.*, **95**, 423–452.
- Pérez, F.L. (1989) Talus fabric and particle morphology on Lassen Peak, California. *Geogr. Ann.*, **71A**, 43–57.
- Perla, R.I. (1978) Failure of snow slopes. In: *Rockslides and Avalanches, 1. Natural Phenomena* (Ed. by B. Voight), pp. 731–752. Elsevier, Amsterdam.
- Perla, R.I. (1980) Avalanche release, motion and impact. In: *Dynamics of Snow and Ice Masses* (Ed. by S.C. Colbeck), pp. 397–462. Academic Press, New York.
- Perla, R.I., Cheng, T.T. and McClung, D.M. (1980) A two-parameter model of snow-avalanche motion. *J. Glaciol.*, **26**, 197–207.
- Perla, R.I. and Martinelli, M. Jr (1975) *Avalanche Handbook*. Agric. Handbook, **489**, 254 pp. U.S. Department of Agriculture, Washington.
- Pierson, T.C. (1980) Erosion and deposition by debris flows at Mt. Thomas, North Canterbury, New Zealand. *Earth Surf. Proc.*, **5**, 227–247.
- Pierson, T.C. (1981) Dominant particle support mechanisms in debris flows at Mt. Thomas, New Zealand, and implications for flow mobility. *Sedimentology*, **28**, 49–60.
- Pierson, T.C. (1986) Flow behavior of channelized debris flows, Mount St. Helens, Washington. In: *Hill-slope Processes* (Ed. by A.D. Abrahams), pp. 269–296. Allen and Unwin, Boston.

- Radbruch-Hall, D.H. (1978) Gravitational creep of rock masses on slopes. In: *Rockslides and Avalanches, 1. Natural Phenomena* (Ed. by B. Voight), pp. 607–657. Elsevier, Amsterdam.
- Ramsli, G. (1981) *Snow and Snow Avalanches*. Universitetsforlaget, Oslo. (In Norwegian.)
- Rapp, A. (1960) Recent development of mountain slopes in Kärkevagge and surroundings, Northern Scandinavia. *Geogr. Ann.*, **42**, 65–200.
- Rapp, A. (1963) The debris slides at Ulvådal, western Norway: an example of catastrophic slope processes in Scandinavia. *Nach. Akad. Wissen. Göttingen, Math.-Phys. Kl.*, **13**, 195–210.
- Rapp, A. (1987) Extreme weather situations causing mountain debris flows. In: *Climatological Extremes in the Mountains: Physical Background, Geomorphology and Ecological Consequences* (Ed. by H. Alexandersson and B. Holmgren), pp. 171–181. UNGI Rapport 65, University of Uppsala.
- Rapp, A. and Nyberg, R. (1981) Alpine debris flows in northern Scandinavia. *Geogr. Ann.*, **63A**, 183–196.
- Rapp, A. and Nyberg, R. (1988) Mass movements, nivation processes and climatic fluctuations in northern Scandinavian mountains. *Nor. Geogr. Tidsskr.*, **42**, 245–253.
- Reading, H.G. and Collinson, J.D. (1996) Clastic coasts. In: *Sedimentary Environments: Processes, Facies and Stratigraphy* (Ed. by H.G. Reading), pp. 154–231. Blackwell Science, Oxford.
- Reite, A.J. (1967) Lokalglasiasjon på Sunnmøre. *Nor. Geol. Unders.*, **247**, 262–287.
- Rickenmann, D. (1990) Bedload transport capacity of slurry flows at steep slopes. *Tech. Hochsch. Zürich, Versuch. Wasser. Hydrol. Glaziol. Eidgen. Mitteil.*, **103**, 249 pp.
- Rickenmann, D. (1991) Bed load transport and hyperconcentrated flow at steep slopes. In: *Fluvial Hydraulics of Mountain Regions* (Ed. by A. Armanini and D. Di Silvio), pp. 429–441. Lecture Notes in Earth Sciences, **37**. Springer-Verlag, Berlin.
- Rickenmann, D. and Zimmermann, M. (1993) The 1987 debris flows in Switzerland: documentation and analysis. *Geomorphology*, **8**, 175–189.
- Salm, B. (1982) Mechanical properties of snow. *Rev. Geophys. Space Phys.*, **20**, 1–19.
- Salm, B. and Gubler, H. (1985) Measurement and analysis of the motion of dense flow avalanches. *Ann. Glaciol.*, **6**, 26–34.
- Sandersen, F., Bakkehoi, S., Hestnes, E. and Lied, K. (1996) The influence of meteorological factors on the initiation of debris flows, rockfalls, rockslides and rockmass stability. *Rep. Norw. Geotech. Inst.*, **585910–10**, 21 pp.
- Savage, S.B. (1983) Granular flows down rough inclines — review and extension. In: *Mechanics of Granular Materials: New Models and Constitutive Relations* (Ed. by J.T. Jenkins and M. Satake), pp. 261–282. Elsevier, Amsterdam.
- Savage, S.B. and Hutter, K. (1989) The motion of a finite mass of granular material down a rough incline. *J. Fluid Mech.*, **199**, 177–215.
- Savage, S.B. and Hutter, K. (1991) The dynamics of avalanches of granular materials from initiation to runout. Part 1: Analysis. *Acta Mech.*, **86**, 201–223.
- Savage, S.B. and Lun, C.K.K. (1988) Particle size segregation in inclined chute flow of dry cohesionless granular solids. *J. Fluid Mech.*, **189**, 311–335.
- Schaerer, P.A. (1981) Avalanches. In: *Handbook of Snow* (Ed. by D.M. Gray and D.H. Male), pp. 475–518. Pergamon Press, Toronto.
- Schaerer, P.A. and Salway, A.A. (1980) Seismic and impact-pressure monitoring of flowing avalanches. *J. Glaciol.*, **26**, 179–187.
- Schumm, S.A. (1956) The role of creep and rainwash on the retreat of badland slopes. *Am. J. Sci.*, **254**, 693–706.
- Scott, A.M. and Bridgwater, J. (1975) Interparticle percolation: a fundamental solids mixing mechanism. *Industr. Engin. Chem., Fundam.*, **14**, 22–26.
- Selby, M.J. (1982) *Hillslope Materials and Processes*. Oxford University Press, Oxford.
- Selby, M.J. (1994) Hillslope sediment transport and deposition. In: *Sediment Transport and Depositional Processes* (Ed. by K. Pye), pp. 61–87. Blackwell Scientific Publications, Oxford.
- Sharp, R.P. and Nobles, L.H. (1953) Mudflow of 1940 at Wrightwood, Southern California. *Bull. Geol. Soc. Am.*, **64**, 547–560.
- Sharpe, C.F.S. (1938) *Landslides and Related Phenomena*. Columbia University Press, New York.
- Solem, T. (1989) Blanket mire formation at Haramsøya, Møre og Romsdal, western Norway. *Boreas*, **18**, 221–235.
- Sollid, J.L. and Sørbel, L. (1979) Deglaciation of western Central Norway. *Boreas*, **8**, 233–239.
- Statham, I. (1973) Scree slope development under conditions of surface particle movement. *Trans. Inst. Br. Geogr.*, **89**, 41–53.
- Statham, I. and Francis, S.C. (1986) Influence of scree accumulation and weathering on the development of steep mountain slopes. In: *Hillslope Processes* (Ed. by A.D. Abrahams), pp. 245–267. Allen and Unwin, Boston.
- Suwa, H. (1988) Focusing mechanism of large boulders to debris-flow front. *Trans. Jap. Geomorph. Union*, **9**, 151–178.
- Suwa, H. and Okuda, S. (1983) Deposition of debris flows on a fan surface, Mt. Yakedake, Japan. *Z. Geomorph. N.F.*, **46**, 79–101.
- Svendsen, J.I. and Mangerud, J. (1987) Late Weichselian and Holocene sea-level history for a cross section of western Norway. *J. Quat. Sci.*, **2**, 113–132.
- Svendsen, J.I. and Mangerud, J. (1990) Sea-level changes and pollen stratigraphy on the outer coast of Sunnmøre, western Norway. *Nor. Geol. Tidsskr.*, **70**, 111–134.
- Takahashi, T. (1991) *Debris Flow*. A.A. Balkema, Rotterdam.
- Tusima, K. (1973) Tests of the repeated loadings on snow. *Low Temp. Sci.*, **A31**, 37–48.
- Van Asch, Th.W.J. (1984) Creep processes in landslides. *Earth Surf. Proc. Landf.*, **9**, 573–583.

- Van Steijn, H. (1988) Debris flows involved in the development of Pleistocene stratified deposits. *Z. Geomorph., (Suppl.) Bd.*, **71**, 45–58.
- Van Steijn, H. (1996) Debris-flow magnitude-frequency relationships for mountainous regions of Central and Northwest Europe. *Geomorphology*, **15**, 259–273.
- Van Steijn, H., Bertran, P., Francou, B., Hétu, B. and Texier, J.-P. (1995) Models for the genetic and environmental interpretation of stratified deposits: review. *Permafr. Periglac. Proc.*, **6**, 125–146.
- Van Steijn, H. and Coutard, J.-P. (1989) Laboratory experiments with small debris flows: physical properties related to sedimentary characteristics. *Earth Surf. Proc. Landf.*, **14**, 587–596.
- Van Steijn, H. and Filippo, H. (1987) Laboratory experiments about the role of debris flows in the formation of grèze-litée type slope deposits. In: *Loess and Periglacial Phenomena* (Ed. by M. Pécsi and H.M. French), pp. 235–252. Akadémiai Kiado, Budapest.
- Voellmy, A. (1955) Über die Zerstörungskraft von Lawinen. *Schweiz. Bauzeit.*, **73**, 159–162, 212–217, 246–249 & 280–285.
- Voight, B. (Ed.) (1978) *Rockslides and Avalanches, 1. Natural Phenomena*. Elsevier, Amsterdam.
- Voitkovskiy, K.F. (1977) *Mechanical Properties of Snow*. Nauka, Moscow. (In Russian.)
- Walton, O.R. (1983) Particle-dynamics calculation of shear flow. In: *Mechanics of Granular Materials: New Models and Constitutive Relations* (Ed. by J.T. Jenkins and M. Satake), pp. 327–338. Elsevier, Amsterdam.
- Washburn, A.L. (1979) *Geocryology – A Survey of Periglacial Processes and Environments*. Edward Arnold, London.
- Washburn, A.L. and Goldthwaite, R.P. (1958) Slush-flows. *Bull. Geol. Soc. Am.*, **69**, 1657–1658.
- Wasson, R.J. (1979) Stratified debris slope deposits in the Hindu Kush, Pakistan. *Z. Geomorph., N.F.*, **23**, 301–320.
- Watanabe, Z. (1980) Tensile strain and fracture of snow. *J. Glaciol.*, **26**, 255–262.
- Weirich, F.H. (1989) The generation of turbidity currents by subaerial debris flows, California. *Bull. Geol. Soc. Am.*, **101**, 278–291.
- Whalley, W.B. (1984) Rockfalls. In: *Slope Instability* (Ed. by D. Brunson and D.B. Prior), pp. 217–256. John Wiley & Sons, Chichester.
- Whalley, W.B. and Martin, H.E. (1992) Rock glaciers: II. Models and mechanisms. *Prog. Phys. Geogr.*, **16**, 127–186.
- Wieczorek, G.F. and Jäger, S. (1996) Triggering mechanisms and depositional rates of postglacial slope-movement processes in the Yosemite Valley, California. *Geomorphology*, **15**, 17–31.
- Williams, V.S. (1984) Pedimentation versus debris-flow origin of plateau-side desert terraces in southern Utah. *J. Geol.*, **92**, 457–468.
- Wyroll, K.H. (1977) Causes of rock slope failures in a cold area: Labrador-Ungava. In: *Landslides* (Ed. by D.R. Coates). *Geol. Soc. Am., Rev. Engin. Geol.*, **3**, 59–67.
- Young, A. (1978a) *Slopes*. Longman, London.
- Young, A. (1978b) A twelve year record of soil movement on a slope. *Z. Geomorph., N.F.*, **29**, 104–110.

Manuscript received 16 February 1997;

revision accepted 28 January 1998